THE UNIVERSITY *of* EDINBURGH

KANK:
A Novel EB1 Interactor and *Drosophila* Orthologue of a Conserved Tumour Suppressor

Sara Clohisey

PRESENTED FOR THE DEGREE OF DOCTOR OF PHILOSOPHY

UNIVERSITY OF EDINBURGH

2013

Declaration

I hereby declare that I alone have composed this thesis and that the work presented is my own, unless stated otherwise.

Sara Clohisey
September 2013

Contents

Figures

Tables

Acknowledgements

First and foremost, I would like to express my very great appreciation to Professor Hiro Ohkura for his valuable help and discussion during the course of this research. His willingness to give his time and energy so generously and his amazing efforts to be available for any and all problems have been very much appreciated. I wish to thank Cancer Research UK for funding me and this project, and giving me a chance to come study at The University of Edinburgh.

I would also like to thank all the wonderful past and present members of the Ohkura lab for all their help, banter and for a making my PhD so pleasant. An extra special thanks goes to Fiona (who always makes sure we get to tea on time!) and Manuel (who has put up with my pokes in the shoulder followed by a scientific enquiry for three years!). Additionally I would like to thank the PhD students who started in the lab with me: Agata, Karolina and Elvira, for their support and friendship over the past few years. I would like to acknowledge Hiro, Manuel and Robin for critical reading and helpful suggestions during the writing of this thesis.

A massive thank you goes to my parents, Joseph and Roslyn. Besides being the most caring and supportive parents anyone could ask for they're also some of my best friends. I would also like to thank my siblings, Jessica and Peter, and all my family and friends back home for their encouragement throughout my studies.

Finally, I want to thank my wonderful boyfriend, John, for his support, encouragement and for motivating me (read: bringing me tea!) when I most needed it.

Abstract

The conserved human protein KANK1 has been identified as a tumour suppressor and its expression is down-regulated in several tumour types. Roles for this protein in actin regulation, cell migration and cell polarity have been documented in cultured mammalian cells. In *C. elegans* the KANK1 orthologue, VAB-19, is required for normal development as it helps stabilise attachment structures between muscle and epidermal cells. Despite these studies, the precise cellular role of KANK remains elusive.

It was found that the *Drosophila* KANK orthologue binds directly to EB1, a crucial regulator of microtubule plus-end dynamics. I aimed to determine the role of KANK with respect to this indirect microtubule interaction using *Drosophila*. I identified residues which mediate the interaction between KANK and EB1, and showed they are essential for localisation of KANK to microtubule plus-ends in *Drosophila* culture cells. I found that KANK expression increases during embryogenesis and peaks in the late embryonic development when KANK is shown to localise to sites of attachment between muscle and epidermal cells. This suggests a role for the protein in stabilisation of muscle attachment during embryonic development, a process previously shown to require EB1. I generated a KANK deletion mutant and found they are viable and fertile but show a mild neuronal phenotype, specifically early branching of the neurons and less organised neuron bundles. My results suggest previously unknown roles for KANK in myogenesis and neurogenesis in *Drosophila* embryogenesis.

Abbreviations

+TIP	Plus-end Tracking Protein
ANKRD	Ankyrin Repeat Domain Protein
APC	Adenomatous Polyposis Coli
ATP/ADP	Adenosine Triphosphate/Diphosphate
CAP-Gly	Cytoskeleton-Associated Protein Glycine Rich
CH	Calponin Homology
CLIP	Cytoplasmic Linker Protein
CNS	Central Nervous System
DAPI	4’,6-diamidino-2-phenylindole, dihydrochloride
DNA	Deoxyribonucleic Acid
dsRNA	Double Stranded RNA
EB(H)	End Binding (Homology)
ECM	Extracellular matrix
EMT	Epithelial-Mesenchymal Transition
EST	Expressed Sequence Tag
FBS	Foetal Bovine Serum
FC	Founder Cell
FCM	Fusion Competent Myoblast
FGF	Fibroblast Growth Factor
GST	Glutathione-S Transferase
GTP/GDP	Guanosine Triphosphate/Diphosphate
MAP	Microtubule Associated Protein
MBP	Maltose Binding Protein
MTJ	Myotendinous Junction
MTOC	Microtubule Organising Centre
NBP	Numb Binding Protein
NES	Nuclear Export Signal
NLS	Nuclear Localisation Signal
PI3K	Phosphoinositide 3-Kinase
PNS	Peripheral Nervous System
RNA	Ribonucleic Acid
RNAi	RNA interference
S2 Cell	Schneider Cell
SDS	Sodium Dodecyl Sulphate
TOG	Tumour Over-expressed Gene
Tris	2-amino-2-(hydroxymethyl)-1,3,-propanediol
VAB	Variable Abnormal Morphology

Chapter 1
Introduction

1.1 The Cytoskeleton

The cytoskeleton, consisting of microtubules, actin and intermediate filaments in eukaryotes, has three main functions. Firstly, the cytoskeleton is so called as it is analogous to the skeleton of the human body in that its components can coordinate to structurally support the cell in 3 dimensions. The cytoskeleton, however, differs from the rigid human skeleton; it is dynamic and constantly changes shape as the filaments it is composed of grow and shrink. Secondly, the cytoskeleton can act as the tracks on which transport of vesicles, proteins and other cellular material can occur. Finally, the cytoskeleton maintains communication between the cell and its surroundings. Eukaryotic cells typically contain all three components of the cytoskeleton, with some exceptions. *Drosophila melanogaster* cells, for example, contain actin and microtubules just like other eukaryotic organisms, but do not contain any cytoplasmic intermediate filaments. *Drosophila* cells contain only nuclear intermediate filaments, lamins, which are important components of the meshwork architecture of the nuclear envelope. Owing to their near-absence in *Drosophila,* intermediate filaments will not be discussed further. What follows is a brief introduction to the actin cytoskeleton and a more thorough introduction to the microtubule cytoskeleton.

1.1.1 The Actin Cytoskeleton

Actin was originally identified in muscle preparations by Halliburton et al in 1887. It was once thought to be a purely muscular protein (Straub, 1942) (Jakus and Hall, 1947). However, in the 1960s it was realised that actin was a ubiquitous protein, necessary for eukaryotic cell function (Ohnishi, 1962). Actin filaments enable cell motility and provide structure to the cell during interphase. Actin is distributed throughout the cytoplasm of the cell but is more concentrated at the cell cortex where it provides support and shape to the plasma membrane. During cytokinsesis, actin in the cell transiently reorganises to form a contractile ring which tightens, eventually separating two daughter cells (Sanger, 1975; Schroeder, 1973).

Actin is highly conserved throughout evolution (Hightower & Meagher 1986). Actin filaments are two-stranded helical polymers composed of monomeric

globular actin molecules (Egelman, 1985; Holmes et al., 1990; Kabsch et al., 1990). Monomeric actin is referred to as G-actin (for globular) while linear actin polymers are referred to as F-actin (for filamentous). Filaments are 5-9nm in diameter. Actin filaments are polar, with a minus-end prone to depolymerisation and a plus-end prone to polymerisation. The plus and minus ends differ structurally due to the structure of adenosine triphosphate (ATP)-bound G-actin monomers which assemble head-to-tail in the filament. When assembled as a filament polymer, actin hydrolyses ATP to adenosine diphosphate (ADP) (Frieden, 1982; Frieden and Patane, 1985) and addition of new monomers becomes energetically unfavourable. Rapid polymerisation and depolymerisation enable actin to be dynamic and to respond quickly to the needs of the cell. These processes are tightly controlled by many actin-associated proteins (Campellone and Welch, 2010; Hall, 1994).

Actin is naturally linear but flexible and can form structures in two dimensions. Actin binding proteins can facilitate bundling, branching and crosslinking enabling actin to form a wealth of 3-dimensional structures including protrusive lamellipodia and filopodia at the cell membrane, giving actin a vital role in cell motility.

1.1.2 The Microtubule Cytoskeleton

Similar to actin filaments, microtubules are dynamic, polar polymers. They perform vital functions in eukaryotic cells; forming the spindle during cell division and functioning as the tracks for vesicular transport. Structurally, microtubules are composed of heterodimers of α-tubulin and β-tubulin monomers. These monomers have been shown to have high sequence similarity (Keskin et al., 2002) though they have slightly different functions within the microtubule structure. The α/β heterodimers bind head-to-tail and are organised into protofilaments (Amos and Klug, 1974). These protofilaments are bound in a longitudinal fashion to form a cylindrical ‘tubule’ shape which has an outer diameter of 24nm and a hollow inner lumen. The number of protofilaments can vary from 9 to 15 and this number can correlate to the function of the microtubule (Bounoutas et al., 2009). 13 protofilaments is most commonly seen (Tilney et al., 1973). The cylindrical structure makes microtubules far more rigid than actin microfilaments, though still dynamic.

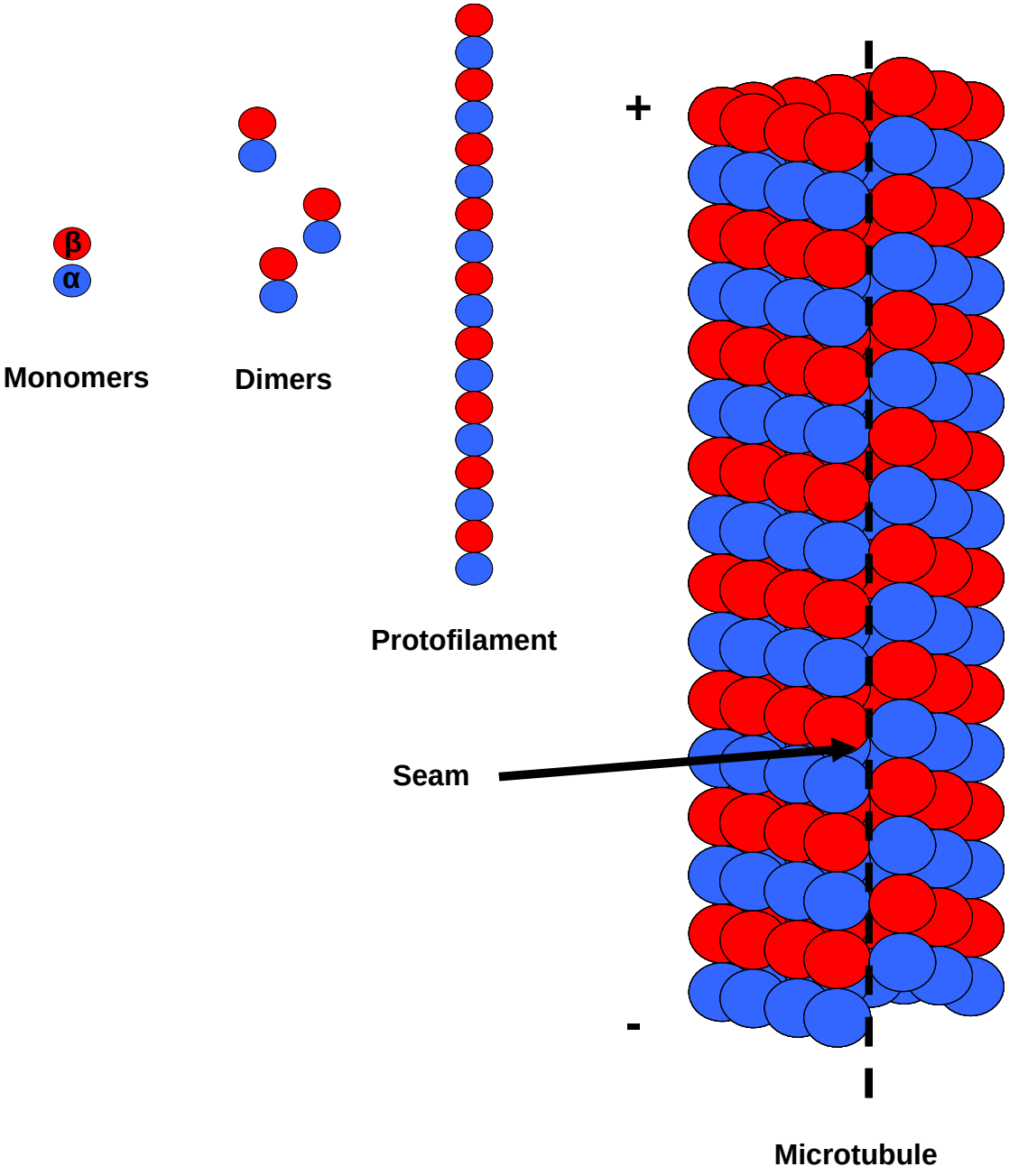

Figure 1.1 Microtubules are composed of α/β-tubulin heterodimers organised into protofilaments which bind laterally to form polar cylindrical tubules.

In a 13 protofilament tubule the protofilaments are arranged such that the monomers are bound laterally α to α and β to β, apart from two protofilaments in which the monomers are bound laterally α to β and β to α, this is known as the seam (Figure 1.1) (Mandelkow and Schultheiss, 1986).

Nucleation of microtubules typically occurs at γ-tubulin containing microtubule organising centres (MTOCs) (Joshi et al., 1992; Oakley and Oakley, 1989) such as centrosomes (Mitchison and Kirschner, 1984a). Like actin filaments microtubules are structurally polar, with a dynamic plus end and a less dynamic minus end both of which undergo constant polymerisation and depolymerisation. Microtubules exist in a state of dynamic instability (Mitchison and Kirschner, 1984b) and are able to rapidly switch between polymerisation and depolymerisation in response to the needs of the cell. The minus (non-growing) end of the filament often remains anchored at the MTOC allowing the plus (growing) end to extend towards the periphery of the cell.

During polymerisation, α-β tubulin heterodimers are added to the growing tubule. These heterodimers are in a guanosine triphosphate (GTP) bound state. β-tubulin contains a GTP exchange site allowing for hydrolysis of GTP to guanosine diphosphate (GDP) as the microtubules polymerise and grow (David-Pfeuty et al., 1977). Incorporation into the microtubule lattice is associated with GDP-bound α-β tubulin. GTP bound β-tubulin and GDP bound β-tubulin have conformational differences. GTP bound β-tubulin promotes formation of straight tubules while GDP bound β-tubulin encourages more curved tubules, which are not energetically favourable (Müller-Reichert et al., 1998) and therefore an unstable structure. A GTP cap i.e. a region of GTP bound α-/β-tubulin, at the growing ends constrains the GDP bound α-/β-tubulin, keeping microtubules straight and preventing disassembly of the older regions of protofilaments (Hill and Chen, 1984; Mitchison and Kirschner, 1984b). If this GTP cap is lost depolymerisation occurs and the protofilaments cannot maintain a straight structure, they peel back becoming splayed.

The dynamic instability of microtubules is tightly regulated, spatially and temporally, by microtubule associated proteins (MAPs) (Sloboda et al., 1975) and allows the architecture of the microtubule network to change quickly. The most clear and striking example of this is when cells enter mitosis. In interphase the microtubule

network consists of astral arrays, emanating from MTOCs at the centre of the cell out towards the periphery. This network allows for structural stability of the cell and forms a network for transportation within the cell. When cells enter mitosis this lattice quickly rearranges to form the mitotic spindle, a vital structure which acts during cell division to pull sister chromatids apart and segregate them into separate daughter nuclei.

1.2 Microtubule Associated Proteins and +TIPs

Microtubule associated proteins (MAPs) is the name given to a wide range of proteins with varied structures and functions which can interact with tubulin *in vivo* and/or *in vitro* and often affect microtubule structure and dynamics. A subset of MAPs are the +TIPs, proteins which localise to the growing ends of microtubules and often have roles in regulation of microtubule dynamics or have structural roles in linking microtubules to cellular structures and each other. These proteins can bind the growing end of the microtubule directly or through other +TIPs which facilitate their localisation. +TIPs can be loosely categorised by the domains and motifs they contain, as described below:

TOG (tumour over-expressed gene) domains are flat domains containing six HEAT-repeats, side by side (Al-Bassam et al., 2007). HEAT repeats are structural elements which form protein-protein interaction sites (Kennedy et al., 2009). Multiple TOG domains, arranged in tandem, allow proteins to bind tubulin directly and track microtubule growing ends (Brouhard et al., 2008; Spittle et al., 2000). Proteins containing TOG domains include the related proteins: *Drosophila* Msps (Cullen et al., 1999) human TOGp (Charrasse et al., 1998) and *Xenopus* XMAP215 (Gard and Kirschner, 1987), along with Cytoplasmic Linker Associated Proteins (CLASPs) such as mammalian proteins CLASP1 and 2 (Komarova et al., 2002; Maiato et al., 2003) and the related *Drosophila* protein MAST/Orbit (Akhmanova et al., 2001). TOG domain-containing proteins have roles in promoting microtubule polymerisation. The Msps family of proteins have been shown to act as antipausing factors by promoting microtubule stabilisation and destabilisation (Brittle and Ohkura, 2005; Gard and Kirschner, 1987). CLASPs have been shown to

promote microtubule dynamics, specifically rescue (Al-Bassam et al., 2010) and to promote microtubule pausing in interphase (Sousa et al., 2007). TOG domain containing proteins affect microtubule dynamics directly.

Calponin Homology (CH) domains were first identified as actin binding domains (Castresana and Saraste, 1995), however the conserved N-terminal region of EB (End Binding) proteins was found to contain a CH domain that functions in microtubule binding (Bu and Su, 2003; Hayashi and Ikura, 2003). The CH domain recognises the growing ends of microtubules by recognising the conformational difference between GDP and GTP bound β-tubulin (Maurer et al., 2012). This domain allows proteins to bind autonomously to and track microtubule growing ends. Since then, other CH domain containing MAPs have been identified including CLAMP (Dougherty et al., 2005) and Ndc80. The latter of which binds microtubules as part of the Ndc80 complex, attaching them to the kinetochore during spindle formation (Ciferri et al., 2008).

Cytoskeleton-associated protein glycine rich (CAP-Gly) domain was first identified in the N-terminus of cytoplasmic linker protein (CLIP)-170 (Pierre et al., 1992, 1994). It is a ~80 amino acid unit that can bind (via a conserved motif: GKNDG) a three amino acid motif (the EEY/F motif) in a hydrophobic environment (Pierre et al., 1994; Weisbrich et al., 2007). The EEY/F motif is found at the C-terminal of α-tubulin allowing proteins with a CAP-Gly domain to bind microtubules directly. It has been shown that detyrosylation of α-tubulin can inhibit the recruitment of CAP-Gly domain containing proteins (Peris et al., 2006). Other EEY/F motif containing proteins include the EB family of proteins and CLIP-170 itself.

The C-terminal region of the EB family of proteins is highly conserved and contains the end binding homology (EBH) domain (Miller et al., 2000; Zimniak et al., 2009) which recognises a four amino acid motif, **SxIP** or, less often, **TxIP** or **SxLP**. This motif goes by many names; EB1 binding motif, Microtubule Tip Localisation Signal (MtLS) (Buey et al., 2012) or SxIP motif (Honnappa et al., 2009). This motif is readily recognised by the EBH region of EB1. It is seen as a putative marker for EB1 binding and thus, microtubule plus end localisation and tracking.

1.3 EB1: The 'Hub' of Microtubule Plus Ends and its Interactors

Interaction with EB1 has emerged as a common characteristic of +TIPs. EB1 has been referred to as the "Master Controller" of microtubule plus ends (Vaughan, 2005). However, it would be more accurate to refer to it as a "hub of +TIP machinery" as it is becoming apparent that sequences and domains identified which target proteins to the growing ends of microtubules often act through EB1 and EB1 does not have a direct effect on microtubule ends itself. EB1 was identified as a binding partner of APC (adenomatous polyposis coli) when a yeast two hybrid screen was carried out for proteins that bind the carboxyl terminus of APC, a region often deleted in colo-rectal tumours (Su et al., 1995). Afterwards, it was realised that EB1 is a MAP that dynamically localises to the growing ends of microtubules throughout the cell cycle (Berrueta et al., 1999; Mimori-Kiyosue et al., 2000; Morrison et al., 1998). EB1 was thought to primarily increase the rate of catastrophe and rescue of microtubules (Tirnauer et al., 1999) however it has become clear that the primary function of EB1 is to recruit proteins to the growing ends of microtubules. EB1, like other EB proteins, functions as a homodimer (Sen et al., 2013) and binds microtubules directly via the conserved CH domain found in its N-terminus (Bu and Su, 2003).

EB1 can bind to and track polymerising ends exclusively. How EB1 recognises the growing ends of microtubules, in contrast to the lattice, has recently been determined. Studies of the fission yeast (*S. pombe*) EB1 homologue, Mal3, have determined that the CH domain of EB proteins binds microtubules between protofilaments, except at the seam, close to the GTP-exchange site in the GTP-cap. This allows the CH domain to directly respond to structural changes which occur in tubulin when GTP has been hydrolysed to GDP, leading to dissociation of the CH domain from tubulin when such hydrolysation occurs (Maurer et al., 2012).

The EBH domain of the protein family recognises proteins which contain SxIP motifs. This enables these 'cargo proteins' with very different sequences, structures and functions to localise with EB1 at microtubule ends. Very few identified +TIPs bind microtubules directly. The vast majority have been shown to

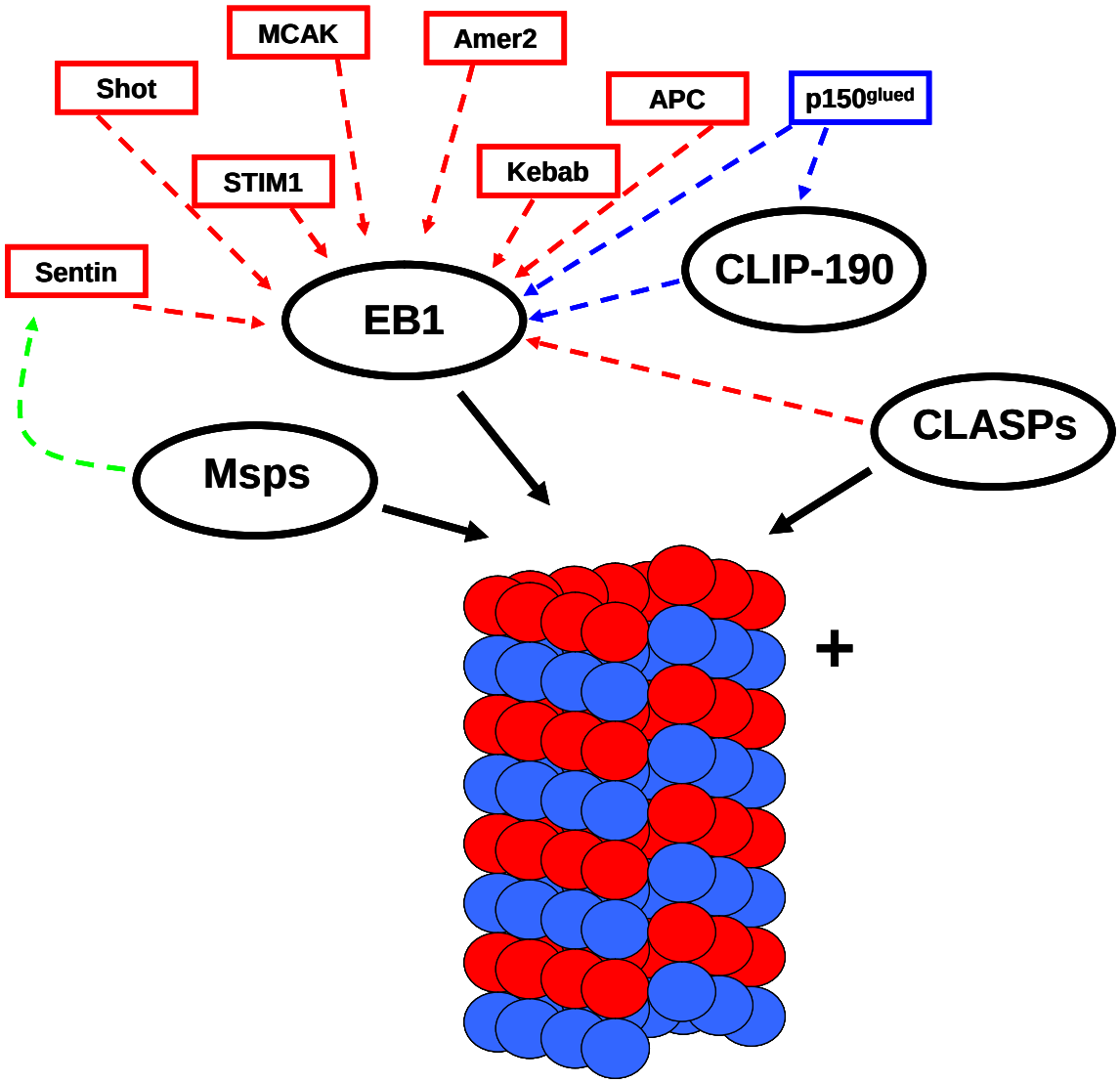

Figure 1.2 Some +TIPs bind tubulin directly while others 'hitchhike'. While some +TIPs can bind microtubules directly (black) many +TIPs localise to microtubule plus ends via association with EB1 (red) while a minority associate through other, established +TIPs. References: msps (Cullen et al. 1999), Shot (Slep et al. 2005; Alves-Silva et al. 2012), STIM1 (Grigoriev et al. 2008), Sentin (Wenjing et al., 2011, Li et al. 2011), Amer2 (Pfister et al. 2012), Kebab (Meireles et al. 2011), APC (Slep et al. 2005), CLIP-170 (Dzhindhev et al. 2005; Dixit et al. 2009), P^{150}-Glued (Watson et al. 2006), CLASPs (Akhmanova et al. 2001).

localise to microtubule growing ends via EB1 interaction (Figure 1.2). EB1, therefore, is the most important regulator of the microtubule growing ends, albeit indirectly. Below is a (by no means exhaustive) list of some identified EB1 interactors:

APC is a conserved protein, strongly associated with colon cancer (Groden et al., 1991) which has been studied, along with its yeast homologue Kar9, in great detail. APC has been shown, among other roles, to regulate the degradation of β-catenin, a transcription factor which acts as part of the canonical Wnt pathway and a component of the cadherin complex which functions in cell-cell adhesion (Rubinfeld et al., 1993). EB1 was originally identified as an APC binding protein (Su et al., 1995) and the EB1 binding region of APC was further studied. A small unstructured region, later found to contain an SxIP motif, in the C-terminus of APC was identified as being responsible (Honnappa et al., 2005, 2009). Although EB1 remains the primary recruiter of proteins to the microtubule plus end, some proteins may require the EB1/APC complex to localise such as mDia2, an actin nucleator with a function in microtubule dynamics, which localises to the plus-ends of microtubules (Bartolini et al., 2008; Wen et al., 2004).

Cytoplasmic-linker protein-170 (CLIP)-170 was identified as Restin in human white blood cells (Bilbe et al., 1992) and in the same year as CLIP-170, a 170kDa protein which linked microtubules and endocytic vesicles (Pierre et al., 1992). CLIP-170, and its *Drosophila* homologue CLIP-190, require EB1 to bind and track microtubule plus-ends (Dixit et al., 2009; Dzhindzhev et al., 2005). CLIP-170 and -190 localise to unattached kinetochores in early mitosis (Dujardin et al., 1998; Dzhindzhev et al., 2005) in an EB1 independent manner (Coquelle and Caspi, 2002; Tai et al., 2002). Binding to EB1 by CLIP-170 and its orthologues is through the CAP-Gly domain of the CLIP proteins (Dzhindzhev et al., 2005)(Section 1.2).

The *Drosophila* spectraplakin **Short stop (Shot**)/Kakapo/Groovin was identified as an embryonically expressed protein with an important role in cell adhesion (Gregory and Brown, 1998) and a role in the correct localisation of the signalling protein Vein at the myotendinous junction (MTJ) between developing muscle and tendon cells (Strumpf and Volk, 1998), two possibly related functions.

More recently, Shot has been shown to localise to the growing ends of microtubules in an EB1 dependent manner (Slep et al., 2005). In developing tendon cells of *Drosophila* embryos, Shot associates with microtubules via the EB1/APC complex and this enables the plus ends of microtubules to grow towards the membrane at the developing myotendinous junction, between tendon cells and muscle cells (Subramanian et al., 2003). Shot also binds microtubules in growing axons in an EB1 dependent manner to facilitate axon growth and organisation of microtubules (Alves-Silva et al., 2012). This latter study found that Shot binds EB1 through SxIP motifs in its C-terminal.

Stromal interaction molecule 1 (STIM1) is a tumour suppressor (Sabbioni et al., 1999)which regulates store-operated Ca^{2+} channels, the control of which is necessary to regulate important cellular functions. Such functions include activating enzymes and refilling intracellular Ca^{2+} stores (Liou et al., 2005; Sabbioni et al., 1999). STIM1 binds to EB1 through a variant of the SxIP motif, a TxIP motif. Mutation of this motif was shown to disrupt EB1-STIM1 binding (Jiang et al., 2012; Pozo-Guisado et al., 2013).

Mitotic-centromere associated kinesin (MCAK) is a member of the kinesin-13 family of kinesin related proteins that depolymerise microtubules (Desai et al., 1999; Wordeman and Mitchison, 1995). Although related to kinesins, MCAK is not motile. Depletion of MCAK in mammalian cells leads to lagging chromosomes (Maney et al., 1998) which indicated a role in microtubule depolymerisation during mitosis. MCAK associates with EB1 which targets it to the polymerising ends of microtubules (Lee et al., 2008; Moore et al., 2005).

1.4 Identification of Kank as an EB1 Binding Protein

EB1 has been described as a “master regulator” of microtubule growing ends and has been observed to influence microtubule dynamics indirectly through its binding partners. Therefore, a genome-scale screen was carried in the Ohkura lab (Ohkura and Dzhindzhev, personal communication) to identify EB1 interactors via *in vitro* expression cloning. First, genes from a collection of annotated *Drosophila* cDNA were transcribed and translated *in vitro*. The proteins expressed were radioactively

labelled using ^{35}S methionine during translation and then EB1 interactors were pulled down with MBP-EB1 coupled to amylose beads. The beads could then be prepared as protein samples, run on an SDS gel and the interactors identified on an autoradiograph (modified from Lee et al., 2005). The technique has proven effective and has so far identified a number of novel EB1 interactors, including Kebab (Meireles et al., 2011). Among the identified interactors was CG10249, the *Drosophila* homologue of the human ANKRD15. This protein, also known as Kank1, was identified as a tumour suppressor protein (Sarkar et al., 2002a) which, so far, has no known association with microtubules. Kank1, and its *C. elegans* homologue VAB-19, have been implicated in a number of molecular processes, outlined below. However, there are major gaps in our understanding of Kank1 and its functions. *Drosophila* provides a powerful means to address this problem as outlined in Section 1.11.

1.5 Kank is a Tumour Suppressor Protein

A loss of heterozygosity (LOH) in tumour cells from patients suffering renal cell carcinomas (RCC) was mapped to chromosome 9 and expressed sequence tags (EST) were used to determine the sequence that was deleted. This analysis identified the gene ANKRD15 as a putative tumour suppressor as it had lower levels of transcripts in six out of eight RCC cell lines examined, when compared to normal cells from the same patients (Sarkar et al., 2002a). Loss of wild type expression levels was due to a deletion of one allele of the gene in tumour cells coupled with various degrees of methylation in regulatory regions of the second allele, resulting in reduced expression, not seen in normal tissues from the same patients. No nonsense mutations were identified in the ANKRD15 region during this study.

The ANKRD15 gene was confirmed as a tumour suppressor in cell culture and *in vivo*. Firstly, HEK293 cells, human embryonic kidney cells which were determined to have no expression of the gene, were transfected with a vector containing ANKRD15 or an empty control vector. Those containing the ANKRD15 vector grew much slower than control cells and after 15 days had reached numbers only 20% that of cells transfected with the empty vector. Cells also displayed

morphological differences; specifically they were larger and flatter than control cells. Secondly, nude mice were injected with HEK293 cells transfected with either the ANKRD15 or the empty vector. After 40 days, mice injected with the empty vector had formed visible kidney tumours while those injected with the ANKRD vector containing cells had a complete absence of tumours (3/4 mice) or a slow growing tumour (1/4 mice).

The 1192 amino acid ANKRD15 protein was predicted to contain a coiled-coil region towards the N-terminus and an ankyrin repeat region towards the C-terminus. The protein was renamed Kidney Ankyrin repeat containing protein (Kank1). An antibody raised to Kank1 confirmed, through western blotting, a lower expression of the protein in 60% of the RCC lines examined. This antibody was used to determine the subcellular localisation of human Kank1, which localises to the cytoplasm and is strongly localised to the periphery of the cells, specifically at sites of membrane ruffling (Chandra et al., 2005).

Further evidence for the role of Kank1 in the progression of some cancers has since emerged. Kank1 has been identified in a study which sought to catalogue genes which showed homozygous deletions in human lung cancer (Kohno et al., 2010) and found to be down-regulated in a myeloproliferative disorder (disease of the bone marrow indicative of progression to leukaemia) known as polycythemia vera (Kralovics et al., 2005).

1.5.1 The Kank Family of Proteins is Conserved Across Species

It was later determined that humans express two isoforms of Kank1, termed Kank-L (for long) and Kank-S (for short). Kank-L has an extended N terminus compared to Kank-S of 158 amino acids (Aoyagi and Kiyama, 2005). While Kank-S is expressed ubiquitously in human tissues, Kank-L expression was shown to be somewhat tissue specific as higher levels of expression are seen in kidney, heart, liver and skeletal muscle tissues. It has been hinted that the two forms of Kank may have somewhat different functions as, although there is a nuclear localisation signal and nuclear export signal common to both Kank isoforms, the 158 amino acid region unique to Kank-L contains further NLS and NES which may alter its function compared to Kank-S (Wang et al., 2006a).

A further 3 members of the human ankyrin-repeat domain protein (ANKRD) family have been identified which share a similar structure to Kank1 (Zhu et al., 2008). These 4 proteins have been collectively referred to as the 'Kank family' and the founding member, ANKRD15, has been designated Kank1. Not much is known about Kank2-4. As all 4 members of this protein family are not highly expressed in kidney tissues the acronym Kank now refers to 'KN motif and ankyrin repeat domain-containing protein'. Orthologues of Kank1 have been identified in other species, vertebrate and invertebrate, leading to the conclusion that Kank is reasonably well conserved within the animal kingdom. No plant or fungi orthologues have been identified.

The Kank family of proteins and their orthologues share a similar, conserved structure (Kakinuma et al., 2009) consisting of an N-terminus coiled-coil region, a mid-region and a C-terminus ankyrin repeat domain. The coiled-coil domain may enable Kank to form a homodimer (Kakinuma et al., 2009; Medves et al., 2010). A conserved 'KN motif' located in the N-terminal region has been shown to be important in Kank-L (Wang et al., 2006) for nuclear localisation and nuclear export and may have similar functions in other Kank-family members. The ankyrin domain is found towards the C-terminus. Ankyrin-repeat domains are very common in nature and often mediate protein-protein interactions as they are known to recognise and bind a wide range of protein motifs (Mosavi et al., 2004). Proteins containing ankyrin domains have a wide range of functions, though they are predominantly scaffolding proteins, the most well-known of which are the ankyrin domain containing adaptor proteins which link the plasma membrane to spectrin, a cytoskeletal scaffolding protein. The Kank family differ from these classical ankyrin proteins as Kank proteins lack spectrin binding and transmembrane domains.

1.5.2 VAB-19 is Necessary for Viability in C. elegans

Disruption of the Kank orthologue VAB-19 in *C. elegans* during development is lethal (Ding et al., 2003). VAB-19 localises to epidermal attachment structures, specifically those attachment structures between epidermal and muscle cells, in developing nematode embryos and later at the circumferential actin bands that cover the length of the worm. These circumferential bands are necessary for elongation. It

was found that disruption of VAB-19 function in temperature sensitive mutants caused growth arrest soon after elongation and weak muscle contractions began. Susceptibility at this stage was confirmed by temperature shift experiments. If the worms are shifted to the restrictive temperature after this stage, development is morphologically normal, though there is a delay.

1.5.3 A Role for Kank Proteins in Cell Adhesion

In humans, Kank1 has been shown to bind β-catenin and accompany its translocation from the cell periphery to the nucleus (Wang et al., 2006a). β-catenin is a well known component of the canonical Wnt pathway in development and acts as a transcription factor activator. β-catenin is also a subunit of the cadherin protein complex, which plays a major role in cell adhesion. Kank2 (ANKRD25) has been identified as a growth regulatory factor (Harada et al., 2005). When chicken embryo fibroblasts were transfected with Kank2, they were found to proliferate at an increased rate and gained the ability to grow in culture without cell-cell contact. In the same study Kank2 was found to be expressed quite highly in mouse heart, liver and kidney tissues, particularly in the glomerulus of the kidney (Harada et al., 2005). The zebrafish homologue of Kank3, Numb-binding protein (NBP) has recently been found to interact with the developmental regulator Numb and localise at the basal poles of cells (Boggetti et al., 2012). Mutants for NBP show an abnormal distribution of cadherin proteins, leading to disruption of cell adhesion in developing zebrafish embryos.

In *C. elegans vab-19* mutants, components of attachment structures (specifically myotactin a transmembrane scaffold protein, VAB10A a spectraplakin and some intermediate filaments (IFs)) (Bosher et al., 2003) become delocalised from the muscle adjacent regions of epidermal cells after the two-fold stage of development, disrupting the adhesion between the two cell types and leading to growth arrest (Figure 1.3). This shows that VAB-19 is essential to maintain these attachment structures and thus cell-cell adhesion between epidermal and muscle cells during elongation. Myotactin, VAB10A and IFs also localise to the circumferential actin bands that promote elongation at later stages of development and maintenance of their localisation at this stage is not dependent on VAB-19. However VAB-19

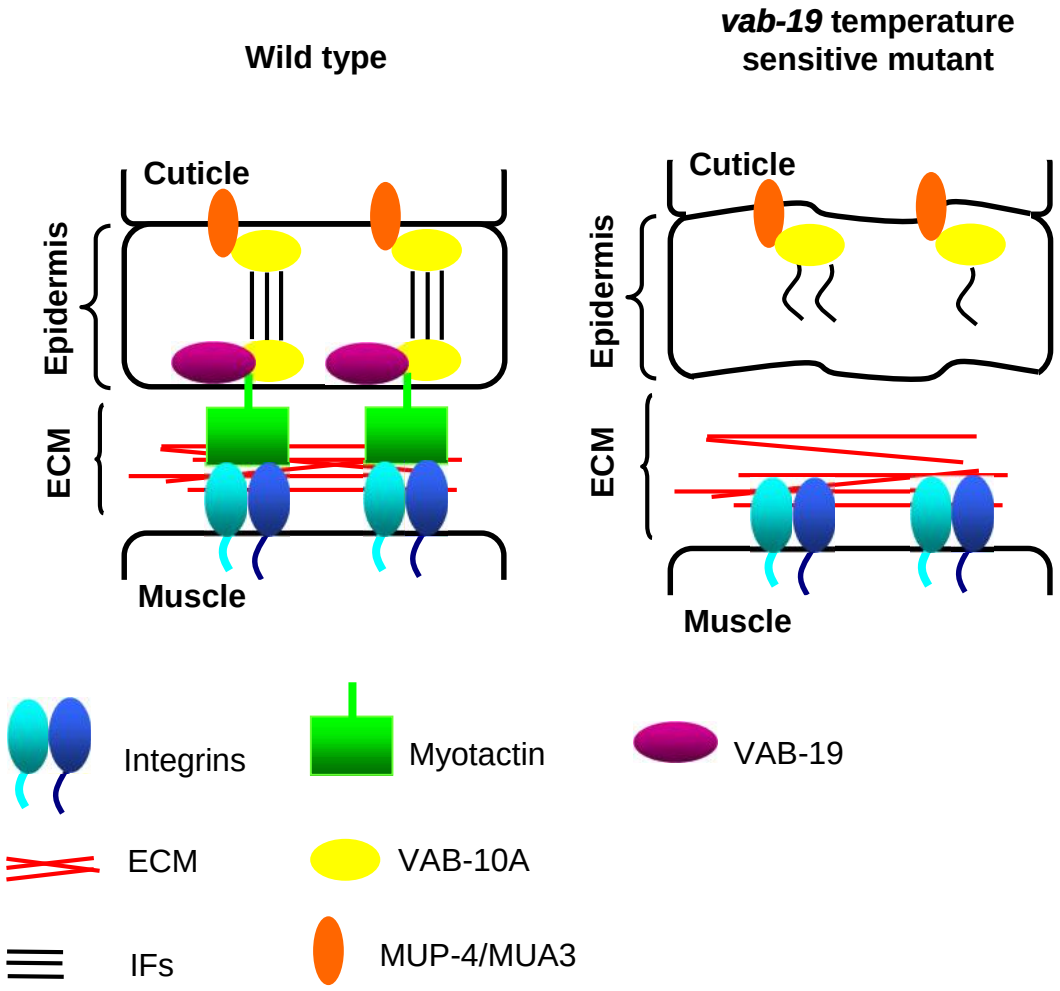

Figure 1.3 VAB-19 stabilises attachment structures between muscle and epidermal cells in *C. elegans*. VAB-19 localises on the epidermal side of the attachment structure that forms between the muscle and epidermal cells of *C. elegans* during development and maintains the localisation of VAB-10A, Myotactin and intermediate filaments (IFs) during elongation of the worm. In *vab-19* temperature sensitive mutants VAB-10A, Myotactin and IFs become mislocalised, leading to detachment of the epidermis from the muscle cells and resulting in lethality. ECM – extra cellular matrix, MUP-4/MUA3 – transmembrane proteins which enable VAB-10A localisation on the cuticle side (apical) of epidermal cells. Adapted from Bosher et al. 2003.

localisation to the actin bands is affected in mutants for any of these three proteins, but its localisation to attachment structures is not (Ding et al., 2003).

RNAi of VAB-19 indicates a further, indirect, role in cell adhesion during development. It was found that invagination during uterine-vulval attachment in *C. elegans* required VAB-19 to maintain basement membrane sliding (Ihara et al., 2011). If VAB-19 expression was disrupted, cells could no longer 'sense' the distance they should slide to allow for invaginating cells, causing holes to form on the basement membrane.

1.5.4 Kank Proteins Affect Actin Organisation

Mammalian Kank has been shown to localise to actin rich membrane ruffles of human kidney cells and to affect β-actin distribution directly in cultured human kidney cells (Sarkar et al., 2002a). Studies have shown that Kank1 can affect actin polymerisation in two ways via the phosphoinositide 3-kinase (PI3K) pathway. Firstly, Kank1 has been shown to be phosphorylated by Akt. This allows Kank1 to bind to an isoform of 14-3-3, which is then unable to activate the small GTPase RhoA (Kakinuma et al., 2008) (Figure 1.4 A). RhoA acts upstream ROCK and mDia. ROCK is a kinase which phosphorylates and inhibits actin depolymerisers such as cofilin (Maekawa, 1999) and mDia is a member of the formin family of actin polymerising proteins (Krebs et al., 2001). This leads to Kank1 indirectly influencing the polymerisation of actin through inhibition of RhoA.

Secondly, Kank1 has also been shown to bind to IRSp53 (insulin receptor substrate p53) and inhibit the interaction between IRsP53 with an activated form of the small GTPase Rac1 ($Rac1^{G12V}$) but not the similar molecule $CDC42^{G12V}$ (Roy et al., 2008) (Figure 1.4B). IRsP53 acts as the 'link' between Rac1 and the WASP and WAVE family of proteins which function as actin regulators (Miki et al., 2000; Takenawa and Miki, 2001) during lamellipodia and fillopodia formation. By inhibiting the IRsP53/Rac1 interaction Kank1 inhibits the formation of lamellipodia (Roy et al., 2008).

In *C. elegans vab-19* mutants were shown to have disorganised bundling of actin, a phenotype which was suppressed by a reduction in SMA-1 function, a βH

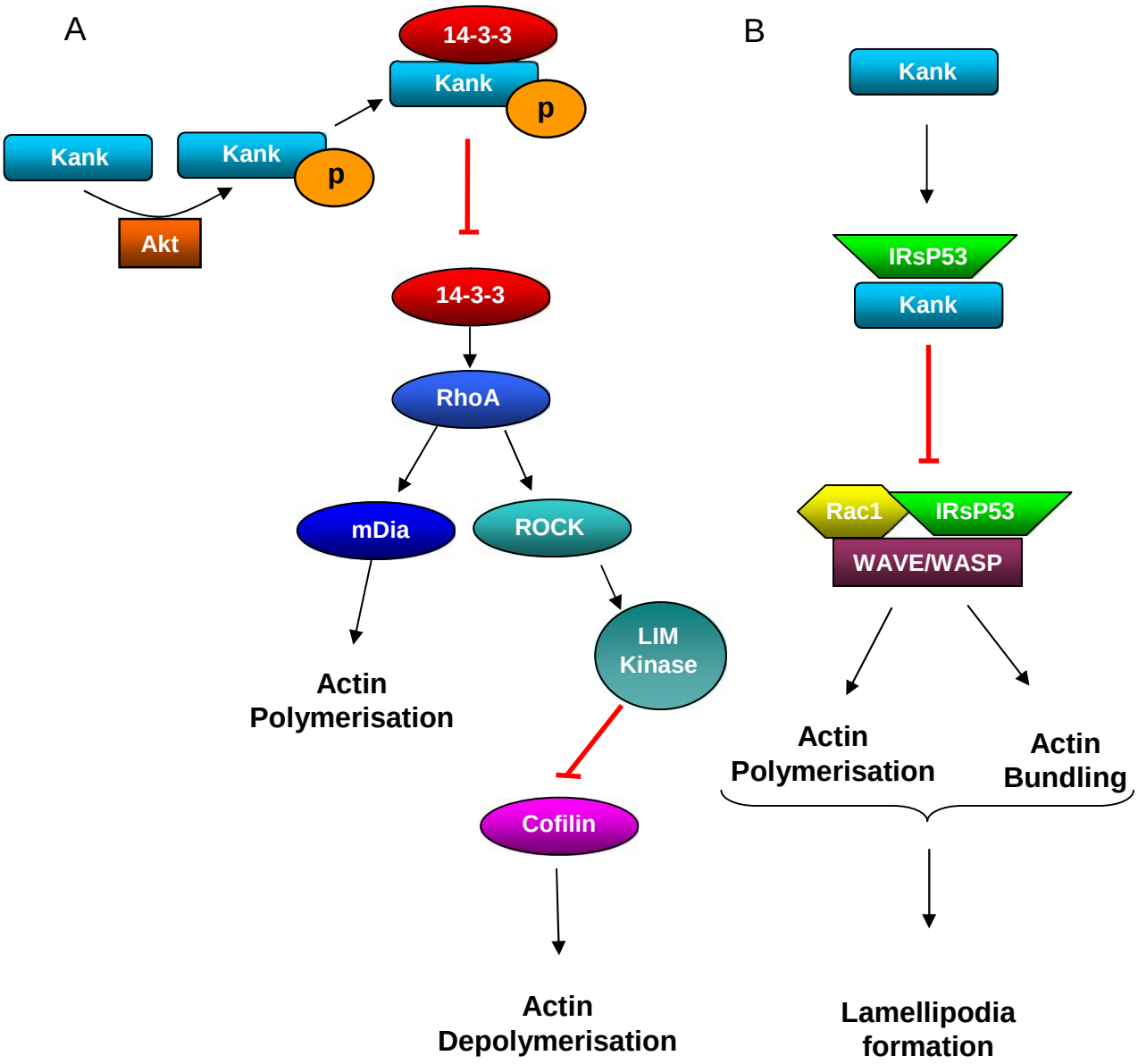

Figure 1.4 Kank1 affects actin organisation in mammalian culture cells (A) Human Kank1 can be phosphorylated by Akt, which enables Kank to bind 14-3-3. This binding leads to inhibition of RhoA activation by 14-3-3. RhoA can therefore not activate mDia, which regulates actin polymerisation, and ROCK, which activates LIM kinase leading to inhibition of Cofilin – an actin depolymerising protein. (B) Human Kank1 can directly bind IRsP53, preventing IRsP53 from binding to and activated Rac1 and forming a complex with proteins from the WAVE and WASP family of actin regulators. This prevents actin polymerisation by the downstream effectors of WAVE/WASP thus inhibiting lamellipodia formation.

spectrin protein (McKeown et al., 1998), suggesting that VAB-19 and SMA-1 have antagonistic roles (Ding et al., 2003).

1.5.5 Kank May Affect Muscle Development in Humans

Cerebral Palsy is a disorder characterised by loss or deficiency in motor control, present from birth. Loss of Kank1 expression has been shown to cause familial cerebral palsy (Zlotogora et al., 2005). In the case examined, expression of Kank1 has been down-regulated however the exact mechanism through which this might occur remains unclear. In this report it is suggested that epigenetic changes in the promoter region of a nearby gene may affect Kank1 expression.

Congenital Fibrosis of the Extraocular Muscles Type 1 (CFEOM1) is a genetic disorder characterised by ophthalmolpegia, an inability to move the eyes. CFEOM1 has been associated with mutations in KIF21A, a plus-end directed kinesin motor. KIF21A was identified as a Kank binding protein in an immunoprecipitation assay (Kiyama et al., 2009). KIF21A was found to enhance Kank1 translocation to the membrane of cells examined. It is suggested that this translocation of Kank may play a role in the regulation of membrane outgrowth or cell migration, specifically during development. Interaction between Kank1 and KIF21A, along with the protein BIG1 (Brefeldin-A inhibited nuclear exchange 1), has been shown to maintain transport along microtubules during establishment of cell polarity in human hepatocytes and fibroblasts (Li et al., 2011).

1.5.6 Kank and Transcriptional Regulation

Kank family proteins contain the ‘KN motif’ (Zhu et al., 2008) which contains nuclear localisation and nuclear export signals. As previously mentioned, Kank1 has been shown to facilitate translocation of β-catenin from the cell periphery to the nucleus (Wang et al., 2006a). β-catenin is a well known transcription factor regulator, implying Kank1 may have an indirect role in gene expression under certain circumstances, which remain unknown. In addition, Kank2 has been shown to regulate transcription by sequestering steroid receptor co-activators to the cytoplasm (Zhang et al., 2007).

1.5.7 Kank in Drosophila Melanogaster

No studies have focused on the *Drosophila* orthologue of Kank1, hereafter referred to as KANK, which is the only Kank family orthologue present in *Drosophila.* KANK has, however, been identified in two screens and referred to by CG number only. Firstly, KANK was identified in a genome-wide RNAi screen for genes involved in neural outgrowth (Sepp et al., 2008). This screen indicated that KANK was expressed in primary neurons from gastrula stage embryos which were cultured *in vitro*. RNAi of KANK in these cells led to very mild effects on neuron development.

Secondly, KANK was recently identified as a target of the notch pathway. Specifically, KANK was found to be up-regulated in imaginal wing discs over-expressing the active domain of notch and thus displaying hyperplasia (Djiane et al., 2013).

A very recent paper has indicated that KANK may be expressed from stage 10 of embryogenesis and this expression is regulated by *single-minded (*Sim), a basic helix-loop-helix transcription factor (Hong et al., 2013). KANK has also been identified as a protein that is phosphorylated in S2 cells (Bodenmiller et al., 2007; Gnad et al., 2007) and embryos (Zhai et al., 2008) in large scale mass-spectrometry screens for phosphorylated proteins in *Drosophila.*

1.6 Formation of Embryonic Abdominal Muscles in *Drosophila Melanogaster*

1.6.1 Introduction

Muscle formation in *Drosophila* has been extensively studied over the years and much is known about the manner in which muscles are specified and develop (Bate, 1990; Miller, 1950). Muscle which is associated with internal organs and tracts is known as ‘smooth muscle or ‘visceral muscle’ while muscle associated with the body wall is referred to as ‘somatic muscle’.

Drosophila embryos become segmented during development, forming 9 abdominal segments referred to as a1-9 from anterior to posterior, 3 thoracic segments, t1-3 from anterior to posterior and the anterior head segment. For simplicity, we will focus on the highly similar abdominal segments, ignoring the

head and thoracic segments which have a slightly different topography of their somatic musculature. Abdominal segments a2-a7 contain identically patterned musculature (Figure 1.5), while a8/a9, where a9 is more commonly referred to as the telson, have a slightly altered form to accommodate the anal plate and spiracles and a1 accommodates the adjacent thorax. Each hemisegment in a2-a7 contains 30 individual muscles which are distinguishable based on their size, shape, location, attachment sites, number of nuclei and innervation. The muscles are arranged in three layers: external, intermediate and internal (Figure 1.6). *Drosophila* is a holometabolous organism that undergoes major morphological reconstruction during pupation. This section will briefly discuss some of the processes and pathways that contribute to the formation of *Drosophila* embryonic, and thus larval, somatic musculature.

1.6.2 Early Mesoderm Formation

The mesoderm is specified when Dorsal, expressed in a dorso-ventral gradient (Nüsslein-Volhard and Lohs-Schardin, 1980), induces the expression of the two basic helix-loop-helix transcription factors *twist* and *snail* in the ventral-most cells of the blastoderm (Leptin, 1991). These transcription factors are conserved and have similar functions in vertebrates (Hopwood et al., 1989; Sargent and Bennett, 1990; Smith et al., 1992; Wolf et al., 1991) and in *Drosophila* their expression is associated with the invagination of mesodermal cells along the ventral furrow, forming an epithelial tube during gastrulation (Seher et al., 2007). The mesodermal cells undergo epithelial-to-mesenchymal transition (EMT), losing their epithelial cell identity and instead becoming unpolarised and interacting with each other transiently via focal adhesion sites. The EMT allows for migration of the mesoderm and is closely followed by collapse of the mesodermal tube and the formation of a monolayer at stage 9 of embryogenesis.

After the monolayer has formed, mesodermal cells begin to migrate inwards and become segmented (Borkowski et al., 1995). Around stage 10 the arising layers of muscles, which will have diverse cell fates as somatic muscle, visceral muscle and the fat cell body of the organism, begin to differentiate. Around stage 11 of embryonic development the progenitors of future muscles become specified, the

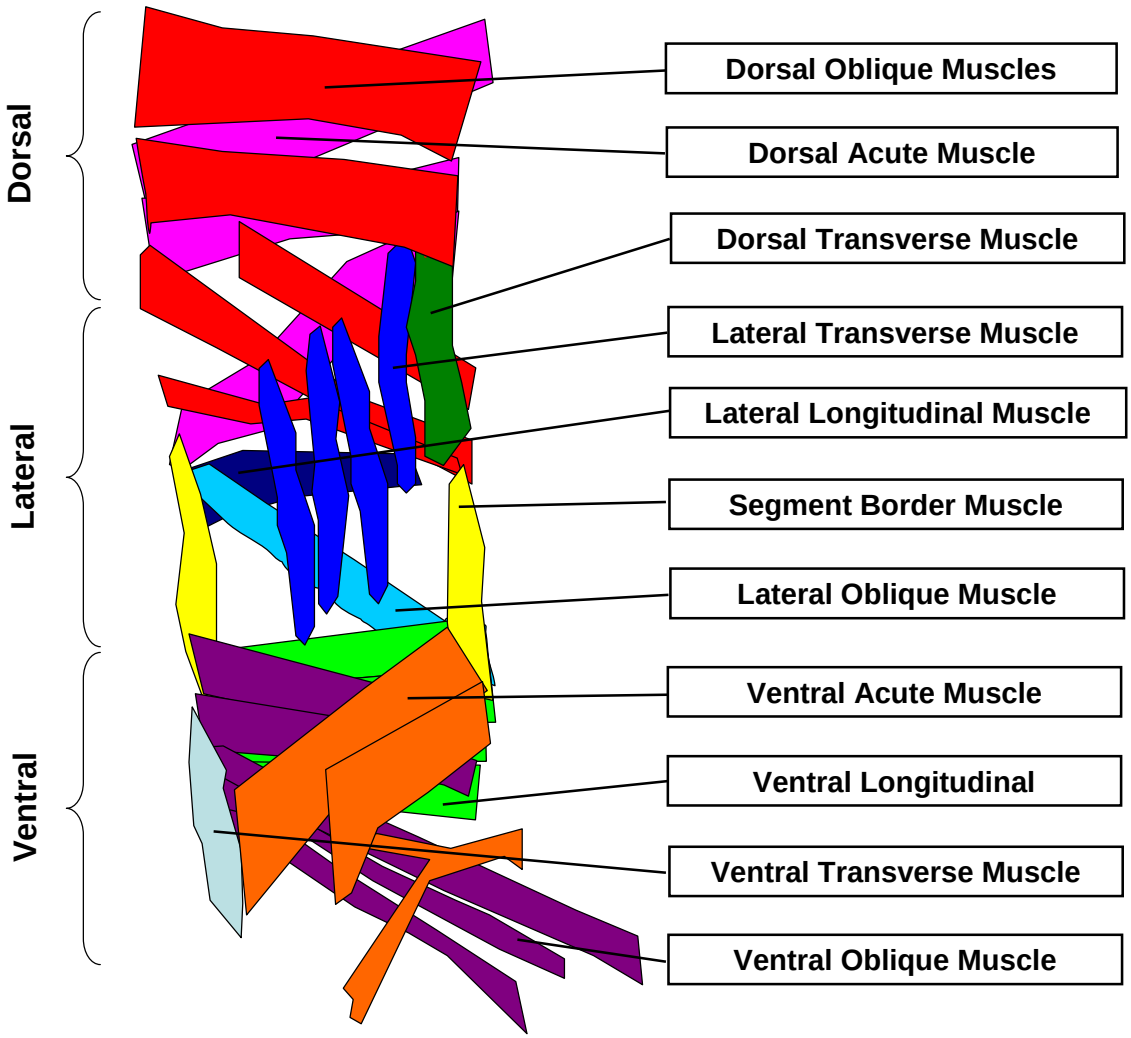

Figure 1.5 Muscle pattern of *Drosophila* embryo and larval abdominal segments a2-a7. Each hemisegment contains 30 individual muscles which are arranged in a repeating pattern and are individually distinguishable based on their size, shape, position and innervation. These muscles can be grouped based on location as outlined above. Adapted from Bate 1990

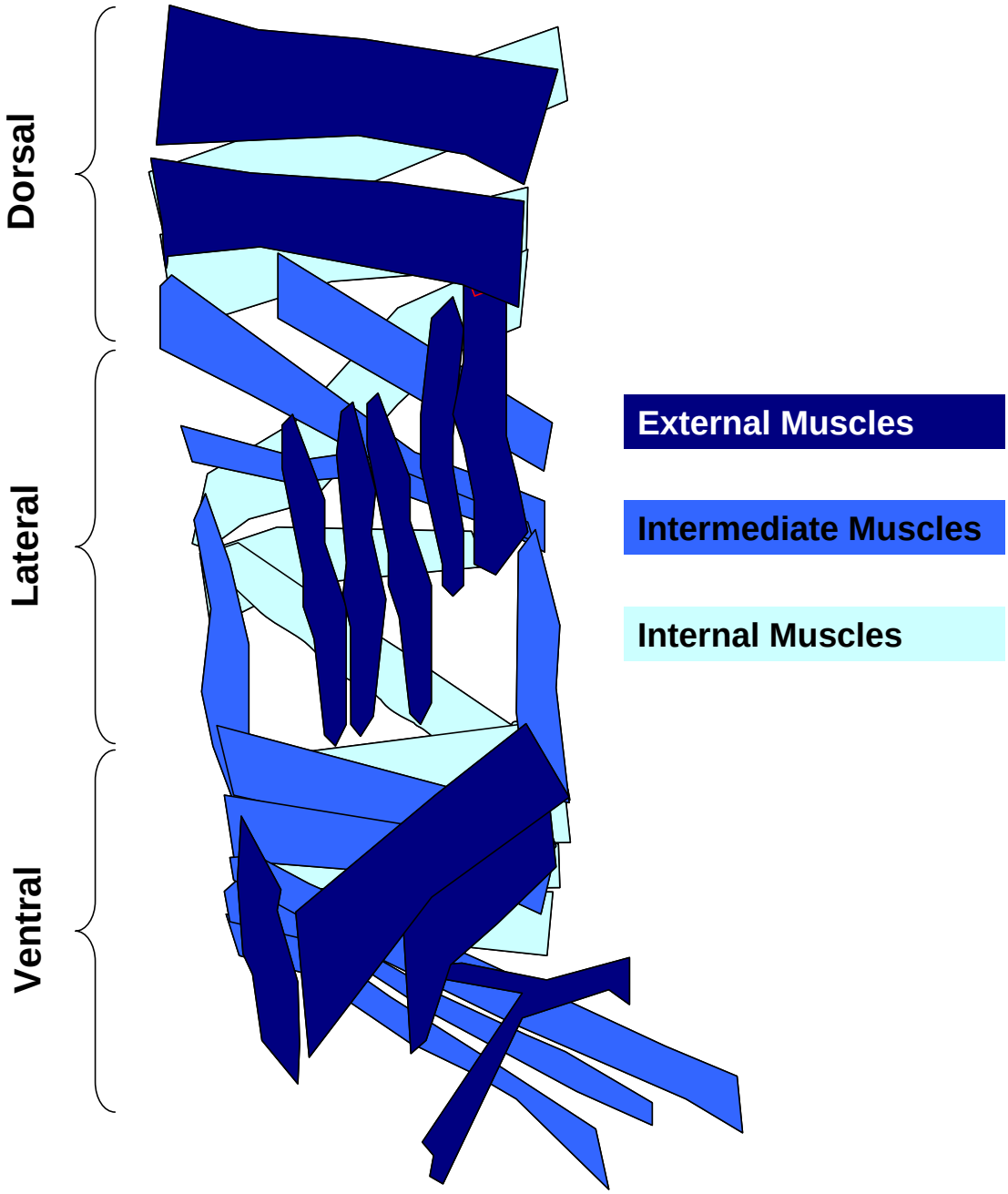

Figure 1.6 Muscle pattern of *Drosophila* embryo and larval abdominal segments a2-a7. Muscles lie in three layers: external, intermediate and internal. This diagram is based on Bate 1990.

mesodermal cells divide asymmetrically, controlled by lateral inhibition of Notch signalling to form two cell types, ‘founder cells’ and ‘fusion competent cells’. Between this stage and hatching the muscle fibres develop, grow and become innervated.

Each muscle fibre in a developed *Drosophila* embryo, and thus *Drosophila* larva, is a single, multinucleate cell. Muscle fibres form when multiple ‘fusion competent myoblasts’ fuse with a single ‘founder cell’. ‘Founder cells’ contain all the necessary information for muscle fibre growth. They are seeded at particular sites and their positioning determines the final pattern of somatic musculature (Ho et al., 1983; Rushton et al., 1995).

The developed muscle fibres form attachments with epidermal cells in the very late stages of embryogenesis. These points of attachment are known as myotendinous junctions.

1.6.3 The Myotendinous Junction

The myotendinous junction (MTJ) in *Drosophila* embryos is made up of extracellular matrix (ECM) proteins deposited at integrin mediated hemi-adherens junctions between epithelial tendon cells of epidermal origin and muscle fibres of mesodermal origin. A hemi-adherens junction is simply a junction between membrane and the surrounding ECM. In this way, ECM proteins physically connect the two cell types forming the junction. The MTJ functions in force generation and muscle contraction, leading to overall movement of the embryo.

The *Drosophila* integrin Myospheroid (βPS) was identified as a *Drosophila* homologue of vertebrate integrin β subunits (MacKrell et al., 1988; Leptin et al., 1989) and subsequently found to play a vital role in myogenesis during embryonic development (McMahon et al., 2010). βPS integrin is found on both the muscle and the tendon sides of the MTJ and is in a heterodimeric complex with one of two αPS integrins, leading to a difference in binding specificity for the two complexes. These integrins are αPS1 (also known as *multiple edematous wings-mew*) or αPS2 (also known as *inflated-if*)

The muscle-ECM hemi-adherens junction is composed of the αPS2βPS heterodimers which interacts with the ECM proteins Thrombospondin, Slowdown

and Tiggrin. Thrombospondin and Slowdown are secreted by tendon cells (Chanana et al., 2007; Gilsohn and Volk, 2010) and Tiggrin is secreted by muscle cells (Bunch et al., 1998). The tendon-ECM hemi-adherens junction is composed of αPS1βPS heterodimers which interact with Laminin in the ECM. Laminin is tendon-derived (Gotwals and Fessler, 1994).

1.6.4 Formation of the Myotendinous Junction

Tendon cell precursors are specified by expression of the tendon specific transcription factor *Stripe* (Hatini and DiNardo, 2001) which has been shown to be necessary and sufficient for expression of tendon specific genes (Frommer et al., 1996; Volk and VijayRaghavan, 1994). Stripe positively regulates its own expression and the expression of tendon specific genes, such as *Thrombospondin* (*Tsp*) (Chanana et al., 2007). Stripe activates the expression of signalling molecules to attract the developing muscle fibres to the tendon cells. For example, *slit* is expressed in tendon cells under the control of Stripe and, despite being known to generally act as a repulsive signal, it acts as a muscle attractant for some muscles expressing *Roundabout* (*Robo*) (Englund et al., 2002; Kramer et al., 2001).

Vein is a protein secreted by muscle cells which attracts developing tendon precursor cells and binds to EGFR on their surfaces (Yarnitzky et al., 1997). Binding of Vein to a tendon precursor cell sets off a cascade of signals which induces the cell to become a mature tendon cell including expression of some Stripe controlled genes such as *β1 tubulin*, *Delilah* and *Shot.* Tendon cell precursors which are not 'activated' in this way by Vein do not become mature tendon cells.

Moleskin, *Drosophila* importin-7, is a muscle specific nuclear import protein which is required for formation and maintenance of tendon cells at the MTJ as part of the Vein-Egfr signalling pathway in mature tendon cells (Liu and Geisbrecht, 2011). Stripe and MAPK are reduced in *msk* mutant embryos, which display muscle attachment defects. These defects can be rescued with Vein or activated MAPK implying that Moleskin acts upstream of these proteins to attract tendon cells and assist the formation of the MTJ.

1.7 Microtubule Organisation in *Drosophila* Embryonic Musculature and MTJs

In vertebrates, the integrin mediated hemi-adherens junctions of the MTJs are linked to the cytoskeleton via intermediate filaments. As *Drosophila* lack such cytoplasmic intermediate filaments it seems that microtubules play the part, assembling into arrays with the help of the spectraplakin *Shot.* These arrays stabilise the tendon cells. It has been shown that Shot recruits EB1 and APC to the MTJ (Subramanian et al., 2003) where EB1/APC may encourage assembly of the microtubule array in tendon cells and help stabilise the MTJ.

Although the +TIP EB1 is necessary for muscle formation in vertebrates (Zhang et al., 2009) there is no available information as to whether EB1 is required for muscle formation in invertebrates. Microtubule organisation in Drosophila embryonic musculature has not been particularly widely studied. It remains to be seen if the microtubule network of *Drosophila* muscle cells has a significant role in elongation during myogenesis. Studies of the *Drosophila* gene *spastin* found that over expression of Spastin in muscle cells led to dissolution of the tubulin network (Sherwood et al., 2004). This was, as expected, lethal. It has also been postulated, based on observed phenotypes, that β-1 tubulin (a maternally contributed protein) is required for microtubule formation during myogenesis and enables the muscles to form correctly – despite being undetectable by antibodies in these cells. However, surprisingly, β-3 tubulin, expressed in embryos, is dispensable for muscle formation (Rudolf et al., 2012).

1.8 Neuron Development in *Drosophila Melanogaster* Embryos

1.8.1 Introduction

Drosophila has a complex nervous system. Neurons in the abdomen of *Drosophila* embryos at stages 16/17 of development have a distinct stereotypic pattern which is repeated in each hemisegment, as is observed for the pattern of somatic musculature. Each hemisegment contains: a segmental motor nerve (SN) and an intersegmental muscle nerve (ISN), both of which extend dorsally from the ventrally located central nervous system (CNS) and project motor axons. Each segment also contains the

transverse nerve (TN) which is located along the border of the segment (Figure 1.7 B).

Neuron development occurs in three stages: Neurogenesis and migration, growth of axons, and synaptogenesis which includes formation of the neuromuscular junction and leads to innervation of the somatic musculature of the embryo. What follows is a brief description of neuron development in the *Drosophila* embryo.

1.8.2 Neurogenesis and Migration

Similar to myogenesis, the nervous system begins developing during gastrulation when a subset of the ventral ectoderm forms the neuroectoderm, from which the neural and glial precursors and sensory organ precursors originate (Prokop, 1999). It has been shown that presumptive neuroblasts, can express specific characteristics of their future lineages quite soon after gastrulation (Lüer and Technau, 2009).

Neuroblasts segregate from the ectoderm and divide to give rise to the final neuronal precursors: the mother ganglion cells. Neuroblast identity is temporally controlled as neuroblasts express a range of transcription factors sequentially and, after division, neuroblasts maintain the gene expression profile conferred to them at birth (Isshiki et al., 2001; Kanai et al., 2005). Mother ganglion cells complete their final division – becoming neurons – and at approximately stage 12, growth cones appear and axon extension begins. These neurons are closely associated, forming the ventral nerve chord (Prokop, 1999).

Drosophila sensory organs arise from single precursors (Bodmer et al., 1989). Sensory organ precursors remain in the ectoderm and migrate as the ectoderm migrates. They divide to form single neurons and accompanying sheath cells. The sensory organs grow towards the developing CNS, again beginning by sending out growth cones around stage 12 (Prokop, 1999).

1.8.3 Axon Extension and Pathfinding

Axon extension begins around stage 12 of embryogenesis and is complete by stage 16/17. Firstly, ‘pioneer’ axons extend, followed later in development by other neurons which use the pioneers for guidance. Developing axons have a highly dynamic, motile tip known as a growth cone that searches out the correct pathway in

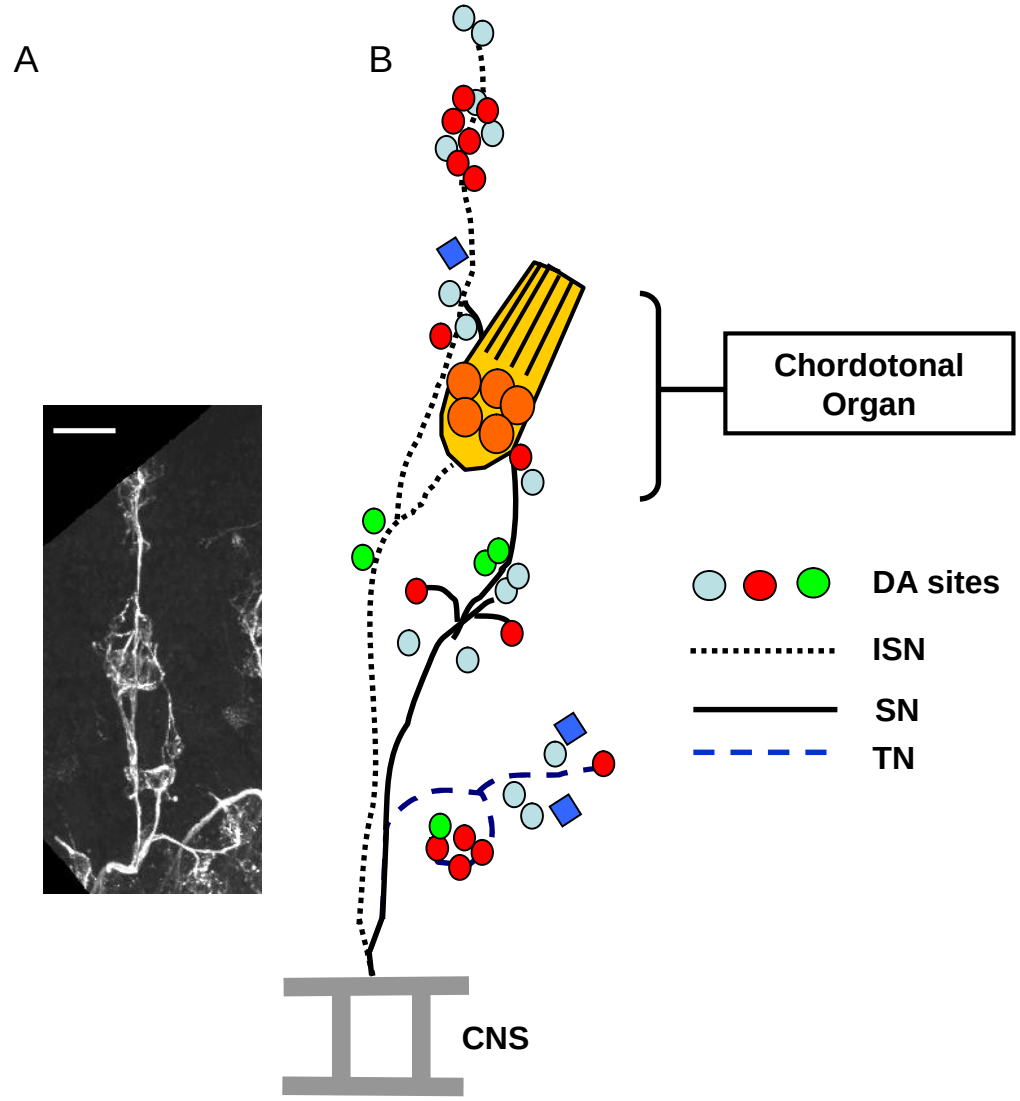

Figure 1.7 Neurons of the peripheral nervous system are arranged in a stereotypic pattern in *Drosophila embryo* abdominal segments. The neurons of the peripheral nervous system are patterned as shown in A and B. (A) shows the neurons of an abdominal hemisegment, stained with the 22c10 antibody which recognises a microtubule associated protein. The structure of the neurons are readily visible. Scale bar 40μm. (B) is a schematic of the neuron pattern in each hemisegment. The Intersegmental nerve (ISN-dashed line) and segmental nerve (SN-line) separate at the boundary of the central nervous system (CNS). The transverse nerve (TN) travels along the segmental border. The coloured circles represent the sites of dendritic arborization (DA), where dendrites and synapses form, making contact with the somatic musculature via the neuromuscular junction. The chordotonal organ, a mechanosensory structure, is also shown.

a process referred to as pathfinding. Growth cones were first observed by Santiago Ramòn y Cajal as amoeboid-like structures at the ends of developing neurons stained with silver chromate in chickens (Cajal, 1890). The growth cone has three basic functions; it is the motile device by which the axon extends, it acts as a sensor for external cues and alters its direction of motility in response to such cues to guide the growth of the axon.

The role of the cytoskeleton in the growth cone has been well studied (Bridgman and Dailey, 1989; Dent et al., 2011; Prokop et al., 2013) The growth cone resembles a poly-dactyl hand, where the fingers consist of actin filopodia and the inter-digital area is composed of actin lamellipodia (Figure 1.8). This F-actin rich region is known as the Peripheral domain (P domain). This is followed by the Central domain (C domain) which is microtubule rich and is the main site of microtubule polymerisation in the developing axon. The area which separates these two domains is known as the Transition zone (T zone) and contains many mitochondria and vesicles. Microtubules in this area are less stable than those in the axon and much less bundled, often curving. The C domain is followed by the axon wrist and the nascent axon, in which microtubule bundling and constriction of the axon occurs.

If attractant cues are present, such as *netrin-1* (de la Torre et al., 1997), microtubules can become stabilised in the P domain and interact with the cell membrane allowing for axon stabilisation. The P domain protrudes into the surrounding ECM during axon extension, driven forward by actin polymerisation (Forscher and Smith, 1988; Geraldo and Gordon-Weeks, 2009). F-actin in the C domain can affect microtubules, causing them to be less dynamic and to elongate more efficiently to enter the P domain (Schaefer et al., 2002). F-actin in the P domain can then act as a scaffold to which actin-microtubule crosslinking proteins such as spectraplakins bind (Applewhite et al., 2010; Bouquet and Nothias, 2007). The trailing ‘nascent axon’ is compressed by cortical actin rings once the route has been established

Signals which repel growth cones work in tandem with attractant cues to keep axons on their path. *Slit* is a well characterised molecule that acts in growth cone repulsion through interaction with Robo receptors present on the membrane of the growth cone (Bhat, 2005; Kidd et al., 1999; Parsons et al., 2003).

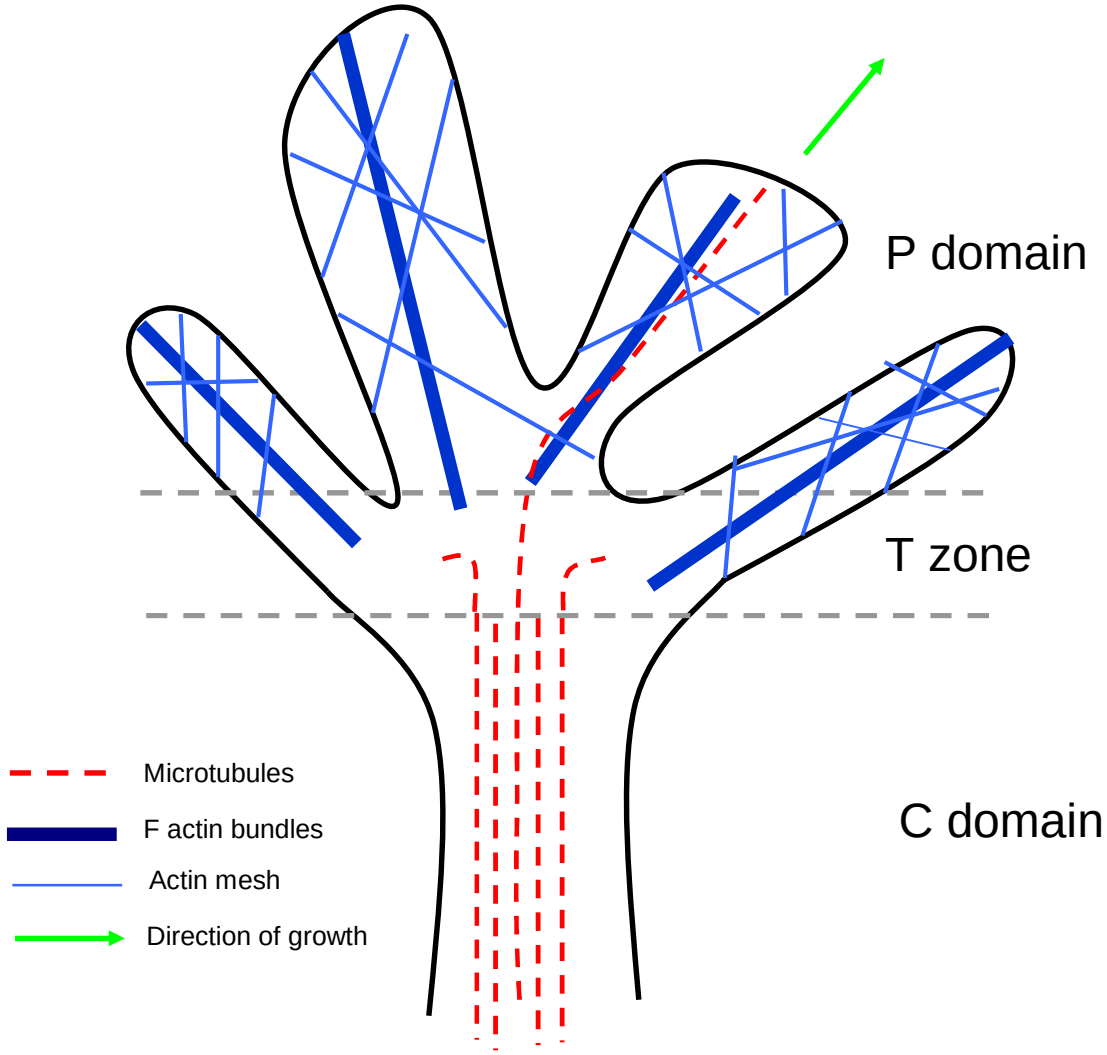

Figure 1.8 Developing axons have a highly dynamic, motile tip known as a growth cone. The growth cone has three regions: the microtubule rich C domain – in which stable microtubules grow, the intermediate T zone – into which microtubules grow, and the highly dynamic P domain – which is actin rich. Microtubules can extend from the C domain to the P domain and become stabilised, upon the growth cone receiving the correct guidance cues, to direct the developing axon in the correct direction.

When growth cones of motor axons make contact with somatic muscle cells, processes from the axon will begin to explore the surface of the muscle cell. Formation of synapses is triggered by interactions between adhesion molecules on these presynaptic (neuron) and postsynaptic (muscle) cells (Biederer and Stagi, 2008) leading to the formation of the glutamatergic neuromuscular junction (Halpern et al., 1989).

Meanwhile, developing glial cells express *reversed polarity* (*repo*) a nuclear transcription factor that is glial cell specific (Xiong et al., 1994). Glia, among other functions, act as 'scouts' for the developing axons thus directing axonal targeting (Pielage and Klämbt, 2001; Sepp et al., 2000).

1.9 The Role of EB1 in Neuron Development

EB1 is a vital +TIP, through which many other +TIPs function (see Section 1.3). The function of EB1 and some of its interactors are necessary for axonogenesis. The importance of EB1 in axonogenesis has been demonstrated in several ways. MAP1B sequesters EB1 in the cytosol during axonogenesis in mouse neuroblastoma cells leading to a delay in axon outgrowth (Tortosa et al., 2013).

Hypomorphic *EB1* mutant *Drosophila* display neuromuscular defects and malformed chordotonal organs (Elliott et al., 2005) indicating that EB1 is required for neuron development in *Drosophila*. The *Drosophila* spectraplakin *Shot* is a +TIP which functions to stabilise microtubules and to guide microtubules in the direction of axon growth. *Shot* requires EB1 to localise along F-actin tracks in growth cones (Alves-Silva et al., 2012). EB1 also has further functions in axonogenesis, as it is required, with the kinesin KIF3, for the targeting of K^+ voltage gated channels to the axon membrane (Gu et al., 2006).

1.10 Drosophila as a Model Organism

Drosophila is a model organism known for its dichotomous complexity as a multicellular animal and its simplicity of use in the laboratory. The widespread use of *Drosophila* in genetic and developmental laboratories, and as a teaching tool for genetics, is due to practical as well as historical reasons.

Drosophila is a practical animal to keep. The flies are small, cheap, easily cultured and require very basic food. They have short lifecycles of about two weeks and are extremely fecund, particularly when compared to mammals. *Drosophila* has four pairs of chromosomes, one pair of sex chromosomes and three pairs of autosomes. This is much simpler than a mammalian system such as humans with twenty three pairs, mice with twenty pairs or *C. elegans* which has 11/12 depending on gender. *Drosophila* also has a lifecycle stage where many rounds of DNA replication are not followed by cell division (endoreduplication), leading to giant polytene chromosomes which can be observed under a reasonably low magnification. Historically, this polytene chromosome made DNA easily visible to scientists before more modern staining techniques were available. These natural attributes make *Drosophila* a good organism for use in genetic studies and has contributed to their historical significance in biology in the first half of the 20th century.

The laboratory of Thomas Hunt Morgan at Colombia University took *Drosophila* as their organism of choice. Over the course of approximately a decade this laboratory, relying on acute observation and spontaneous mutations, developed many of the basic concepts of genetics we take for granted today. Papers they produced gave evidence for: chromosomes as the location of genes (Morgan and Lynch, 1912; Muller, 1914; Sturtevant, 1913), non-disjunction (Bridges, 1913), chromosome recombination (Morgan, 1911), the concept of the balanced lethal system for maintenance of mutations – which would later lead to balancer chromosomes (Muller, 1918), and proof that recombination does not occur in male *Drosophila* (Morgan, 1914).

In the 1930s it was observed that polytene chromosomes displayed a clear banding pattern which led to the physical mapping of genes. Theophilus S. Painter is credited with realising the importance of these bands and attributing chromosomal localisation of several genes (Painter, 1934), which was quickly followed by detailed polytene maps of great accuracy (C. B. Bridges, 1935). These studies contributed to cementing *Drosophila* as an invaluable organism for cytogenetic studies.

In the second half of the 20th century the foundations for the use of *Drosophila* as a model organism were built upon and its usefulness was extended to other fields, particularly developmental biology. Nüsslein-Volhard and Wieschaus

examined the effects of gene mutations on morphological development of the *Drosophila* embryo, leading to the discovery of segmentation genes (Nüsslein-Volhard and Wieschaus, 1980) and later, a Nobel prize. Meanwhile the discovery of HOX (homeobox) genes was through experimentation in *Drosophila* that established *Bithorax* and *Antennapedia* as essential for *Drosophila* development, genes which were subsequently found to be highly conserved in other organisms (McGinnis et al., 1984).

In more recent times the *Drosophila* genome has been sequenced and annotated, an invaluable tool in genetic research (Adams, 2000; Misra et al., 2002; Oliver and Leblanc, 2003). This has allowed for the creation of vast databases where information on individual genes can be collated and easily accessed, for example FlyBase (http://flybase.org)(St Pierre et al., 2014). This has allowed us to compare *Drosophila* to other animals, such as humans and though both organisms differ in gene number and are morphologically very distinct, of the genes identified in humans which lead to disease 75% are thought to have functional homologues in *Drosophila* (Reiter et al., 2001). *Drosophila* models of human diseases such as neurodegenerative disorders, diabetes, metabolic disorders and cancer are now well established (Pandey and Nichols, 2011).

With regards to this project, *Drosophila* has several advantages over the models which have been used to collect data thus far. The *Drosophila* genome, for example, contains one *kank* gene unlike humans which contain four (Kank1-4). This makes studying the overall function of the protein much simpler and reduces, though does not abolish, the risk of functional redundancy in deletion experiments.

By using *Drosophila*, there is the opportunity to study the protein in a multicellular animal, in natural conditions. So far, data on Kank family proteins has depended mainly on human tumour cell lines and other mammalian cell culture lines. Although these represent a good system for studying the protein in the context of cancer, often cell culture lines can have genetic alterations which can make them unrepresentative of an *in vivo* situation. As Kank proteins have so far demonstrated roles in cell growth and cytoskeletal regulation, a multicellular context may be more helpful in elucidating precise functions. Notably, work in *C. elegans* using temperature sensitive mutants and RNAi has been invaluable in demonstrating

developmental roles for VAB-19 and thus the advantage of using a multicellular system (Ding et al., 2003b; Ihara et al., 2011).

Techniques in targeted insertion and targeted deletion have been refined over the last decade making genetic manipulation in *Drosophila* less cumbersome than it once was (Bateman et al., 2006; Thibault et al., 2004) and tools for RNAi in whole flies have been developed and improved (Dietzl et al., 2007; Ni et al., 2011). Moreover, *Drosophila* cultured cells can be utilised to examine localisation in single cells and for techniques such as RNAi (Goshima and Vale, 2003) which may help uncover some of the functional roles of KANK and can be later confirmed in the context of the multicellular organism.

In conclusion, *Drosophila* is practically and historically an important and useful model organism for which, versatile methods and techniques have been established. They are particularly suited to this project because of the tools available and their adaptability as a model for studying the role of KANK.

1.11 Aims of this Project

The conserved *Drosophila* KANK protein was identified in the laboratory of Hiro Ohkura as an EB1 binding protein. A review of the literature indicates that this protein may have an important developmental role in humans as well as acting as a tumour suppressor and also has a role in the development of *C. elegans.* However, the data available does give any indication of the function of the KANK-EB1 interaction nor satisfactorily define a cellular role for KANK. Therefore, it is my intention to determine the function of KANK in *Drosophila* and to determine its cellular role with respect to its EB1 interaction.

Firstly, I aim to determine if the KANK-EB1 binding occurs in *Drosophila* cells and if so, which regions of KANK are responsible. Secondly, I aim to localise the protein in cultured cells and in the whole organism. Localisation of the protein will be paramount to determining its function. Finally, I aim to determine if *Drosophila* KANK is differentially expressed throughout the *Drosophila* life-cycle and if so, how this expression affects development. There is evidence from studies in humans and *C. elegans* for a developmental role for KANK (Ding et al., 2003a;

Lerer et al., 2005; Roy et al., 2009). It will be interesting to see if this is also the case in *Drosophila* and to determine if KANK is required for normal development.

Chapter 2

Materials and Methods

2.1 Chemical Reagents

All Chemical Reagents used, unless otherwise stated, were analytical grade and obtained from Fisher Scientific, Invitrogen and Sigma.

2.2 Buffers

Standard buffers and stock solutions were used (Sambrook et al., 1989).

2.3 Enzymes

Restriction enzymes used were supplied by New England Biolabs and Promega. PrimeSTAR (Takara) was used for any cloning PCR while Taq DNA Polymerase (Roche) was used elsewhere.

2.4 PCR Primers

All PCR primers were supplied by MWG-Biotech.

2.5 Antibodies

All primary and secondary antibodies used for immunoblotting or immunofluorescence staining are listed, with their typical dilutions in Table 2.1.

2.6 Bacteria, *Drosophila* Cell Lines And Fly Strains

The following *E. coli* strains were used for DNA cloning and protein expression (Invitrogen)

BL21(DE3) pLysS : F^- *ompT hsdS*($r_B^- m_B^-$)*gal dcm* (DE3) pLysS (Cam^R)

One Shot® TOP10: F^- *mcr*A Δ(*mrr-hsd*RMS-*mcr*BC) φ80*lac*ZΔM15 Δ*lac*X74 *rec*A1 *ara*D139 Δ(*ara-leu*) 7697 *gal*U *gal*K *rps*L (Str^R) *end*A1 *nup*G λ-

Drosophila Schneider 2 cell line (S2) was used for immunolocalisation and dsRNAi. *Drosophila melanogaster* strains used are listed in Table 2.2.

Primary Antibodies	Secondary Antibodies	Dilution for Immunoblotting	Dilution for Immunofluorescence	
			S2 cells*	Embryos
Rb-α-KANK(525-924)[1]		1:100	1:20	1:500
Rat-α-KANK(525-924) [1]		1:100		
Rb-α-KANK(925-1224) [1]		1:100		
Rat-α-KANK(925-1224) [1]		1:100		
Rb-α-GFP[2]		1:500	1:500	
Mouse-α-GFP[2]			1:500	
Mouse-α-alpha-tubulin[3]			1:250	
Rb-α-EB1[4]			1:200	
Mouse-α-futsch[5]				1:500
Mouse-β-Actin[6]				1:500
	α- Rb; α-Mouse; -Cy3	1:500	1:1000	1:1000
	α-Rb; α-Mouse; -Alexafluor 488	1:500	1:1000	1:1000
	α-Rb; α-Rat – HRP	1:1000		

Table 2.1 Dilutions of Antibodies Used.

References:
1: This work
2: Life Technologies
3: (α-alpha Tubulin [DM1A] antibody) Sigma-Aldrich
4: (Elliott et al., 2005)
5: (22c10) Developmental Studies Hybridoma Bank
6: Sigma-Aldrich

Fly Strain Genotype	Reference
w[1118]	BDSC
y[1] w[*]; [Sco]/CyO [y+]	BDSC
w[1118]; Df(2R)ED2423/SM6a	DGRC
y[*] w[*]; P{GawB}NP6204 / CyO, P{UAS-lacZ.UW14}UW14	DGRC
w[1118]; P{GD6584}v15009	VDRC
wg[Sp-1]/CyO; ry[506] Sb[1] P{ry[+t7.2]=Delta2-3}99B/TM6	BDSC
w[1118]; PBac{w[+mC]=WH}CG10249[f01478]/CyO	BDSC
w[1118]; PBac{w[+mC]=WH}CG10249[c00393]	BDSC
P{UAS-Dcr-2.D}1, w[1118]; Pin[1]/CyO	BDSC
y[1] w[*]; P{w[+mC]=Act5C-GAL4}25FO1/CyO, y[+]	BDSC
y[1] w[*]; P{w[+mC]=Act5C-GAL4}17bFO1/TM6B, Tb[1]	BDSC

Table 2.2 Fly strain genotypes
References: BDSC: Bloomington *Drosophila* Strain Centre
DGRC: *Drosophila* Genetic Resource Centre
VDRC: Vienna *Drosophila* RNAi Centre

2.7 Media For Bacterial, Cell Culture And Fly Growth

The bacterial and fly media were graciously prepared by the University of Edinburgh ICMB kitchen staff. LB medium (1% w/v bacto-tryptone; 0.5% w/v yeast extract; 0.1% w/v glucose; 1% w/v NaCl) and LB-agar plates, supplemented with the appropriate antibiotics were used for bacterial cultures (Sambrook et al., 1989). S2 cells were cultured in Schneider's medium (Gibco) supplemented with 10% heat inactivated Foetal Calf Serum (Gibco). Flies were grown on standard yeast-cornmeal agar medium (Ashburner, 1989).

2.8 *Drosophila* Techniques

Standard *Drosophila* handling techniques were used (Ashburner, 1989). *Drosophila* were grown and maintained at 25°C while stocks were maintained at 18°C.

2.8.1 RNAi in Adult Flies and Embryos

RNAi was performed by introducing an Act5c-GAL4 driver into a background containing an insert expressing dsRNA under a UAS promoter. A strain from the Vienna Drosophila RNAi Centre with an insert expressing 400bp hairpin RNA was used to perform RNAi in adult flies. A strain from the Drosophila RNAi Screening centre expressing a 40bp hairpin RNA was used to perform RNAi in embryos.

2.8.2 P-element Remobilisation

P-element remobilisation was performed by introducing a transposase gene into the P-element background according to the crossing scheme detailed in Figure 3.X. The P[NP6204] line was crossed to the Δ2-3 transposase source. Jumpstarter males from the progeny were crossed to balancer females. Males with a balanced excision were then crossed to deficiency flies, containing a deletion which uncovered the gene region corresponding to the excision. Resulting progeny were examined by PCR to determine the extent of the excision.

2.8.3 Generation of a Synthetic Deletion

A synthetic deletion was generated within the *kank* gene region using *piggyBac* transposons which contain FRT sites. A heat inducible flippase, on the X chromosome, was introduced to a strain containing PBac{PB}c00393. Male progeny from this cross were then crossed with females containing PBac{WH}f01478.

Fertilised adult females were incubated at 37°C for 1 hour. Female progeny were then crossed with males which contained a balancer, to maintain possible deletions. Recombination between the transposons which results in a deletion leads to elimination of the w^+. Progeny with balanced deletions can be identified by the white eye phenotype. Male progeny with balanced deletions were crossed were crossed with female progeny containing balanced deletions. A balanced stock was established and male flies with homozygous deletions were examined by PCR to confirm deletion of the gene region.

2.8.4 Transformation of Drosophila

Drosophila transformations were performed by Genetic Services Inc. Briefly, 30-50µg of purified the BAC plasmid CH322-155 P17 was purified from Qiagen midiprep kit and used for germline transformation.

2.9 DNA Techniques

2.9.1 DNA Purification

Unless otherwise stated, plasmid DNA was purified from *E. coli* using the Wizard® Plus SV Miniprep Kit (Promega) and the QIAprep Spin Midiprep Kit (QIAGEN) according to the manufacturer's protocol. PCR products were purified using the QIAquick PCR purification Kit (QIAGEN) according to the manufacturer's protocol. DNA purification from agarose gels was performed using QIAquick Gel Extraction Kit (QIAGEN) according to the manufacturer's protocol.

2.9.2 Preparation of Drosophila Adult Genomic DNA

Drosophila adult genomic DNA was prepared by homogenising 1 adult male fly in 40µl homogenisation buffer (10mM Tris; 1mM EDTA pH8; 25mM NaCl; 200µg/ml Proteinase K) The Proteinase K (Roche) was added freshly prior to use of buffer. The homogenate was incubated at 37°C for 30minutes followed by 95°C for 1 minute. 1µl was used for each PCR reaction.

2.9.3 Agarose Gel DNA Electrophoresis

DNA fragments were separated on 0.7% agarose gels. The gels were prepared by boiling agarose (Cambrex) in TAE buffer (40mM Tris; 20MM acetic acid; 1mM

EDTA pH8) until it was dissolved. Ethidium bromide was added at a final concentration of 0.5µg/ml for visualisation of the DNA under UV light on a transilluminator (Herolab UVT-28M). Images were recorded with a digital camera (Herolab E.A.S.Y. 429K) HyperLadder^{TM} 1kb was used as a standard size marker.

2.9.4 Sequencing

Cycle sequencing was performed using BigDye Terminator v3.1 (ABH PRISM) in a Hybaid PCR Thermal cycler. The following programme was used

96°C	30 sec	
50°C	15 sec	X 25
60°C	4min	

2.9.5 Site-Directed Mutagenesis

Site-directed mutagenesis was carried out using the QuikChange XL Site Directed Mutagenesis Kit (Stratagene). To mutate the EB1 binding motif in KANK (SectionX) two single nucleotide substitutions were introduced. To change amino acid 764 (I→N) nucleotide 2339 of GH03482 was mutated (T→A) using the following primer pair:

5' – CGGCGGACTCGAGAAATCCGCGACCCAAGC – 3'

5' – GCTTGGGTCGCGGATTTCTCGAGTCCGCCG – 3'

To change amino acid 765 (P→K) nucleotides 2341 and 2342 of GH03482 were mutated (CC→AA) using the following primer pair:

5' – CCGTCGGACTCGAGAAATAAGCGACCCAAGCACCTC – 3'

5' – GAGGTGCTTGGGTCGCTTATTTCTCGAGTCCGACGG – 3'

2.9.6 DNA Cloning

Standard DNA cloning techniques were followed (Sambrook et al., 1989). Insert fragments were prepared from plasmid or PCR-amplified DNA by digestion with appropriate restriction endonucleases followed by separation on an agarose gel

2.10 Protein Techniques

2.10.1 SDS-Polyacrylamide Gel Electrophoresis (SDS-PAGE)

Proteins were analysed by standard discontinuous SDS-PAGE (Sambrook et al., 1989). Resolving gels with 8%, 10% and 12% acrylamide concentrations and a 5% stacking gel were assembled using the Mini-PROTEAN II (BioRad) system. Protein samples were prepared by boiling for 3 minutes in 2X sample buffer (100mM Tris pH6.8, 4% SDS, 20% glycerol, 0.2% bromophenol blue) supplemented with 5% β-mercaptoethanol. Gels were run using SDS-running buffer (25mM Tris, 250mM glycine, 0.1% SDS) at 100-200V until the desired separation was reached. Separation was judged by the separation of protein bands on the standard protein marker. Prestained Protein Marker (Broad Range, New England Biolabs) was used for proteins over 160 kDa and PageRuler Prestained Protein Ladder (Thermo Scientific) was used for other proteins. To visualise separated proteins, gels were stained with Bio-Safe Coomassie (BioRad) according to the manufacturer's instructions.

2.10.2 Immunoblotting

Gels were sandwiched with nitrocellulose membrane (Whatman) between two filter papers and assembled, with an ice cooling unit, into the Mini-Trans Blot cell (BioRad) according to the manufacturer's instructions. The transfer was performed in transfer buffer (25mM Tris, 250mM glycine) at 100V for 30 minutes. The success of the transfer was monitored by membrane staining using a reversible protein stain kit (Thermo Scientific) according to the manufacturer's instructions. The membrane was washed in washing solution of 0.08% Tween 20 in PBS (137mM NaCl, 2.7mM KCl, 4.3mM Na_2HPO_4, 1.4mM KH_2PO_4 pH 7.5) and then blocked in blocking solution (washing solution with 3% non-fat milk powder) for 1 hour. The membrane was incubated in primary antibody diluted in blocking solution (see Table 2.1 for dilutions) overnight. Three 15 minute washes with washing solution were followed by a one hour long incubation with the horseradish-peroxidise conjugated secondary antibody in blocking solution. After 3 more washes, the membrane was covered with the ECL reagent (Amersham) for 1 minute and exposed to Hyperfilm ECL chemiluminescent film (Amersham) for 5seconds-10 minutes. The film was developed using a SRX-101A developer.

2.10.3 Expression and Purification of Recombinant Proteins

GST and MBP labelled KANK proteins were expressed in the BL21 strain (Invitrogen) of *E. coli*. Bacteria were grown in LB medium with the appropriate antibiotics at 37°C overnight. After a 1/100 dilution in fresh medium, culturing was continued until OD_{600} reached ~0.5 which typically took 1.5-2 hours. Expression was induced with 1mM IPTG for 4 hours at 37°C. Solubility at 18°C was also determined, though the proteins used were from bacteria cultured at 37°C. Bacteria were collected by centrifugation and resuspended in 2ml PBS prior to storage at -20°C. Bacterial pellets in 2ml PBS were further suspended in ice-cold washing buffer (PBS, 1% Triton-X100 Complete EDTA-free Protease Inhibitor cocktail (Roche), 0.001% PMSF) and lysed by sonication. Insoluble material was cleared by centrifugation at 14000 rpm, 4°C.

To purify soluble proteins, in this case MBP-KANK(489-900), the soluble fraction was then applied to an amylose column (New England Biolabs) and washed with 30ml PBS. The protein was eluted from the column in three stages using 2ml PBS supplemented with 10mM maltose. The first eluant was obtained after a 10 minute room temperature incubation of the column in the maltose solution. The second eluant was obtained after an overnight incubation of the column at 4°C. The final elution was a 10 minute room temperature incubation.

To purify insoluble proteins, in this case GST-KANK(889-1224), the insoluble pellet was resuspended in 5ml PBS supplemented with 0.5% Triton X-100 and incubated at room temperature for 30 minutes after which the sample was centrifuged at 13000 rpm for 5 minutes. This process was repeated for the pellets obtained from this centrifugation. The remaining pellet was resuspended in 0.5ml PBS and 0.5ml 2 XSB was added. 5% β-mercaptoethanol was added and the sample boiled at 95°C for 5 minutes. The protein sample was run on a large (15 x 21cm) SDS-PAGE gel assembled in a TE42 large gel rig (Hoefer Pharmaci Biotech). The large protein band was cut from the SDS-gel and crushed between 2 pieces of glass. The crushed gel was added to a solution of 0.2M $NaHCO_3$ and 0.2% SDS and was incubated overnight at 37°C. The following day the sample was spun at 13000 rpm for 1 minute. The supernatant was collected while the pellet was filtered using a 5ml syringe and a syringe filter (Millipore), and the filtered solution added to the supernatant. The sample was then purified using an Amicon Ultra-4 centrifugal filter

unit (Millipore) centrifuged at 6000 rpm for 10 minutes at room temperature. Protein purification and concentration was determined by SDS-PAGE.

2.10.4 Antibody Production and Affinity Purification

A rat and rabbit antibodies were raised to GST-KANK(925-1224) and MBP-KANK(525-924) by Scottish National Blood Transfusion Service in the following way: Purified proteins (250µg for immunisation of rabbits and 100µg for immunisation of rats) were injected at regular intervals. Animals were bled prior to first immunisation (pre-immune sera) and one week after each immunisation, apart from the first one. The final third bleed from each antibody was used for antibody purification by a method using antigen immobilised on nitrocellulose membrane (Smith and Fisher, 1984). ~20µg of purified antigen was run on an SDS gel and transferred onto a nitrocellulose membrane as described in Section 2.10.2. The membrane was stained with Ponceau S (1g Ponceau S + 1ml acetic acid + 98ml H_2O) and the band of antigen excised. The band was washed and blocked as previously described. The antibody was then bound to the antigen by incubating the membrane in 100µl of the final antiserum diluted 1:10 in blocking solution overnight at 4°C. After extensive washes in washing buffer, the antibody was eluted by three, consecutive 30 second washes with 400µl elution buffer (50mM glycine-HCl pH2.3, 0.5M NaCl, 0.5% Tween 20, 100µg/µl BSA, 0.1% NaN_3). All of the eluates were combined and immediately neutralised by adding Na_2HPO_4 solution to a final concentration of 50mM. The affinity purified antibodies were tested for specificity and optimal dilution in immunoblotting and immunofluorescence experiments. Antibodies were stored at 4°C.

2.10.5 Preparation of Protein Samples From Drosophila

2.10.5.1 Adults

Male and female flies were always prepared as separate protein samples. Two adult flies were frozen for 30 minutes, after which 95µl dH_20 was added and the samples boiled for 3 minutes at 98°C. 95µl of 2xSDS was then added and flies were homogenised using a pestle. 10µl β-mercaptoethanol was added and the samples and they were then boiled for 3 minutes at 98°C, after which they were spun at 13000rpm for 2 minutes. 10µl of protein sample, equating to $1/10^{th}$ of an adult fly, was run per SDS gel lane. Protein samples were stored at -20°C.

2.10.5.2 Pupae

Male and female pharate pupae were prepared as separate protein samples. This was not possible for early pupae. Pupae were prepared as described for adult flies.

2.10.5.3 Larvae

Larvae were prepared as described for adult flies.

2.10.5.4 Embryos

Adult flies were left to lay on grape plates, after which the embryos were aged to the desired age. 100 embryos were collected in 45µl dH_2O. Samples were boiled for 3 minutes at 98°C after which 50µl 2xSDS was added and the embryos homogenised. 5µl β-mercaptoethanol was added and the samples boiled for 3 minutes at 98°C. 20µl of protein samples, equating to 20 embryos, was run per SDS gel lane. Protein samples were stored at -20°C.

2.10.6 In Vitro Pull-Down Assay

MBP-EB1 and MBP alone (as a control) were expressed from pND30 and pAS01 (obtained from Nick Dzhindzhev and Ana Meireles Sousa respectively), purified and bound to amylose beads as follows: Lysates from bacteria expressing MBP-EB1 and MBP were incubated for 1 hour at 4°C amylose beads. After washing three times in PBS with 0.1% TritonX-100, the beads were incubated in *in vitro* pulldown buffer (50 mM HEPES, pH 7.5, 1mM EGTA, 1mM $MgCl_2$, 0.5% Triton X-100, 200mM NaCl, supplemented with 0.5mg/ml BSA). A known amount of beads was run on an SDS gel, alongside protein standards of known concentration, to determine the concentration of protein bound to the amylose beads. KANK, KANK(1-524), KANK(525-924), KANK(925-1224), KANK(1-924), and KANK(525-1224) were expressed *in vitro* using the TNT Quick Coupled Transcription/Translation system from (Promega) according to the manufacturer's instructions. The expressed proteins were radioactively labelled during translation through addition of S^{35} methionine to the mix. Radiolabelled protein fractions were split, $1/5^{th}$ was reserved as input. $2/5^{th}$ was added to beads coupled to 200µg MBP. $2/5^{th}$ was added to beads coupled to 200µg MBP-EB1. Prior to use beads were washed in x2 in BSA-free *in vitro* pulldown buffer, followed by resuspension in 100µl *in vitro* pulldown buffer supplemented with 0.5mg/ml BSA.

The beads with the radiolabelled proteins were incubated for 1 hour at room temperature, after which the beads were washed x5 in *in vitro* pulldown buffer, followed by a final resuspension in 10µl H_2O, 12.5µl 2xSDS and 2.5µl β-mercaptoethanol. The input was also prepared as a protein sample. All samples were boiled at 95°C and run on an SDS-gel. The gel was dried using a Slab Gel Dryer GD 2000 (Hoefer), exposed to autoradiograph paper and developed.

2.11 *Drosophila* S2 Cell Culture

Drosophila S2 cells were cultured in Schneider's Insect Medium (Sigma) supplemented with 10% heat-inactivated FBS (Gibco) in a humidified incubator at 27°C. Cells were diluted 1:10 in fresh medium every 7 days.

2.12 Transfection of *Drosophila* S2 Cells

Transfection of S2 cells was performed using the Effectene Transfection Reagent (Qiagen) according to the manufacturer's instructions. Typically 0.4µg DNA was used for 1.6ml of cell culture at 1-3.5 x 10^6 cell/ml. Cells were incubated for 24 and 48 hours, fixed, stained and analysed by microscopy.

2.13 Immunostaining of S2 Cells

S2 cells were prepared for immunofluorescence analysis by plating onto concanavalin A (con A) coated coverslips.

2.13.1 Preparation of Con A-Treated Coverslips

Coverslips (1mm thick, VWR International) were washed 3 x 5 minutes with dH_2O, treated with 0.5M HCl for 30 minutes, washed 3 x 5 minutes with dH_2O, and treated with 100% ethanol for 30 minutes. After allowing to air dry, the coverslips were coated with 0.5mg/ml con A (Calbiochem) solution and allowed to air-dry again. Coverslips were stored at 4°C.

2.13.2 Immunostaining Procedure

Cells were diluted to 3-6 x 10^5 cells/ml with Schneider's medium + 10% FBS and plated onto the Con A coverslips for 2.5-3hours. Cells were then fixed in cold methanol/formaldehyde mix (90% methanol, 3% formaldehyde, 5mM Na_2CO_3 pH9, pre-chilled in dry ice for a minimum of 30 minutes). 3ml of fixative was used per

coverslip. Coverslips were immediately placed in dry ice for 15 minutes, followed by 15 minutes at room temperature. The coverslips were then rinsed twice with washing buffer (0.1% Triton x-100 in PBS), blocked in blocking solution (10% FBS in washing buffer) for 1 hour and incubated with the primary antibodies diluted in blocking buffer (for dilutions used see table X.X) for 1 hour. After 3 x 5 minute washes with washing buffer, the coverslips were incubated with secondary antibodies diluted with washing buffer for 1 hour. Three x 5 minute washes were followed by a 10 minute incubation with 0.4µg/µl DAPI diluted in washing buffer for DNA staining. Coverslips were finally washed in washing buffer followed by a wash in PBS and then mounted onto slides with mounting medium (2.5% propyl gallate, 85% glycerol). Cells were visualised with an Axioplan-2 fluorescent microscope (Zeiss) and images were recorded with an attached CCD camera (Hamamatsu), controlled by OpenLab 2.2.1 software (Improvision). Images were processed using ImageJ.

2.14 dsRNA Interference on S2 Cells

2.14.1 Generation of dsRNA

The dsRNA required for RNA silencing in S2 cells was generated by two rounds of PCR, followed by *in vitro* transcription reaction. In the first round of PCR a specific exon sequence of *EB1* was amplified from pND30 (obtained from Nick Dzhindzhev) using the following primers

5' – CGACTCACTATAGGAAGAATGGCTGTAAACGTCTAC – 3'

5' – CGACTCACTATAGGGAGATGCCCGTGCTGTTGGCAC – 3'

The dsRNA for β-lactamase was also created from pND30, as a negative control, using the following primer pair:

5' – CGACTCACTATAGGGAGATTCCTGTTTTTGCTCACC – 3'

5' – CGACTCACTATAGGGAGAAGTGAGGCACCTATCTCA – 3'

Each primer begins with 18bp, which correspond to the end part of the minimal T7 promoter sequence, and is followed by 18 bp which are specific to the *EB1* gene. The product of the first round of PCR therefore contains an 18bp inverted sequence at each end. This PCR product was run on an agarose gel and gel purified, after which it served as a template for a 2nd round of PCR. This round of PCR served to add the

remainder of the T7 promoter sequence at either end, using the 27 nucleotide promoter sequence as a primer for both sides. The primer used for this reaction was:
5' – GAATTAATACGACTCACTATAGGGAGA – 3'
The products from the 2nd PCR were purified using a PCR purification kit, quantified by both spectrophotometry and on an agarose gel. A known amount of DNA was used as a template for *in vitro* transcription of both sense and antisense strands. Transcription was performed using the MEGAscript T7 Kit (Ambion) according to manufacturer's instructions. The RNA was ethanol precipitated and resuspended in 40µl RNase-free H_2O and double-stranded RNA was induced by heating to 65°C for 30 minutes and slowly cooled to 0°C. The dsRNA was checked and quantified on an agarose and the quantification confirmed by spectrophotometry. RNA was stored at -20°C.

2.14.2 Induction of RNA Interference

S2 cells were starved of serum as follows: 1 x 10^6 cells were diluted in 1 ml of serum free Schneider's medium and ~15µg of dsRNA was added. After 1 hour of serum starvation, 2ml of serum-supplemented Schneider's medium was added. The cells were incubated for 3-5 days and examined by immunoblotting and immunofluorescnece for reduction in protein expression.

2.15 Preparation of Haemocytes from Third Instar Larvae

A single late third instar larva (~76 hours since hatching) was taken and washed briefly in PBS. The larva was placed in 100µl Schneider's medium supplemented with Complete EDTA-free Protease Inhibitor cocktail (Roche). The larva was ruptured using a sharp dissection forceps. The larval remains were removed and the Schneider's medium, containing the *Drosophila* hemolymph was pipetted onto a Con A coated coverslip and allowed to adhere for 2.5-3 hours. Haemocytes were methanol/formaldehyde fixed and immunostained as described for S2 cells.

2.16 Fixation of *Drosophila* Embryos

Embryos were collected on plates and aged appropriately. Embryos were then washed with deionised water and dechorionated in 2.5% Chloros in water. Dechorionation takes roughly 2 minutes. Embryos are then washed thoroughly, collected on a brush and transferred to a glass vial containing 3ml heptane and 3ml methanol. The vial was

sealed and shook for 1 minute after which the liquid was extracted with a pipette and replaced with fresh methanol. These embryos were then incubated at room temperature for over 4 hours. Embryos in methanol were stored at -20°C.

2.17 Flat preparation of *Drosophila* Embryos.

Embryos were collected, aged and dechorionated as described in Section 2.16. After dechorionation, embryos at three-part gut stage were selected by eye. Embryos were removed to double-sided tape in a drop of PBS on a pre-prepared coverslip. Coverslips were prepared by wiping with ethanol and placing some double sided tape at the edge, coverslips were then either: placed on a slide and a border of Fixogum rubber cement (Marabu) applied or placed on a square of parafilm.

Embryos were placed on roughened double-sided tape. A tungsten needle, with a 1 micron tip, was inserted into the embryo at the posterior end and used to cut through the embryos from posterior to anterior. As the needle reached the anterior, the embryo was lifted, through the PBS, and placed on the slide. Appropriately aged embryos stick to the coverslip while older embryos do not. The tungsten needle was then used to spread the now filleted sides of the embryo, until the embryo lay flat and the central nervous system was visible.

The embryos were then fixed in 4% formaldehyde in PBS for 45 minutes, after which they were stained as described.

2.18 Immunostaining of *Drosophila* Embryos

Rehydration was done by passaging the embryos through increased concentrations of PBS in methanol (20%, 40%, 60%, 80%, and 100%) for 10 minutes at a time. Embryos were incubated in blocking buffer (10% FCS in PBS-Triton(0.1%)) for 30 minutes. Embryos were incubated in primary antibody in blocking buffer for 4 hours to overnight (dilutions of antibodies are given in Table 2.1) then washed 3 times for 10 minutes in PBS-Triton (0.1%). Embryos were then incubated in secondary antibody in blocking buffer (dilutions of antibodies are given in Table 2.1) supplemented with 0.4µg/ml DAPI for >2hrs. Embryos were washed 4 times for 10 minutes each in PBS-Triton (0.1%), followed by a brief wash in PBS. Embryos were then mounted in mounting medium (Section 2.13) and viewed on an LSM 700 confocal microscope. Images were processed using ImageJ.

2.19 Determination of Percentage of Embryonic Lethality in *Drosophila*

Flies were allowed to lay on grape plates for 1 hour after which the embryos were collected and a known number placed on new grape plates using a fine forceps. The embryos were left at 25°C for 24 hours, after which unhatched embryos were then counted.

2.20 Larval Motility Assays

2.20.1 Distance Assay

A Petri dish with 3% agarose was taped down on an A4 page with printed gridlines (6mm x 6mm) such that the gridlines were visible. A single late third instar larva (~76 hours since hatching) was taken and washed briefly in PBS to ensure no food would interfere with its movements. The larva was then placed in the centre of the Petri dish and allowed 60 seconds to acclimatise to its surroundings after which the number of gridlines passed by the moving larva was counted for 120 seconds. A gridline was only counted if both the anterior and posterior of the larva passed over within the allocated time (adapted from Batlevi at al., 2009).

2.20.2 Muscle movement Assay

A single late third instar larva was taken and washed briefly in PBS. The larva was then placed in the centre of a Petri dish with 3% agarose and allowed 60 seconds to acclimatise to its surroundings after which the number of peristaltic waves occurring in the larva was counted for 60 seconds. Both anterior to posterior and posterior to anterior waves were counted (adapted from Feiguin et al., 2009).

2.20.3 Righting assay

A single late third instar larva was taken and washed briefly in PBS. The larva was then placed in the centre of a Petri dish with 3% agarose and allowed 60 seconds to acclimatise to its surroundings after which it is rolled onto its dorsal side. The time it takes for the larva to right itself is then measured with a maximum of 120 seconds allowed (adapted from Ubhi et al., 2007).

2.20.4 Burrowing assay

30 late third instar larvae of each genotype examined were taken and washed briefly in PBS. They were then dropped onto the surface of food in a bottle and put in the dark at 25C for 2 hours, after which the number of larvae remaining on the surface was counted. The surface of the food was checked under the microscope for 'etchings' which may indicate that larvae attempted to burrow but were unable to. This was repeated 3 times for each genotype (adapted from Wu et al., 2003).

2.20.5 Mechanical Nociception Assay

Third instar larvae of each genotype examined were collected from bottles and washed briefly in PBS. These larvae were then placed on a Petri dish with 3% agarose and allowed to acclimatise to the surroundings. The Petri dish was supplemented with a small amount of PBS to allow the larvae full freedom of movement. Stimulation of the abdominal and thoracic muscles was carried out using a home-made Von Frey fibre with roughly 100mN of pressure. Von Frey fibres were made by welding roughly 2cm of fishing line (Blacks Ultra Cast Fishing line, 0.18mm, 6lb) to a glass pipette, allowing a protrusion of 4mm of fishing line. Larvae were stimulated, one at a time, by rapidly depressing and releasing the fiber on the dorsal side of a larva until a positive response was obtained. A positive response was recorded if a larva curled its body, rolled or 'bucked'. Larvae that did not respond were stimulated a minimum of 8 times.

2.21 Bioinformatic Tools

Sequences homology was determined using BLAST (http://blast.ncbi.nlm.nih.gov/). Ankyrin repeat domains were identified using Prosite (http://prosite.expasy.org/). Coiled-coil regions were identified using Paircoil (http://groups.csail.mit.edu/cb/paircoil/cgi-bin/paircoil.cgi). Structure was confirmed using the PredictProtein server (www.predictprotein.org). Alignments and determination of identity was carried out using Lalign (http://embnet.vital-it.ch/software/LALIGN_form.html). Nuclear localisation signals were searched for using NucPred (http://www.sbc.su.se/~maccallr/nucpred/cgi-bin/single.cgi). Nuclear export signal locations were determined using the NetNES 1.1 server (http://www.cbs.dtu.dk/services/NetNES/).

Chapter 3
Expression of KANK in *Drosophila melanogaster*

3.1 *CG10249* Encodes a Protein with Conserved Structural Features

3.1.1 Introduction

CG10249 is a ~27 kb gene located at 51D2 on chromosome arm 2R which has been identified as a member of the Kank family of proteins (Kakinuma et al., 2009). The protein *CG10249* encodes shares structural and sequence similarities with previously identified proteins: human Kank1-4 and the *C. elegans* protein VAB-19. Kank proteins contain an N-terminal KN motif which is unique to the family. This has been shown to contain a Nuclear Localisation Signal (NLS) and a Nuclear Export Signal (NES) (Zhu et al., 2008; Wang et al., 2006). A region of coiled-coils is also present towards the N-terminal of the protein; the number of coiled coils differs between the Kank proteins. The C-terminal region of the Kank proteins contains an ankyrin repeat domain. No significant sequence identity is found in the middle region of the protein paralogues between species.

3.1.2 KANK Contains a Coiled-Coil Region But Lacks a KN Motif.

CG10249 encodes a protein with an isoform dependent predicted molecular weight of 46kDa for the smallest isoform up to between ~102-147kDa for other isoforms. Isoform A of CG10249, obtained from the *Drosophila* Gold Collection of cDNA (GH03482 or '*kank* cDNA') encodes a protein (KANK) of 1224 amino acids, with a predicted molecular weight of ~133kDa (Figure 3.1 A) and which does not contain the KN motif common to other Kank proteins (For a comparison of sequence identities between KANK and other Kank family proteins see Table 3.1). This may affect its function, compared to the function of an isoform which does contain the KN motif region, such as isoforms C, D and G.

KANK contains two putative coiled-coil regions approximately at amino acids 314-379 (CC1) and 457-484 (CC2). CC1 has a 51% identity to a region of Kank1 while CC2 contains 40% identity to a sequence in VAB-19 (Figure 3.2 A-B).

3.1.3 The Ankyrin Repeat Region of KANK is Highly Conserved Between Species

Ankyrin repeats are common structural motifs which mediate protein-protein interactions. The ankyrin repeat domain of KANK lies at the C-terminal of the protein. Each ankyrin repeat consists of a 33 amino acid long helix-loop-helix, which

	% Homology overall	% Homology CC1	% Homology CC2	% Homology ANK	Putative SxIP motif	KN motif
Kank1	46	51	None	43	Yes	Yes
Kank2	47	37	None	36	No	Yes
Kank3	50	30	None	39	No	Yes
Kank4	46	None	None	45	Yes	Yes
VAB-19	44	None	40	44	No	Yes
Mouse Kank1	46	37	None	39	No	Yes
Mouse Kank2	48	35	None	34	No	Yes
Mouse Kank3	45	40	None	39	No	Yes
Mouse Kank4	44	None	None	44	Yes	Yes

Table 3.1 Kank is conserved across species. The structural domains of Kank are conserved across species. The KN motif is thought to contain nuclear localisation and export signals. The SxIP motif does not seem to be conserved across species.

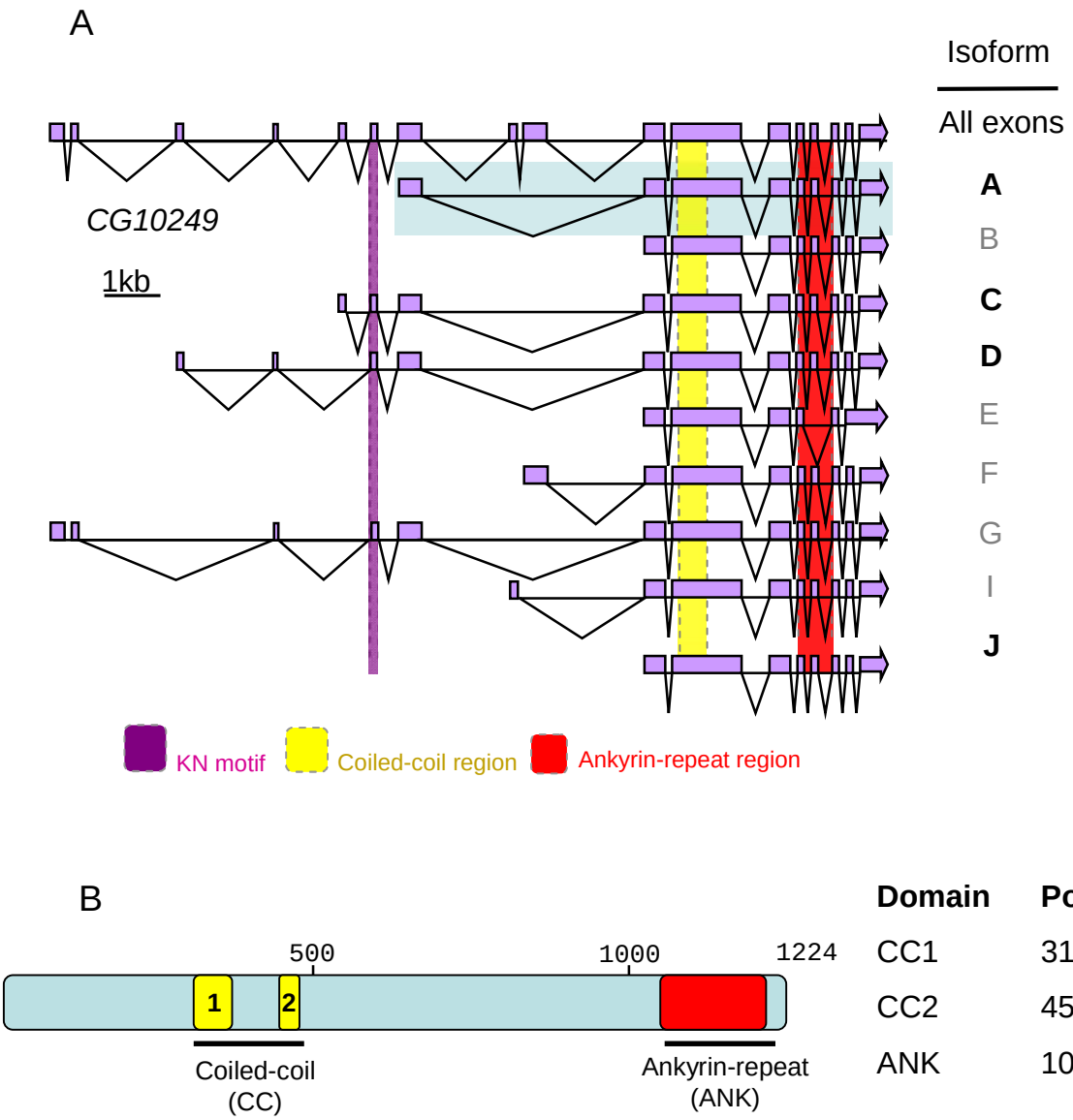

Figure 3.1 CG10249 is a homologue of the human Kank1 gene. (A) CG10249 is a ~27Kb gene found at 51D2 on chromosome arm 2R. Putative isoforms are shown. Those in black are likely to be expressed while those in grey are less likely to be expressed based on ModEncode data. The cDNA clone GH03482 represents isoform A of *kank* (highlighted in blue). This isoform lacks the KN motif found in other Kank proteins (shown in purple) and therefore may have reduced functionality compared to isoforms which contain the motif. (B) A coiled-coil domain is present in the first half of the protein and contains two coiled-coils (CC1 and CC2, shown in yellow in both A and B). An ankyrin repeat domain is found at the C-terminus of the protein (ANK, shown in red in both A and B).

A

CC1: KANK and Kank1

```
KANK  318 LFQIREQMALSLRRLKDLEEQVKVIPDMELELNSLRSEKQKLL 360
Kank1 260 LQHIREQMAIALKRLKELEEQVRTIPVLQVKISVLQEEKRQLV 302
```

B

CC2: KANK and VAB-19

```
KANK    467 VEQALTNAQKQQLRK 481
VAB-19 595 VKKLLTNEQKSNFQR 609
```

C

Ankyrin-repeat Domain: KANK and Kank1

```
KANK  1025 VNLSDSNGNTAMHYAVSHGNFDVVSILLDSKVCDVNQMNNAGYTS 1070
Kank1 1155 INLADGNGNTALHYSVSHSNFEIVKLLLDADVCNVDHQNKAGYTP 1200

KANK  1071 VMLVSLAKLKQPAHRTVVERLFKMADVNIRAKKHCQTALMLAVSH 1115
Kank1 1200 IMLAALAAVEAEKDMRIVEELFGCGDVNAKASQAGQTALMLAVSH 1245

KANK  1116 GNGDMVNMLLDAGADINIQDEDGSTALMCAAEHGRVDVIKHLLSH 1160
Kank1 1246 GRIDMVKGLLACGADVNIQDDEGSTALMCASEHGHVEIVKLLLAQ 1290

KANK  1161 PECDSLVTDVDGSTAFKIAWQAGHRDVGLLIYVHEQMLRSKLPNR 1205
Kank1 1291 PGCNGHLEDNDGSTALSIALEAGHKDIAVLLYAHVNFAKAQSPGT 1335

KANK  1206 GDATRSSLISP 1216
Kank1 1336 PRLGRKTSPGP 1346
```

D

Ankyrin-repeat Domain: KANK and VAB-19

```
KANK   1025 VNLSDSNGNTAMHYAVSHGNFDVVSILLDSKVCDVNQMNNAGYTS 1070
VAB-19 857  VNFCDQNGNTALHYAVSHANFAVVSSILDSGECDLDAPNRAGYTA 902

KANK   1071 VMLVSLAKLKQPAHRTVVERLFKMADVNIRAKKHCQTALMLAVSH 1115
VAB-19 903  VMLAALSQLDDDMEKAVVHRLFQMGNVNAKASQHGQTALMLAVSH 947

KANK   1116 GNGDMVNMLLDAGADINIQDEDGSTALMCAAEHGRVDVIKHLLSH 1160
VAB-19 948  GKKTTTELLLACGANVNEQDQDGSTALMCAAEHGHKELVKMLLAE 992

KANK   1161 PECDSLVTDVDGSTAFKIAWQAGHRDVGLLIYVH 1195
VAB-19 993  NLVNASLTDVDNSTALSIALENDHREIGVMIYAY 1025
```

Figure 3.2 KANK contains conserved structural domains (cont overleaf)

(Cont. from prev page.)

Figure 3.2 KANK contains conserved structural domains KANK shares sequence homology and structural homology with other identified Kank family proteins. Conserved residues are shown in red, while residues with similar chemical attributes are shown in blue. Percentage homology of different regions between KANK and other members of the Kank family are given in Table 3.1.

is arranged in tandem to form the ankyrin-repeat domain. KANK contains 3 ankyrin repeats and the domain stretches roughly from amino acids 1025-1186. The ankyrin repeat domain in KANK has 43% sequence identity with Kank1 and 44% with VAB-19, which in turn have 45% identity with each other (Figure 3.2 C-D).

3.1.4 Putative Motifs and Signals in KANK

Localisation Motifs: Although it lacks the KN motif of the Kank protein family, KANK contains several putative NLS and a putative NES. Three putative classic NLS exist in the KANK primary sequence as indicated in (Figure 3.3 A) the first sequence, KRRK (148-151) is found in Kank1 at amino acids 65-68, as part of the KN motif. This indicates that the KN motif of Kank family proteins may not be conserved as a single motif in other organisms, but its individual elements may be found separately, elsewhere in the protein sequence. This sequence was not found in VAB-19. The next two putative NLS are found in the ankyrin repeat domain, RKK (907-909) and RRK (947-949). These sequences were not found in VAB-19, though the putative NLS sequence KRK (621-623) was. KANK contains a single predicted NES, LLGEDEL, which is found at amino acids 853-859. The sequence does not appear to be found in human Kank proteins 1-3; however a similar sequence may be present in human Kank4. No NES was identified in VAB-19.

Putative SxIP motifs: As it was originally identified as an EB1 binding protein in our laboratory, I searched for putative EB1 binding domains and motifs in the KANK sequence. No EB1 binding domains were found, however two putative SxIP motifs were identified at 762-765 (SRIP) and 1199-1202 (SKLP) as indicated in (Figure 3.3 A). Putative SxIP motifs can be found in Kank1 (SAIP, 1130-1133) and in Kank4 (TRIP, 22-224; SPIP, 291-294). High sequence identity between Kank proteins is not found in those regions which contain putative SxIP motifs. No putative SxIP motif was found in VAB-19.

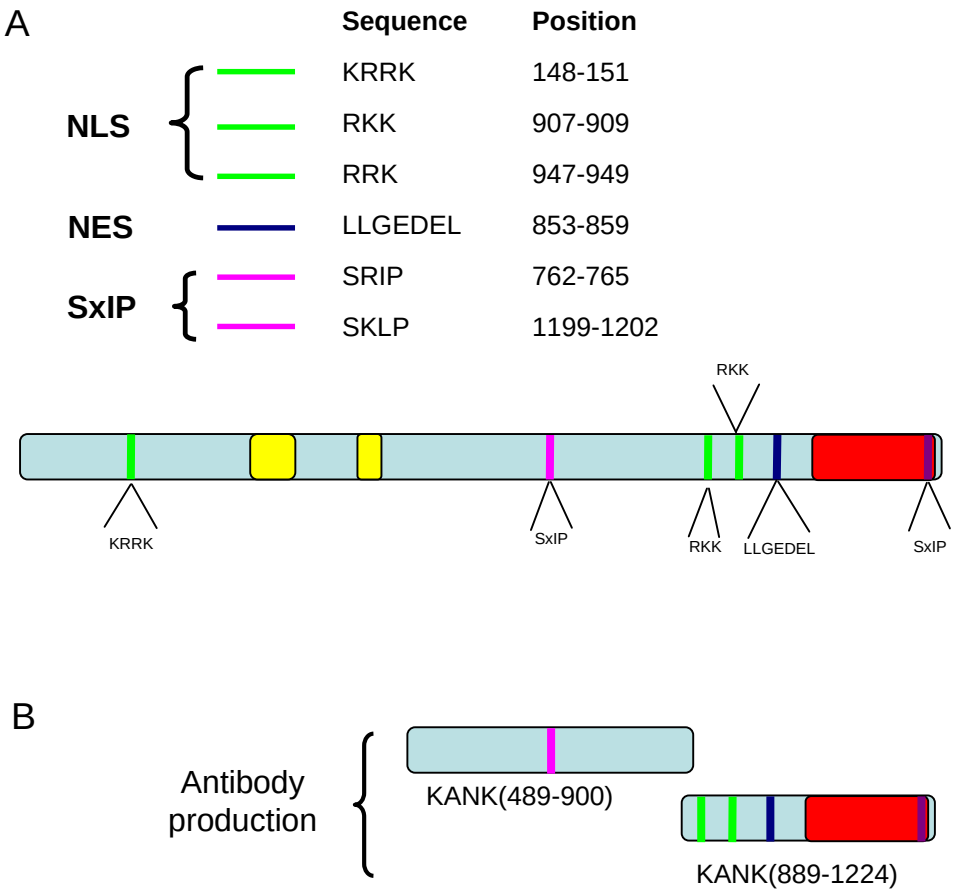

Figure 3.3 KANK contains putative motifs. (A) Putative nuclear localisation signals (green) putative nuclear export signal (dark blue) and putative SxIP motifs (pink) are all found in the KANK sequence (sequences and their positions shown). (B) Rabbit and rat antibodies specific for KANK were generated against two regions of the protein. The first antibody was raised against KANK(489-900) and is the antibody used throughout this thesis. The second was raised against KANK(889-1224).

3.2 KANK is not Essential in *Drosophila*

3.2.1 Background

In order to learn the cellular function of *Drosophila* KANK normal expression of the protein was reduced or abolished in whole flies. This section describes several different approaches which were taken and their outcomes.

3.2.2 KANK RNAi In Vivo

To determine the effect reduction of KANK expression would have in whole flies, RNA interference (RNAi) was used. RNAi relies on the expression of double stranded RNA (dsRNA) for the gene being studied. Cells do not tolerate dsRNA and in destroying it destroy any single stranded RNA with the same sequence. This makes RNAi useful for the disruption of a target protein without alteration of genomic DNA. An advantage of this fact is that RNAi can be driven by tissue specific promoters. RNAi is not 100% efficient and therefore a low amount of protein expression can occur. Occasionally this low level of protein expression is enough to avoid the disruption of normal cellular activities that may occur if expression of the target protein is completely abolished.

The effect of RNAi of KANK on the whole organism was investigated by expression of dsRNA under a GAL4 inducible UAS promoter, specifically the strong, ubiquitous Act5c promoter (For cross see Figure 3.4). Flies which should express *kank* dsRNA survived through to adulthood, had no discernable abnormal phenotype and gave progeny when crossed with w^{1118} and other KANK RNAi flies. The protein levels after RNAi were not quantified as a KANK specific antibody had not been created at the time this experiment was performed.

3.2.3 Remobilisation of a P-element Within the kank Gene Region

In order to disrupt expression of *kank*, a P-element insert (NP6204) that lies within the *kank* gene region was remobilised (Figure 3.5). When a P-element is remobilised imprecise excision of the surrounding genomic DNA sometimes occurs. If this

excised DNA includes part of a nearby exon, indicated by a red arrow in Figure 3.5, it would lead to disruption of KANK in the coiled-coil region, specifically at CC1 (the gene regions which codes for protein structural domains are shown in Figure 3.1). Flies in which P-element remobilisation has occurred will still have heterozygous expression of the gene, it is therefore necessary to introduce through further crosses, a homologous chromosome containing a large deletion, known as a deficiency, which uncovers the desired region.

A transposase is introduced to the P-element background flies creating so-called "jumpstarter" flies, identifiable by their mosaic eye type. Single male progeny were then crossed with balancer females. Single males with remobilised P-elements, selected from the progeny of this cross based on eye colour and body type were then crossed with a deficiency stock containing a deletion that uncovers the *kank* gene. This deficiency stock also contained a balancer chromosome so that a stock of flies with a balanced excision could be established should the excision result in a homozygous lethal phenotype.

Flies with an excision over the deficiency survived to adulthood and had no discernable abnormal phenotype. Moreover, they were fertile, producing progeny when crossed with w^{1118} and each other. Males were screened by PCR, using primers for the P-element and the surrounding genomic DNA, to ensure the P-element had been excised and subsequently to determine how much of the surrounding genomic DNA had been excised with it (Figure 3.6). Out of 768 crosses screened, one gave progeny which had part of the nearby exon of *kank* excised. The resulting homozygous strain ($kank^{\Delta 17}$) had no discernable abnormal phenotype, survived through adulthood and gave progeny when crossed with w^{1118} and $kank^{\Delta 17}$ flies. Partial deletion of the *kank* gene does not adversely affect *Drosophila* adults.

3.2.4 Synthetic Deletion of KANK

The previous 2 methods could not guarantee a 100% loss of expression of the entire KANK protein. RNAi, as previously mentioned, does not completely abolish protein expression. P-element remobilisation, in this case, may allow for some expression of the *kank* gene regions which lie upstream or downstream of the P-element as these regions may not be affected by the excision. Any expressed protein may be sufficient for normal KANK function. For these reasons, a third alternative approach was taken

A

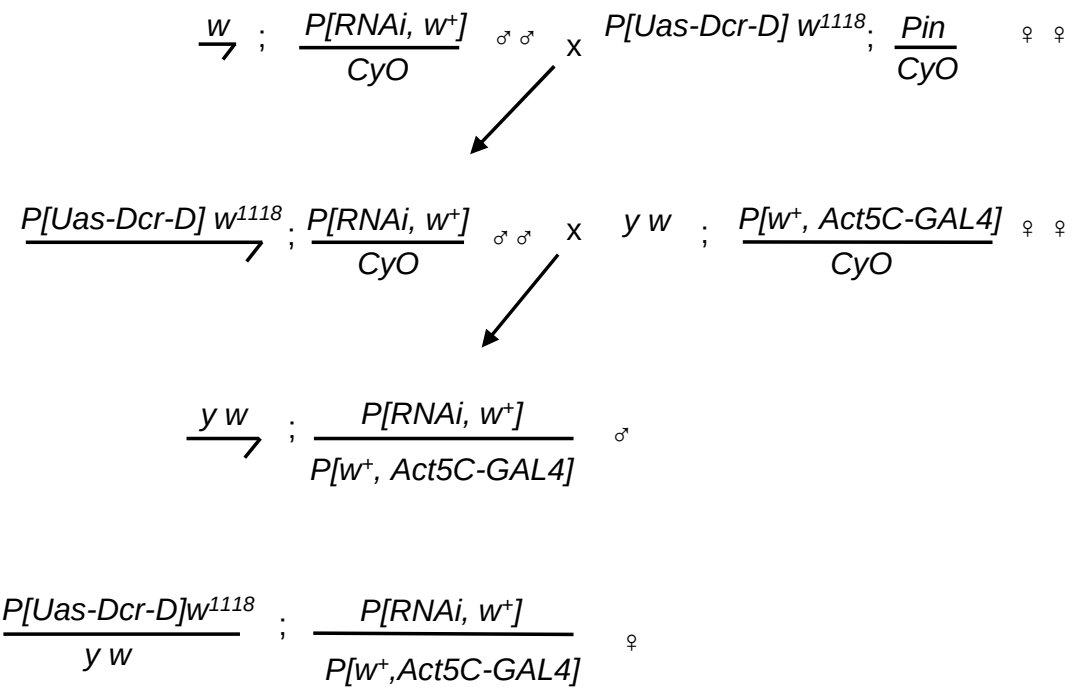

Figure 3.4 Crosses to create RNAi *kank* flies. A fly strain with an insert expressing hairpin RNA was used to create RNAi *kank* flies. Expression of the insert was driven by the Gal4/UAS system under an *Act5C* promoter. This cross used long hairpin RNA. An extra copy of *dicer*, under the same promoter was also introduced, to female progeny, in an attempt to increase the efficacy of the RNAi. No abnormal phenotype was observed.

to create a precise excision using *piggyBac* transposons (Figure 3.7) (Thibault et al., 2004). This method uses the FRT-FLP method of recombination. *PiggyBac* transposons, with correctly oriented FRT sites, are introduced such that they lie on homologous chromosomes. Introduction of a heat inducible flippase facilitates recombination between the FRT sites, when flies are heatshocked, which results in a deletion on one chromosome and a duplication of the gene on the homologous chromosome. Hybrid transposons remain at the sites of recombination (Figure 3.8).

The *kank* gene region contains transposons which are suitable for use and do not seem to affect any nearby genes. The first, PBac{WH}f01478, lies 3.97 kb downstream from the *kank* start site, within the *kank* gene. The 3.97 kb of *kank* which remains contains two putative exons which have been recently shown to be regulatory elements and not protein encoding exons (Hong et al., 2013). The second transposon, PBac{PB}c00393, lies 26 bases downstream from the final exon of the *kank* gene. Recombination between these two transposons will remove all protein encoding exons. Both transposons contained a w^+ marker and when the transposons were reconstituted after recombination both w^+ genes were contained in the hybrid transposon on the chromosome containing the duplicated gene. This facilitated selection of those flies which contain a deletion, as they had white eyes. Single males with a deletion were crossed with balancer females to establish a stock. This resulted in 3 strains which contained deletions (*Δkank1, Δkank2, Δkank3*). The deletion was not homozygous lethal and a homozygous stock was established. Males from this stock were screened using PCR to confirm the absence of *kank* genomic DNA using the transposon containing parental stocks as positive controls (Figure 3.9).

The *Δkank* flies survived through adulthood and exhibited no discernable abnormal phenotype. They also proved to be fertile as they gave progeny when crossed with $w^{1118}$and *Δkank* flies. In future experiments, two strains from *Δkank1* were consistently used after homozygotes for the deletion of *kank* were obtained from two separate stocks. Homozygotes obtained from *Δkank/CyO* will be referred to as $\Delta kank^A$ and homozygotes obtained from *Δkank/Df(2R)ED2423* will be referred to as $\Delta kank^B$. $\Delta kank^B$ flies were predominantly used and therefore will be referred to as *Δkank* in the text.

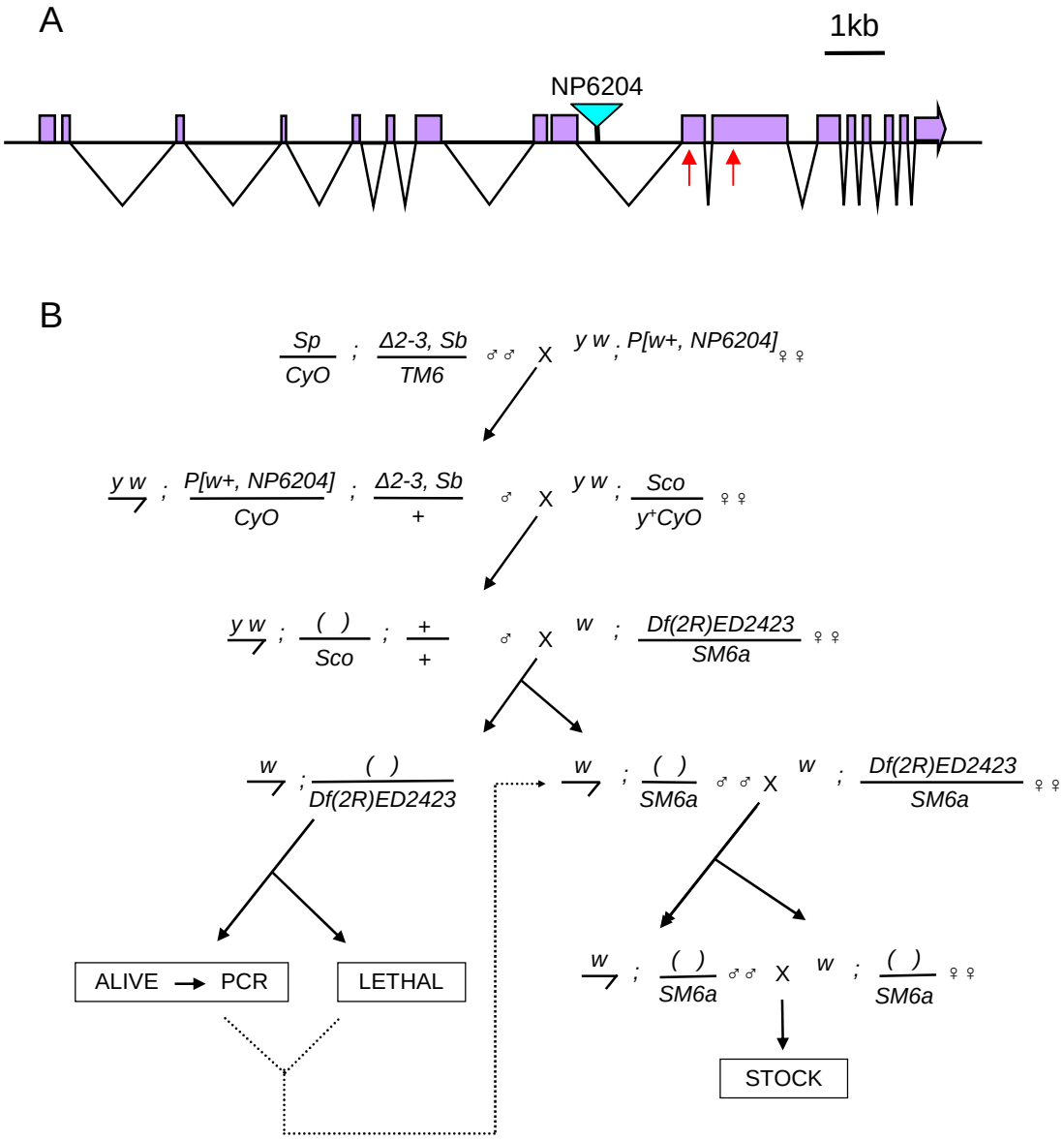

Figure 3.5 KANK expression was disrupted by imprecise P-element excision. (A) The *kank* gene region contains a transposable P-element, *NP6204* that is within 2kb of the nearby exon (exons that may be affected indicated by red arrows). This affects all putative isoforms of *kank*. (B) Imprecise excision of this P-element was carried out by introduction of a transposase, *Δ2-3.* The resulting chromosome with an excised P-element was balanced. Subsequently a deficiency that uncovered the excised region was introduced. If the progeny from this cross survived, PCR was carried out to determine the region of DNA that had been excised with the P-element. Meanwhile, a stock containing the excised region balanced with SM6a was established for further study.

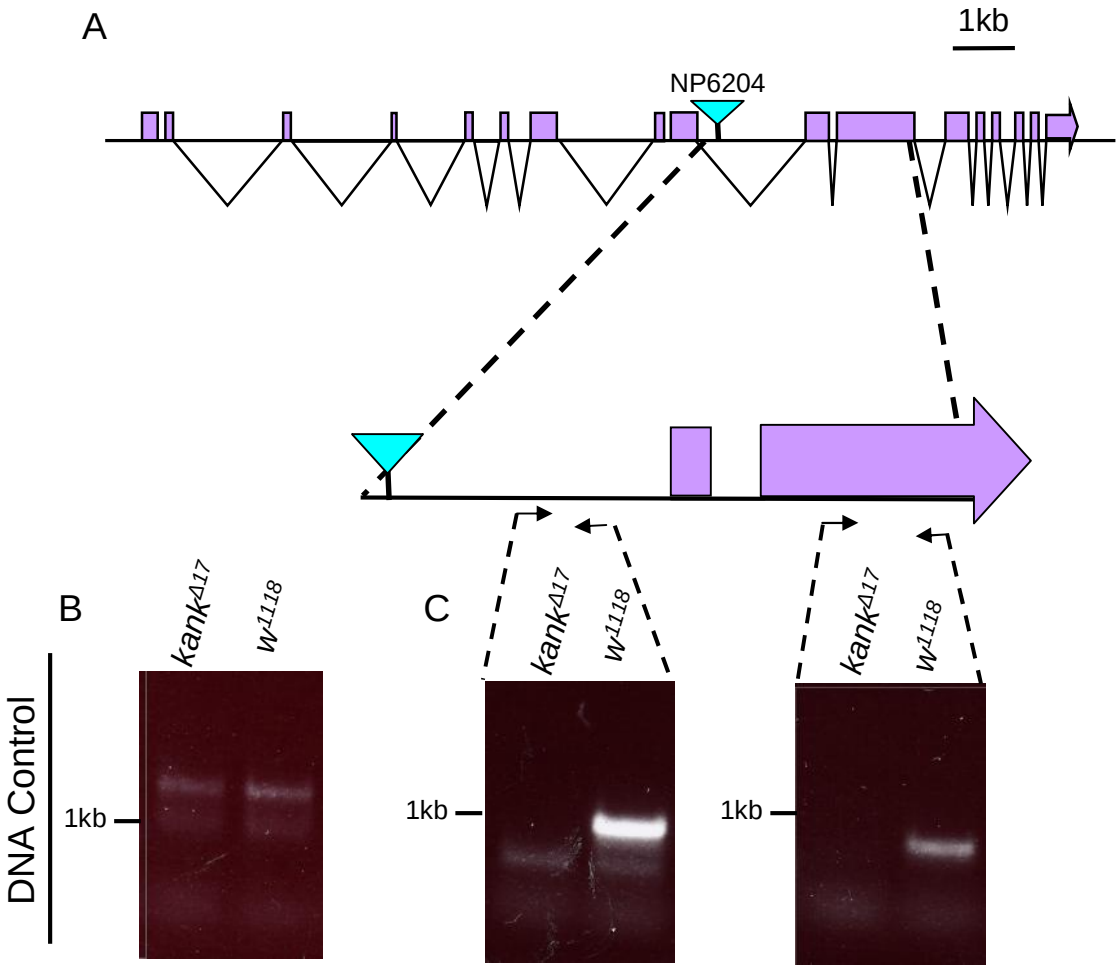

Figure 3.6 PCR confirmed excision of genomic DNA from the nearby exons of *kank*. (A) Imprecise excision of the P-element transposon NP6204 resulted in excision of DNA from nearby exons in the *kank*$^{\Delta 17}$ line. (B) A PCR using primers for a 1kb region on the third chromosome was used to confirm the sample DNA was suitable for PCR. (C) Successful P-element remobilisation was confirmed by PCR using primers for a 0.8kb fragment 0.85 kb from the P-element site. The excision was confirmed to disrupt nearby exons using PCR primers for a 0.6kb fragment 3.3kb from the P-element site.

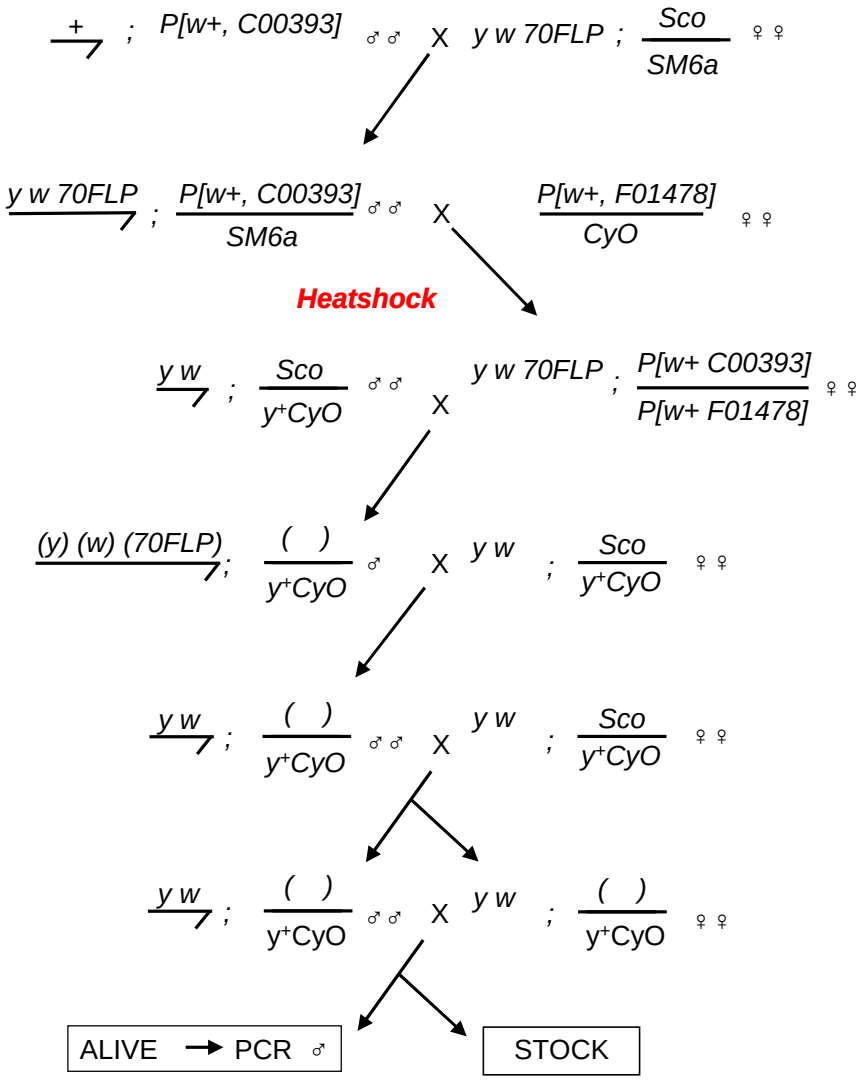

Figure 3.7 *kank* was deleted using FRT-site containing transposable elements. Two transposable elements which were inserted at opposite ends of *kank* were introduced in the trans position in the presence of a flippase, *70FLP*. During fertilisation parents were heatshocked for 1 hour at 37°C. Progeny in which recombination has occurred were selected and chromosomes containing the deletion were balanced with CyO. A stock was established with a balanced deletion. The deletion is not lethal, therefore flies homozygous for the deletion appear in the stock. PCR was carried out on homozygous males to confirm the deletion.

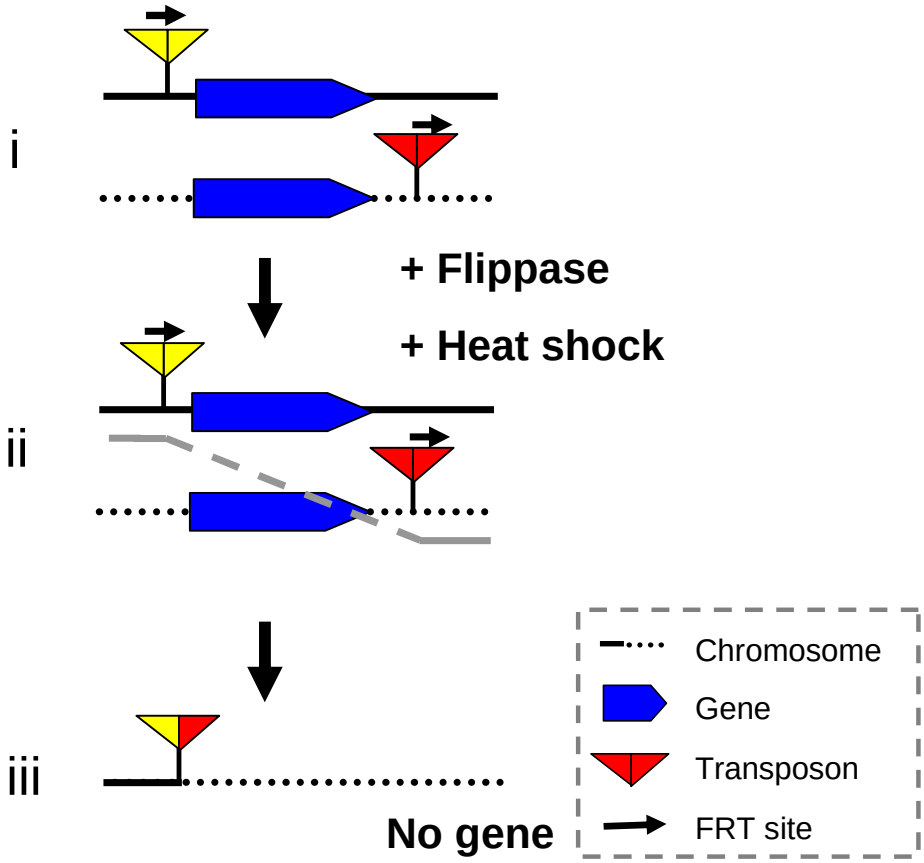

Figure 3.8 Overview of synthetic deletion using FRT containing transposable elements. The appropriate transposons are in the trans configuration on opposite chromosomes (i). A flippase is introduced and flies are heatshocked at 37°C for 1 hour. Recombination takes place at FRT sites (ii) and results in a chromosome lacking the intervening sequence (iii) and a chromosome containing a duplication of the intervening sequence (not shown). The deletion was then balanced to maintain a heterozygous stock. Deletion of the region was confirmed by PCR.

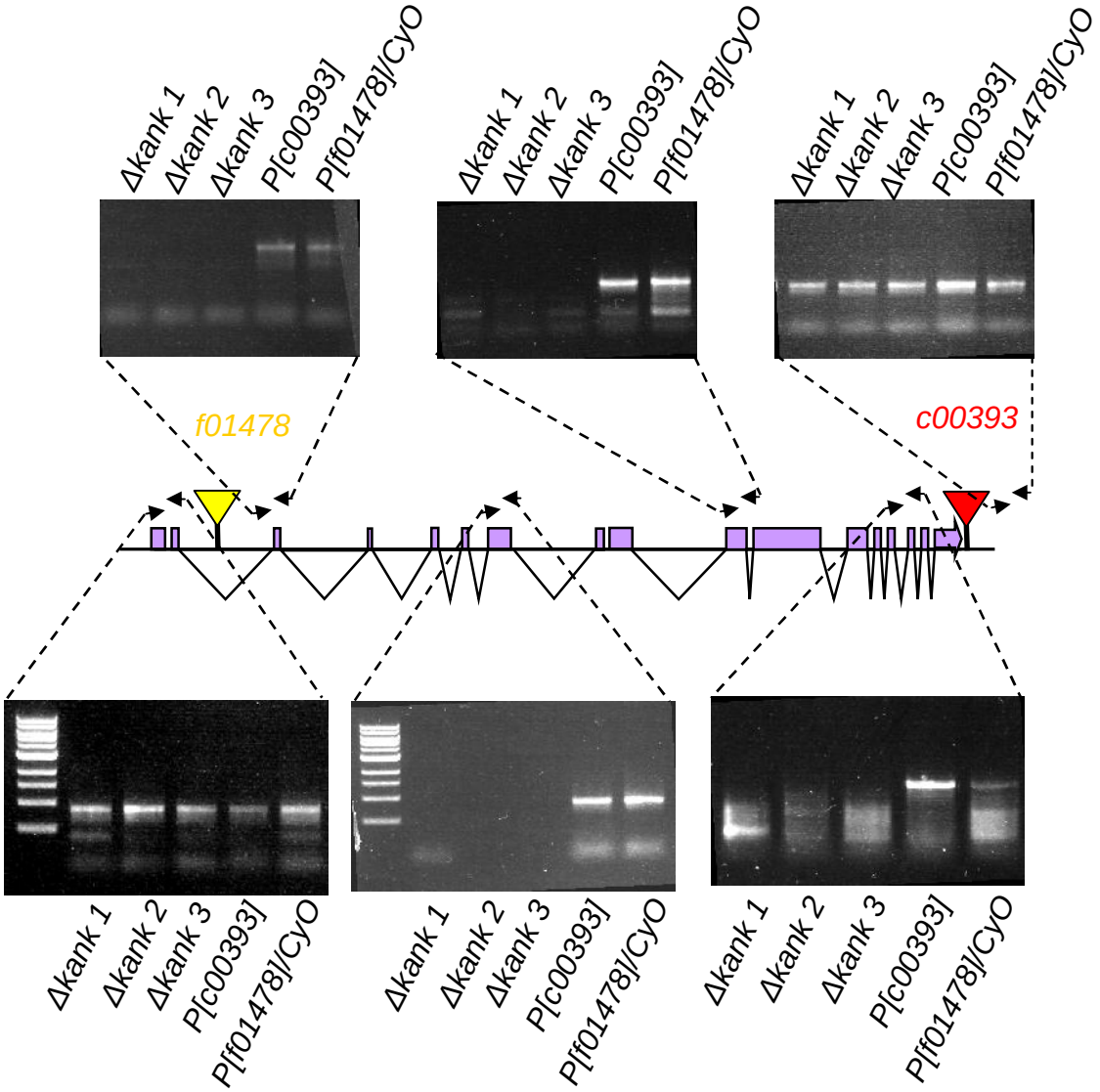

Figure 3.9 Synthetic deletion of *kank* was confirmed by PCR.
PCR was carried out on three *Δkank* lines and two control lines which contained the original FRT site containing transposons used. The gene schematic shows the gene region prior to recombination. Primers for regions both outside and within the *kank* region were used to confirm deletion of the *kank* DNA.

3.3 Disruption of KANK Expression Affects Embryonic Development

3.3.1 Background

Complete deletion of *kank* protein encoding exons did not lead to any discernable abnormal phenotypes and resulted in fertile adult flies. Evidence exists that disrupting the expression of Kank family proteins during development may have adverse effects on an organism, leading to familial cerebral palsy in humans and developmental arrest in *C. elegans* (Ding et al., 2003; Lerer et al., 2005). This led to further examination of *Δkank* strains during embryonic development.

It must be remembered that the stocks used in the following experiments do not have an isogenic background. Therefore any observed phenotype is not necessarily due to the effect of *kank* disruption.

3.3.2 Kank Deletion Flies Have Reduced Embryonic Viability

In order to determine if embryo viability in *Δkank* was comparable to w^{1118}, embryos were collected from both strains and laid on grape juice plates. w^{1118} represents wild type control. The embryos were then left for roughly 24 hours to hatch, and the remaining, unhatched, embryos were counted. Embryonic lethality increased in *Δkank* strains compared to w^{1118} (Figure 3.10 A). In w^{1118} 12% of embryos did not hatch (n=3070) but this increased to 28% for $\Delta kank^{A}$ (n=1250) and 24% for $\Delta kank^{B}$ (n=2770). Similarly, in $kank^{\Delta 17}$embryos embryonic lethality increased to 25% (n=710). The number of embryos hatching for each strain was consistent from day to day.

3.3.3 Kank *Deletion Embryos Do Not Arrest at Any Particular Embryonic Stage*

As *Δkank* embryos had increased lethality, I tested whether growth arrest occurred at any particular stage. Unhatched embryos were dechorionated by hand and viewed on a light microscope in order to determine their stage, as outlined by Bownes (1975). Embryonic stages were placed in 3 categories: Early (stages 1-6), Middle (stages 7-12) and Late (stages 13-hatching) and counted accordingly. No significant difference was found between *Δkank* and w^{1118} unhatched embryos, distribution across all stages was very similar. No particular stage was over-represented (Figure 3.10 B). This

A

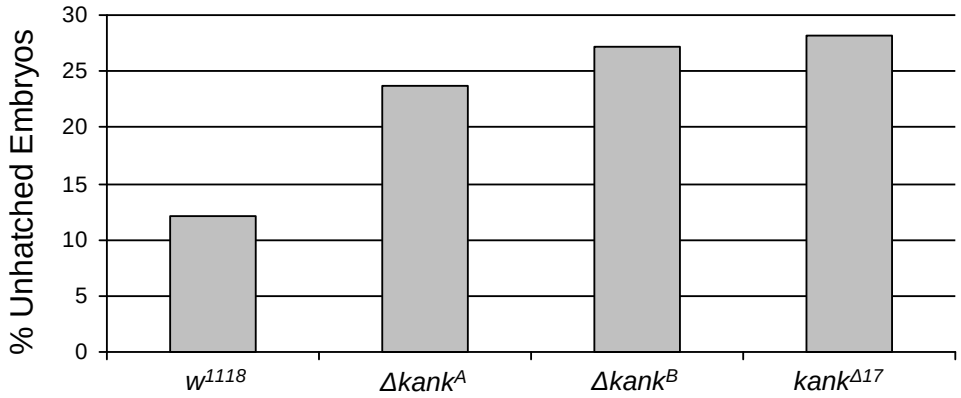

B

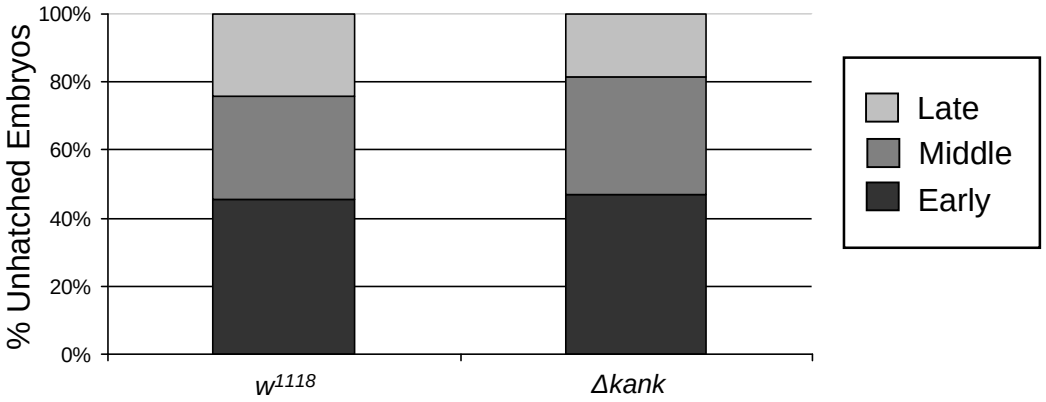

Figure 3.10 Flies with *kank* deletion or disruption show an increase in lethality during embryonic development compared to w^{1118}. Embryos were left at 25°C for 24 hours after which the number of unhatched embryos was counted. While failure to hatch was ~12% in w^{1118} flies. This rose significantly in *Δkank* flies (A). Unhatched embryos were dechorionated and staged according to Bownes (1981). Embryo stages were grouped into Late (13-17), Middle (7-12) and Early (1-6). No significant difference was seen in the stages of arrest between w^{1118} and *Δkank* embryos ($p<0.05$).

result indicates that arrest in *Δkank* embryos does not occur at any particular stage but over the course of embryonic development.

3.4 Antibodies Raised to KANK Can Detect the Endogenous Protein in All Lifecycle Stages

3.4.1 Antibodies Specific to KANK Detect GFP-KANK But Not Endogenous KANK in S2 Cells.

To create the antigens for polyclonal antibody generation, first a region of *kank* cDNA encoding the ankyrin domain region, KANK(889-1224), (Figure 3.3 B) was amplified and sub-cloned into an expression vector containing an N-terminal Glutathione-S transferase (GST) tag. The middle region, KANK(489-900), was amplified and sub-cloned into an expression vector containing an N-terminal Maltose-Binding protein (MBP) tag to generate the antigen for a second antibody. GST- KANK(889-1224) and MBP- KANK(489-900) proteins were then expressed in *E.coli* cells and purified. Purified proteins were used to generate polyclonal antibodies in both rabbits and rats. The crude serum was affinity purified by applying it to the antigen blotted to a nitrocellulose membrane and eluting the specific antibodies with a low pH elution solution.

These antibodies were tested for their specificity using S2 cells expressing GFP-KANK. *Kank* cDNA was cloned into a pAGW plasmid, containing an N-terminal GFP tag under an actin promoter. S2 cells were transfected with this plasmid and expressed GFP-KANK protein. An equal amount of transfected and untransfected cells were run on an SDS gel and were subsequently immunoblotted. Membranes were then probed with the affinity purified KANK antibodies. The precise molecular weight calculated for GFP-KANK from the primary sequence is 175.75kDa while the approximate molecular weight calculated for KANK is isoform dependent and ranges from 46kDa for isoform J up to between 102-147kDa for all other isoforms.

Each antibody gives a strong band at approximately 175kDa for the transfected cells (Figure 3.10). No such band is present in the lanes of the untransfected cells. This band corresponds with the expected size for GFP-KANK.

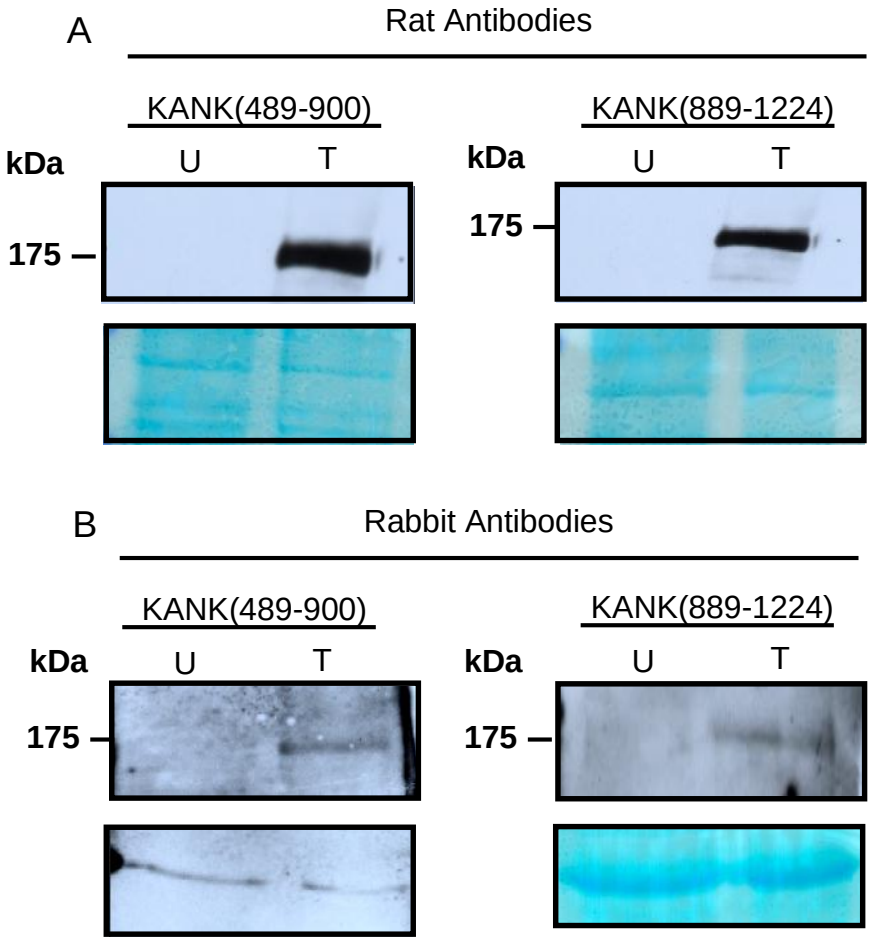

Figure 3.11 Affinity purified antibodies are specific for KANK. Antibodies raised to regions of KANK were affinity purified and used to probe immunoblots of cells transfected with GFP-KANK and untransfected cells. Each antibody gave a band at ~175kDa, the calculated molecular weight of GFP-KANK. Protein staining and non specific bands are shown to indicate equal concentrations of cells were present in each lane.

No band at the expected molecular weight for endogenous KANK is detected in transfected or untransfected cells. The absence of other bands indicates that the antibodies are specific for KANK. No bands were seen on membranes probed with the pre-immune sera.

These antibodies are specific for KANK but do not detect endogenous KANK from S2 cell lysates.

3.4.2 Endogenous KANK is Detectable in All Life-Cycle Stages By Immunoblotting

Publicly available mRNA sequencing data indicates that KANK RNA is expressed at low levels at all lifecycle stages in *Drosophila* (Graveley et al., 2011), apart from in the testis of mated males where expression was high and some embryo stages where expression is moderate. To determine if any protein expression was detectable by immunoblotting; protein samples from adult flies, pharate pupae, early pupae, third instar larvae and embryos 21-24 hours after egg laying were prepared from strains w^{1118} and *Δkank*. Males and females were prepared separately in adult and pharate pupae samples. All samples were run on SDS gels which were then immunoblotted and probed using affinity purified KANK antibodies.

The antibody AbKANK(489-900) gave a strong, specific band at ~160kDa in all w^{1118} samples that was not detected in *Δkank* samples (Figure 3.12A-D). This is somewhat higher than the band expected for endogenous KANK, which may be due to phosphorylation of the protein (as mentioned in Section 3.1) or possibly similar sized isoforms with slightly different mobility. Expression of KANK seemed to be particularly high in late stage embryos and remains reasonably high until adult stages where it is markedly reduced. These results indicate that KANK is expressed throughout the *Drosophila* lifecycle in w^{1118} flies while *Δkank* flies lack KANK expression due to successful deletion of the *kank* gene region.

3.4.3 Expression of KANK Increases During Embryonic Development

mRNA seq data (Graveley et al., 2011) indicates that the *kank* RNA is moderately expressed during *Drosophila* embryogenesis. Our data also indicates that *kank* may have a role in embryogenesis as embryonic lethality is higher in *Δkank* than in w^{1118}. The development of *Drosophila* embryos lasts roughly 24 hours, after which the 1st instar larva hatches. Embryos were collected from grape juice plates kept at 25°C at

3 hour intervals over the course of 24 hours. These embryos were prepared as protein samples and run on an SDS gel, immunoblotted and probed using affinity purified antibodies for KANK(489-900).

A band is visible at ~160kDa, which is not present in $\Delta kank^{A}$ or $\Delta kank^{B}$ (Figure 3.12 D and Figure 3.13 A). The band is visible from 3 hours into development and increased in intensity as the embryos age, until it peaks in intensity at hours 15-18 (Figure 3.12 E).

These results indicate that KANK expression increases over the course of *Drosophila* embryogenesis. The blot shows that expression becomes detectable 3-6 hours after egg laying and expression increases during embryogenesis until roughly 15-18 hours, that is, the late stages 16/17 of embryo development.

3.4.4 KANK Expression is Observed In $kank^{\Delta 17}$

To determine if KANK expression was fully disrupted in $kank^{\Delta 17}$ flies, an immunoblot was performed as previously described. A band for KANK was observed (Figure 3.14) however the amount of protein level seems low compared to w^{1118}. KANK expression is disrupted, but not abolished, in $kank^{\Delta 17}$embryos.

3.5 Increased Lethality in *kank* Deletion Embryos is Not Rescued by Ectopic Expression of *kank*

As stated previously, the embryonic lethality in *Δkank* flies may be independent of the *kank* deletion. For this reason, I introduced a copy of *kank* elsewhere in the genome of $\Delta kank^{B}$ flies, to restore KANK expression and attempt to rescue the phenotype. The p[acman] system uses bacterial artificial chromosome (BACs) and site-directed transformation of *Drosophila*. These BAC plasmids contain large regions of Drosophila genomic DNA, often encompassing genes with their possible promoter regions and regulatory elements, and an attP site which allows site directed integration to inserted attB sites in the genome upon introduction of ΦC31 integrase (Thorpe et al., 2000; Bateman et al., 2006). The BAC plasmid CH322-155P17 ($P[kank,w^{+}]$) containing the *kank* gene region was purified from a single colony bacterial stock and used to transform flies. The insertion site is on the third

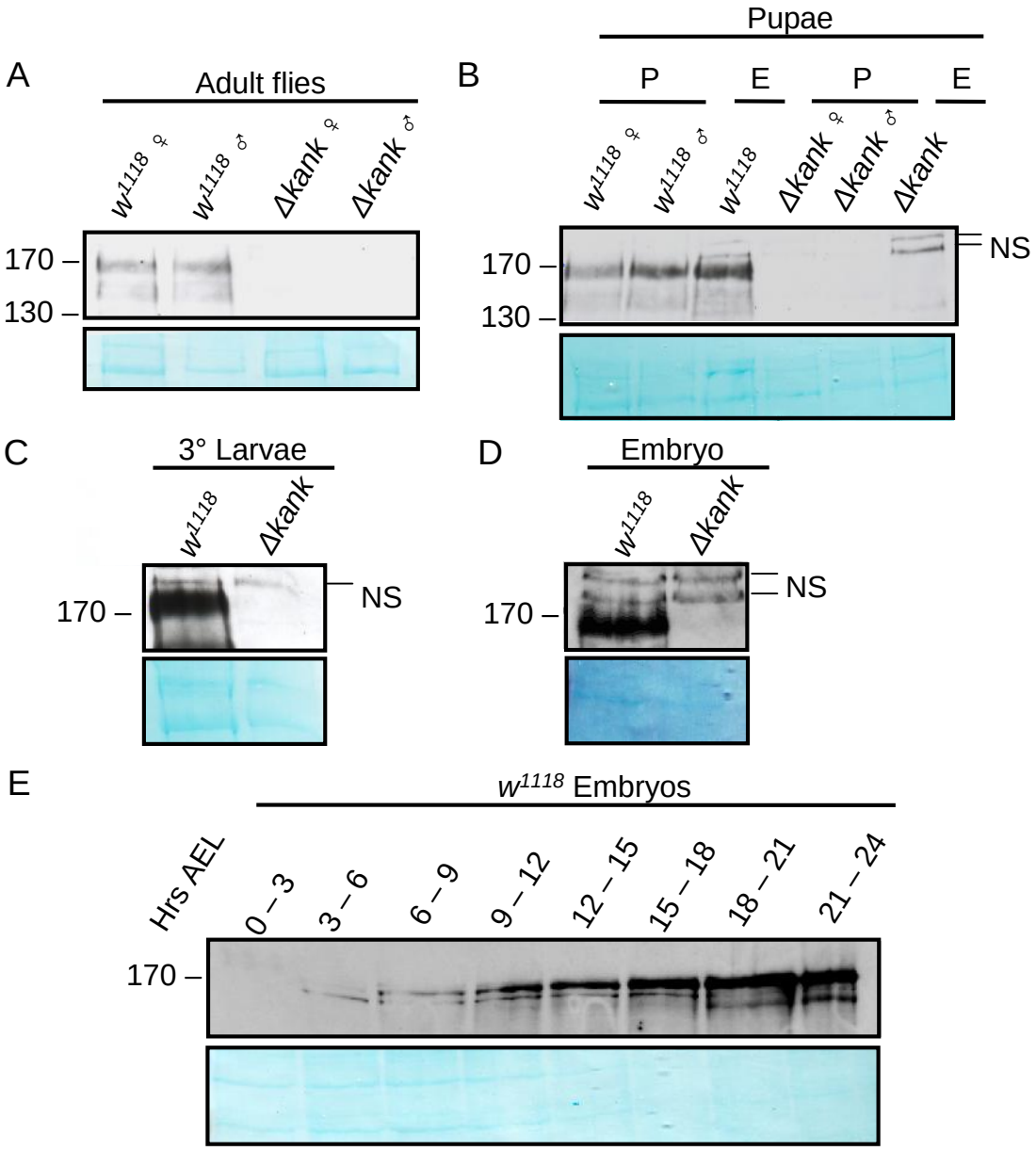

Figure 3.12 KANK is detected by immunoblotting throughout the Drosophila lifecycle. Preparations of *Drosophila* at different stages were probed with a 1:100 dilution of KANK antibody. While some non-specific bands were observed (labelled 'NS') KANK was detected in all lifecycle stages of w^{1118} flies and was not detected in *Δkank* flies. KANK was detected weakly in adults (A). Pharate embryos expressed KANK in levels similar to those seen in adults, while early embryos seemed to have a higher amount of KANK protein (B). Amounts of KANK also seem relatively higher in 3° larvae and *Drosophila* embryos (C & D). The thickness and fuzziness of the band may represent post-translational modifications or possibly different isoforms of KANK with similar molecular weights. Embryo samples were taken every 3 hours after egg laying and immunoblotted for KANK as described. KANK expression begins between hours 3 and 6 and continues to increase during development. Expression peaks between hours 18-21 (E).

chromosome. The insert is approximately 20kb, it begins 714 bases downstream of *kank* start site. The insert does not include first 7147 bases of *kank*. It was not known at the time of experimentation that this region, despite containing no exons, contains regulatory elements, namely sites for transcription factor *sim* binding (Hong et al., 2013). Lack of temporal regulation of *kank* during development may therefore be lost.

Δkank^{B} containing the BAC insert (P[*kank* w^{+}]) were created using the cross shown in (Figure 3.13). These flies (*Δkank*^{B}*;* p[*kank* w^{+}] or *Δkank;P[kank]*) hereafter referred to as *kank;res* were viable and produced progeny. Immunoblotting confirmed expression of KANK, though expression was slightly lower than w^{1118} levels (Figure 3.14 A). Embryonic lethality in *kank;res* was measured and compared to results for w^{1118} and *Δkank* (Figure 3.13 C). Embryonic lethality for *kank;res* was 40.4% (n=1100) much higher than in *Δkank*. Both values were consistently higher than the values obtained for w^{1118} (12%).

Although insertion of P[*kank* w^{+}] to *Δkank*^{B} flies re-establishes the expression of KANK but does not rescue the phenotype of embryonic lethality and leads to increased incidence of lethality (Figure 3.14 B). This result for *kank;res* may reflect mis-regulation of *kank* expression.

3.6 Discussion

3.6.1 KANK Structural Motifs and Sequence Features Are Conserved

KANK is the only member of the conserved Kank family of proteins in *Drosophila*. High identity (>50%) can be found between KANK and both Kank1 and VAB-19 in structural regions, the coiled-coil region and the ankyrin repeat region. The KN motif, unique to Kank proteins, is not present in all *Drosophila* KANK isoforms. However, an important sequence from within this motif, the nuclear localisation signal KRRK, is found elsewhere in the KANK sequence, while the NES found in the KN motif of Kank1 has high sequence identity (~60%) to a putative NES found in KANK.

Drosophila KANK contains 2 putative EB1 binding motifs. As KANK was identified as an EB1 interactor in the Ohkura Laboratory, one, or both, of these

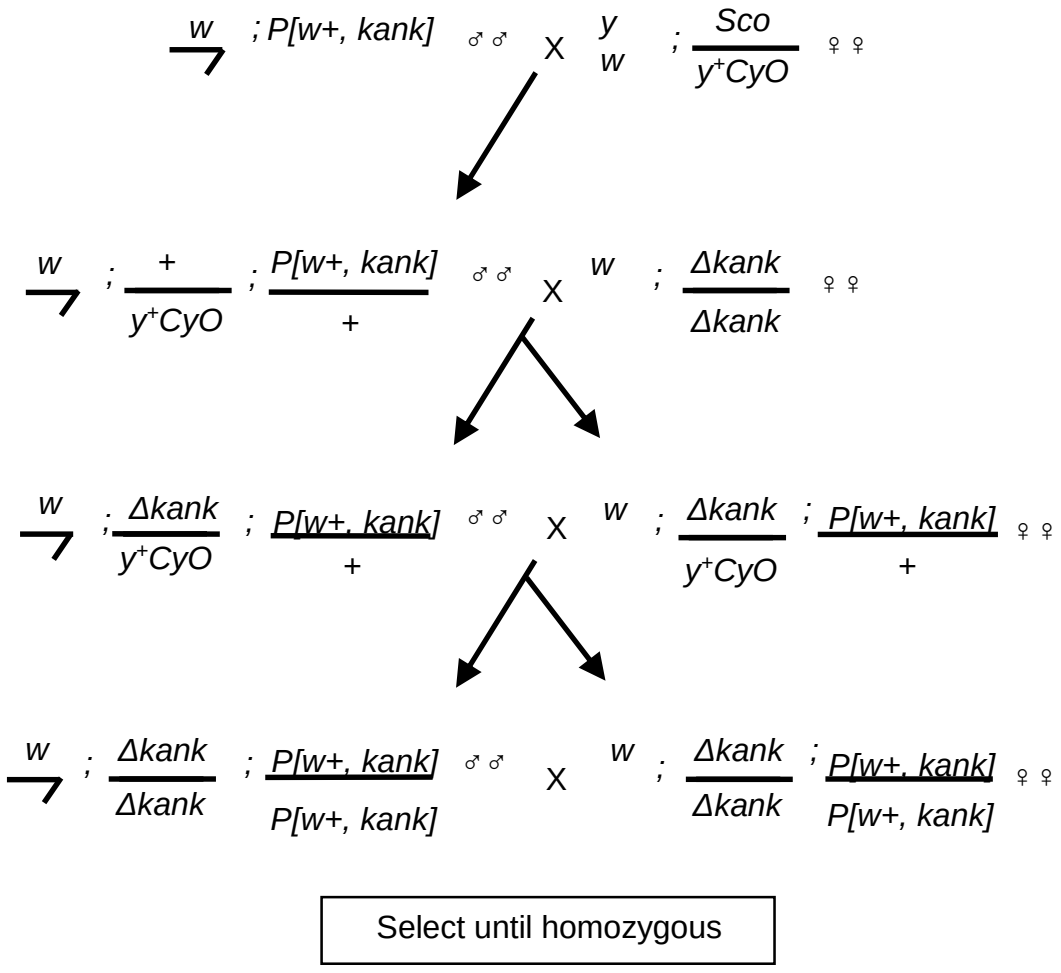

Figure 3.13 To attempt rescue embryonic lethality, *kank* was expressed from an insert in *Δkank* flies. (A) A fly stock containing a 20Kb insert, with the sequence of *kank* genomic DNA containing all protein coding exons, on the third chromosome (3L) was created and was crossed with *Δkank^{B} flies, as shown,* to create *Δkank;P[kank*] (referred to as *kank;res*) flies which express KANK.

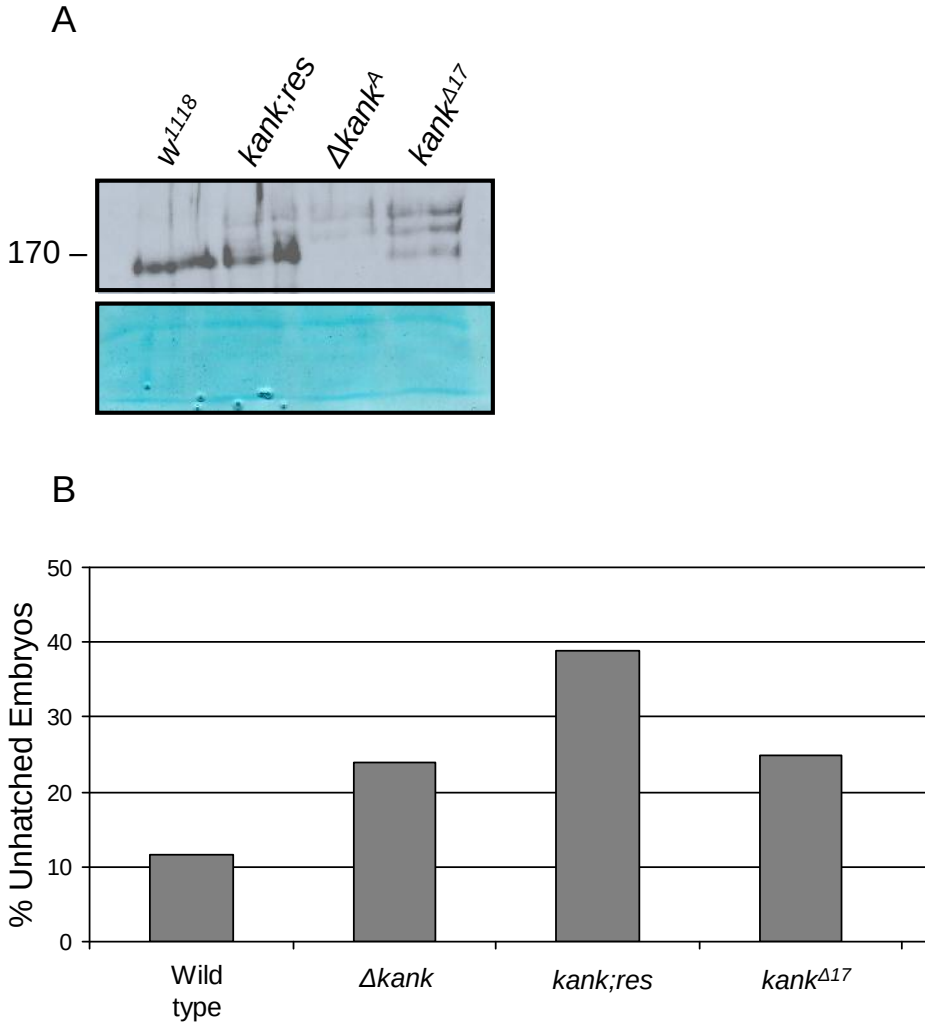

Figure 3.14 Abnormal expression of KANK can affect embryonic lethality. (A) KANK is expressed in *kank;res* and *kank*$^{\Delta 17}$. (B) *kank;res* flies did not rescue the embryonic lethality phenotype seen in *Δkank flies,* in fact, lethality increased significantly. *Kank*$^{\Delta 17}$ flies seem to have an increase in embryonic lethality on par with that seen in *Δkank,* this indicates that disruption of the protein by imprecise P-element excision was successful and a region of *kank* functional in embryogenesis has been affected.

motifs may be significant for KANK function. A recent study of mammalian putative EB1 binding proteins (Jiang et al., 2012) identified human Kank4 as a possible EB1 interacting protein due to the presence of a putative SxIP motif. This study also identified Kank2 in a GST-EB pulldown assay, although it does not contain any known EB1 binding regions or motifs.

3.6.2 KANK Expression Increases During Embryogenesis

KANK is expressed at all stages of the *Drosophila* lifecycle, as demonstrated by immunoblotting using an antibody raised to the middle region of KANK (KANK(489-900)). Expression began 3-6 hours after egg laying, this correlates with a recent study which shows expression of KANK RNA at stage 10 of embryogenesis (Hong et al., 2013). Immunoblotting indicates that KANK expression increases over the course of development, peaking 18-21 hours after egg laying. This represents stages 16 and 17 of embryogenesis. *Drosophila* embryos are approaching full development at this stage and muscle twitching, in preparation for hatching, has begun (Crisp et al., 2008). This is indicative of an important function for KANK in developed embryos, through development to adult stages where a reduction in KANK expression is seen on immunoblots.

3.6.3 Disruption of KANK Expression Results in Increased Embryonic Lethality

A summary of *kank* mutants is given in Figure 3.15. Data from other organisms provides evidence of important, necessary functions for Kank proteins, which may be uncovered in *Drosophila* by disruption of KANK expression. Deletion of the vast majority of the *kank* gene region, including all possible exons, results in an increase in embryonic lethality, from 12% in w^{1118} to 24-28% in *Δkank*, however adult flies displayed no abnormal phenotype and were fertile. The absence of KANK expression was confirmed by immunoblotting. This increase in embryonic lethality was also observed upon imprecise remobilisation of a P-element which resulted in partial deletion of the nearby exons (indicated by red arrow in Figure 3.5) of *kank.* Lethality at embryonic stages increased to 25% in $kank^{\Delta 17}$ flies. Immunoblotting indicates that KANK expression was unaffected in these flies. $Kank^{\Delta 17}$ flies are likely to contain a disruption within the coiled-coil region of the protein, implicating this

A

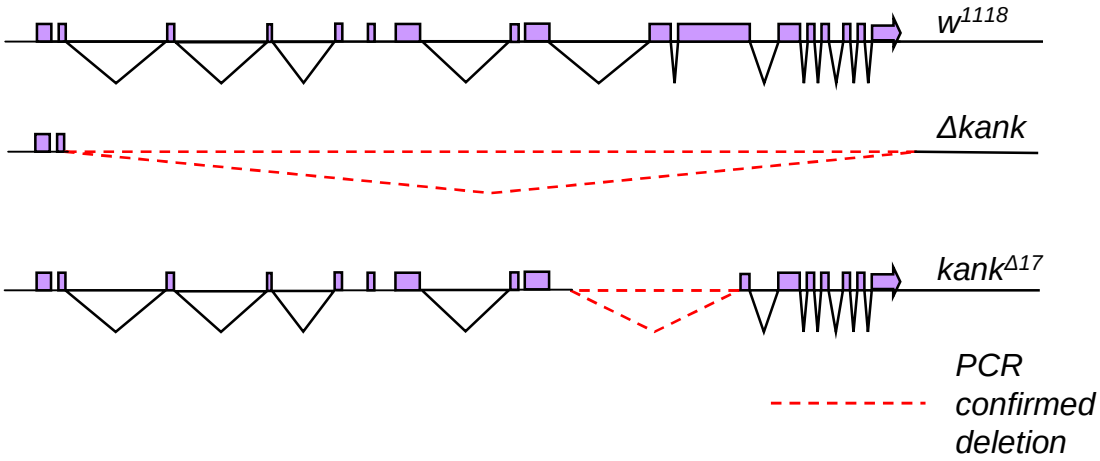

B

Name	Summary	Description	In text
w1118		Wild type control	w^{1118}
Δkank A	Deletion	Homozygote deletion, obtained from Δ*kank*1/CyO	$\Delta kank^{A}$
Δkank B	Deletion	Homozygote deletion, obtained from Δ*kank*1/Df(2R)ED2423	$\Delta kank^{B}$ or *Δkank*
$kank^{\Delta 17}$	P-element excision	Homozygote of imprecise P-element excision (P element: NP5204) which affects two exons.	$kank^{\Delta 17}$
Δkank;P[kank]	*kank* insert in deletion mutant	Δ *kank* homozygous for CH322-155P17 insert on third chromosome. Insert contains w^{+}.	*kank;res*

Figure 3.15 Summary of *kank* mutants created. (A) Schematic showing the regions of *kank* deleted in mutants. (B) Summary of strains used in text with description. For clarity, shorthand names are used in text. *ΔkankB* was the deletion mutant more commonly used and therefore is referred in the main text as *Δkank.*

region in the embryonic function of KANKs. This disruption would affect all putative isoforms (See Figure 3.1). As immunoblotting indicates KANK expression is maintained, it is possible the resulting protein merely lacks a small region of the peptide sequence – likely around the sequence of CC1 (Figure 3.1) – implying that this region may be necessary for KANK function in embryos.

Though the lack of isogenicity between w^{1118}, *Δkank* and $kank^{\Delta 17}$ makes it difficult to draw concrete conclusions, the consistency between the results for *Δkank* and $kank^{\Delta 17}$compared to the control do indicate strongly that the observed phenotype is due to disruption of *kank* expression and that the coiled-coil region is necessary for normal KANK function during embryogenesis.

This result corresponds with that seen in *C. elegans*, where growth arrest occurred early in development when expression of VAB-19 was disrupted. However, in *C. elegans* the arrest was observed in all temperature sensitive mutants at the restrictive temperature. This indicates that, though VAB-19 is essential in *C.elegans,* KANK is not essential for viability in *Drosophila* as >70% of deletion mutants survive to 1st instar larval stage. Additionally, contrary to what is seen in *C. elegans,* where the exact point of growth arrest is clear, observations of unhatched *Δkank* embryos did not indicate any particular stage of arrest. Embryos which failed to hatch were distributed over a range of stages similar to what is seen in w^{1118}.

KANK is non-essential in *Drosophila,* this is in agreement with studies which have indicated that Kank1 is not essential in humans. However, Kank1 is associated with neuromuscular disorders, such as cerebral palsy and congenital fibrosis of the extraocular muscles. Adult *Δkank* flies do not display any such abnormal phenotype.

3.6.4 Expression of KANK May be Tightly Regulated During Embryogenesis

Expression of KANK was restored in *Δkank* by introducing an insert containing ~20kb of the ~27kb *kank* gene that contains all protein coding regions. Although KANK expression was restored, as shown by immunoblotting, it did not rescue the embryonic lethal phenotype and resulted in a further increase in embryonic lethality. This method has been shown to result in the correct expression patterns for the inserted gene, except in cases where identified regulatory regions of the gene have not been included in the insert sequence (Venken et al., 2009). Interestingly, this

insert lacks recently identified regulatory regions of *kank* which are required for *sim* to induce expression of *kank*, beginning at stage 10 of embryogenesis along the ventral midline (Hong et al., 2013). It is possible that mis-expression of KANK during development, either spatially or temporally, results in embryonic death. This recent data was not available when the experiment was performed.

It should be noted that the three strains: w^{1118}, *Δkank* and $kank^{\Delta 17}$, do not share isogenic backgrounds. Therefore, any increased lethality seen may be due to unidentified mutations elsewhere in the genome, particularly as some of the same strains were used in the crosses to create each strain. Although we can not say definitively that *kank* is fully responsible for the observed phenotype, the further increase in embryonic lethality upon insertion of *P[kank]* does increase confidence that *kank* is responsible.

Chapter 4

Localisation of KANK in *Drosophila melanogaster*

4.1 Investigation of KANK localisation in S2 cells

4.1.1 Background

The cellular localisation of a protein can be indicative of function. In the human renal cell carcinoma (RCC) line VMRC-RCW, an antibody raised to human Kank1 stains the cytoplasm (Sarkar et al., 2002b). However, in later studies using a different RCC line, OS-RC-2, nuclear localisation was also observed (Yong Wang et al., 2006). Data from studies of the KANK orthologue in *C.elegans* (VAB-19) indicates that the protein is localised to attachment structures in muscle adjacent epidermal cells. This implies a cytoplasmic localisation of VAB-19, near the membrane of the cell. Localisation of Kank proteins with respect to microtubules has not been examined in any organism.

In this section I use both a GFP labelled form of the protein and a KANK specific antibody to determine the localisation of *Drosophila* KANK in S2 cells.

4.1.2 Detection of Endogenous KANK in S2 Cells

Antibodies specific for KANK were generated (Section 3.5.1) and used to immunostain *Drosophila* culture cells to visualise endogenous KANK. Methanol fixed S2 cells were coimmunostained with antibodies for KANK (1:20) and tubulin. The KANK signal was observed as dots throughout the cytoplasm in both mitotic and interphase cells (Figure 4.1 A and C). Some KANK staining is observed at microtubule ends (Figure 4.1 B) though this is not the primary localisation of the protein. Overall the KANK signal was not much higher than the observed background signal.

4.1.3 GFP-KANK Localises Largely to Microtubule Ends

To determine the subcellular localisation of KANK, S2 cells were transfected with a plasmid expressing GFP labelled full length KANK under an actin promoter, and coimmunostained for GFP and tubulin. This method over-expresses exogenous KANK to aid visualisation of its localisation.

In S2 cells cytoplasmic localisation of the GFP signal was observed, largely localised at the ends of microtubules. The intensity and length of the GFP signal at

A

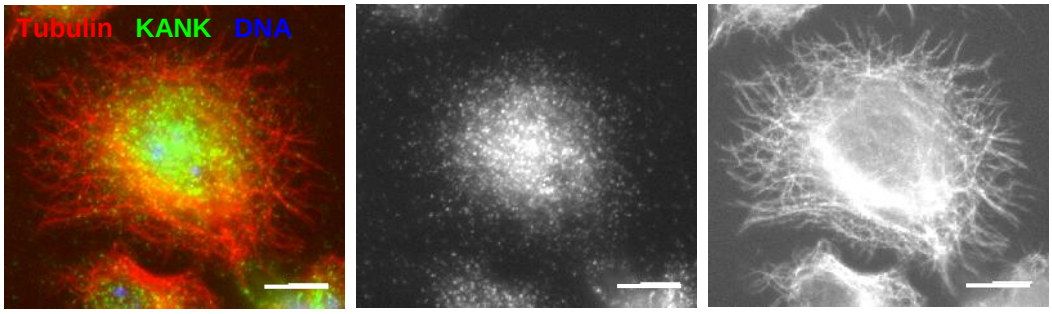

Merge KANK Tubulin

B

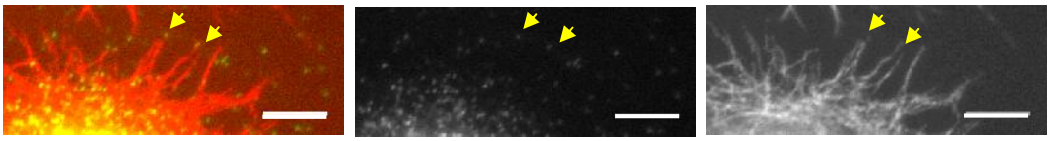

Merge KANK Tubulin

C

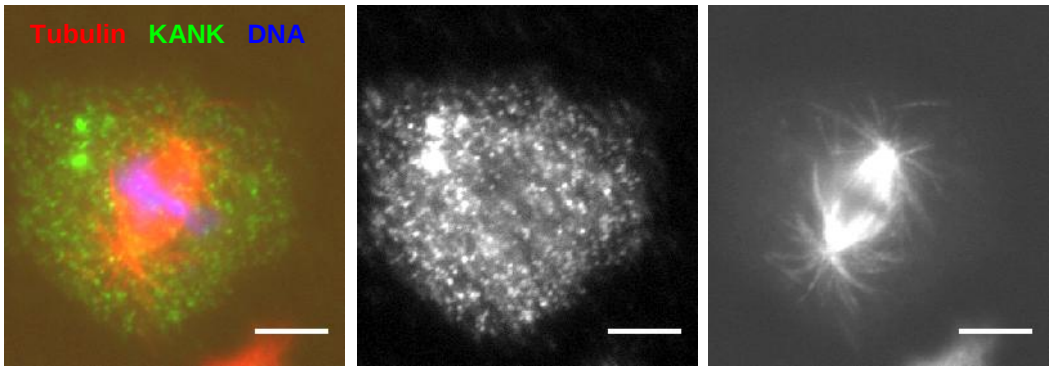

Merge KANK Tubulin

Figure 4.1 Endogenous KANK is not clearly detectable in S2 cells with antibodies specific for KANK. (A) A 1:20 dilution of an antibody specific for KANK(489-900) stains small punctae throughout the cytoplasm of interphase cells. Some staining can be seen at the ends of microtubules in (B) (Yellow arrow) though it is unclear if this is true KANK staining. (C) The KANK antibody stains punctae throughout the cytoplasm in mitotic cells and punctae are observed at microtubule ends. Scale bar 5µm.

microtubule ends was variable. Throughout the cytoplasm there was a weak, diffuse signal which slightly increased in intensity towards the periphery of the cell. (Figure 4.2) An antibody for KANK confirmed that the GFP-signal was GFP-KANK (Figure 4.2 B).

GFP-KANK localises to the cytoplasm of S2 and this localisation is mainly to the ends of microtubules towards the periphery of the cell during interphase.

4.1.4 GFP-KANK co-localises with EB1 at microtubule plus ends

EB1 is well known to form distinct 'comets' at the growing ends of microtubules. Although GFP-KANK does not form such 'comets' it also localises to growing ends of microtubules and has been shown to directly bind EB1 *in vitro* (Dzhindzhev & Ohkura, personal communication) Colocalisation of KANK and EB1 in S2 cells was therefore investigated.

Fixed GFP-KANK transfected S2 cells were coimmunostained for GFP and EB1 (Figure 4.3). The number of cells with GFP localised to more than half of the visible EB1 comets was ~76%. The GFP-KANK signal did not overlap entirely with the EB1 comets. It is possible that GFP-KANK may associate with the 'trail' of the EB1 comet – closer to the microtubule lattice than the tip. KANK colocalises with EB1 at microtubule plus ends in S2 cells.

4.1.5 GFP-KANK Exhibits Nuclear Localisation

The KN motif of KANK proteins contains nuclear localisation signals which have been shown to facilitate nuclear import of Kank1 in renal carcinoma culture cells. A sequence which matches that found in Kank1 is found in KANK. It is therefore possible that a small amount of KANK may localise transiently to the nucleus in S2 cells. Leptomycin B is an inhibitor of CRM1, a receptor which recognises leucine rich nuclear export signals. S2 cells transfected with GFP-KANK were treated with leptomycin B for 3 hours. After this time the cells were fixed and stained for GFP and tubulin. Nuclear localisation of GFP-KANK was seen in 13.6% of cells, compared to <2% of untreated control cells (Figure 4.4 A-B). This difference was significant (Figure 4.4C). This shows that, as in mammalian cells, KANK can localise transiently to the nucleus and is exported in a CRM1 dependent manner.

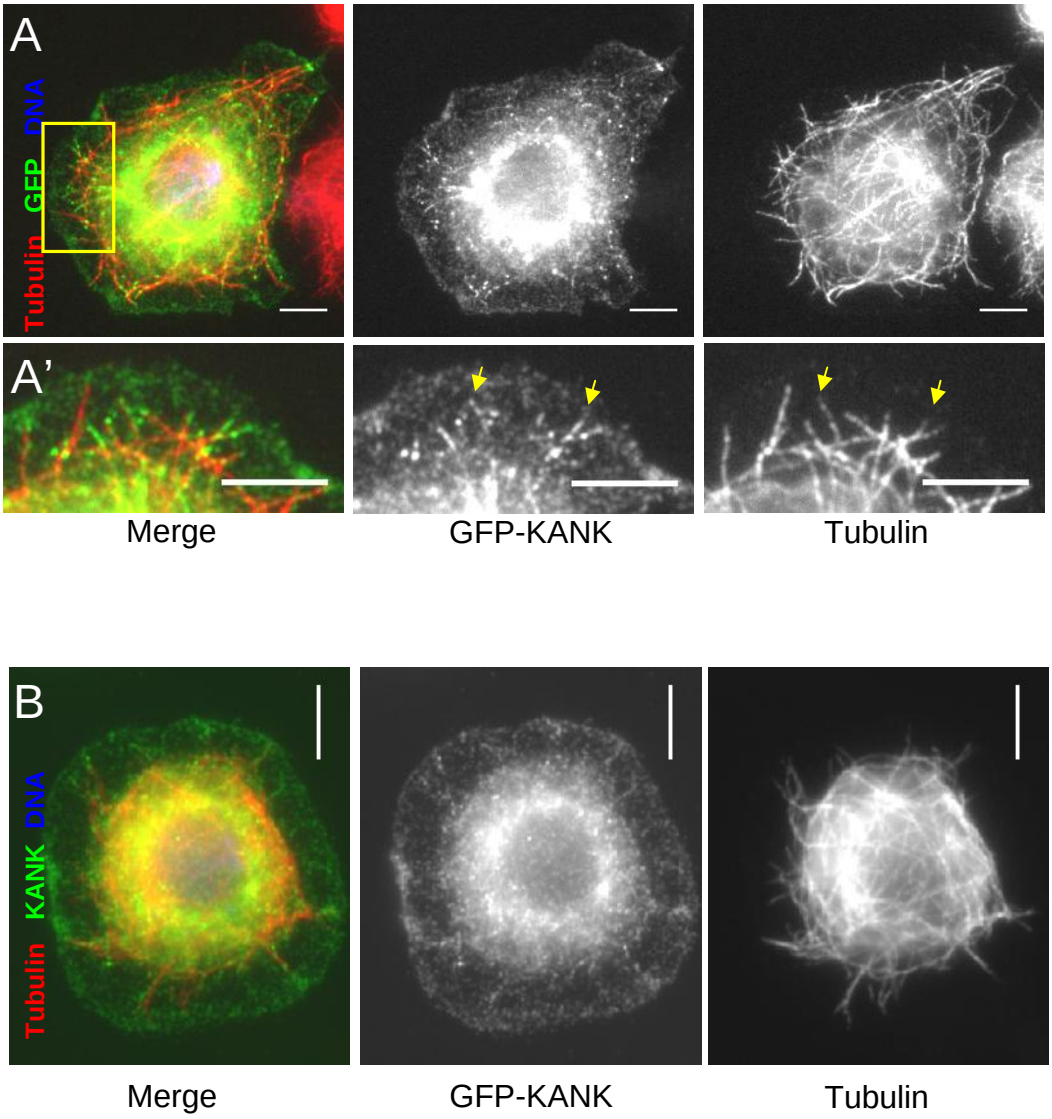

Figure 4.2 KANK localises to microtubule ends in interphase S2 cells. S2 cells transfected with GFP-KANK show a diffuse localisation of KANK to the cytoplasm (A) with slightly increased intensity in the nuclear region and at the cell periphery. KANK mainly localises to microtubule ends (A'). (B) GFP-KANK was detected in S2 cells using an antibody specific for endogenous KANK(489-900) Scale bar is 5µm.

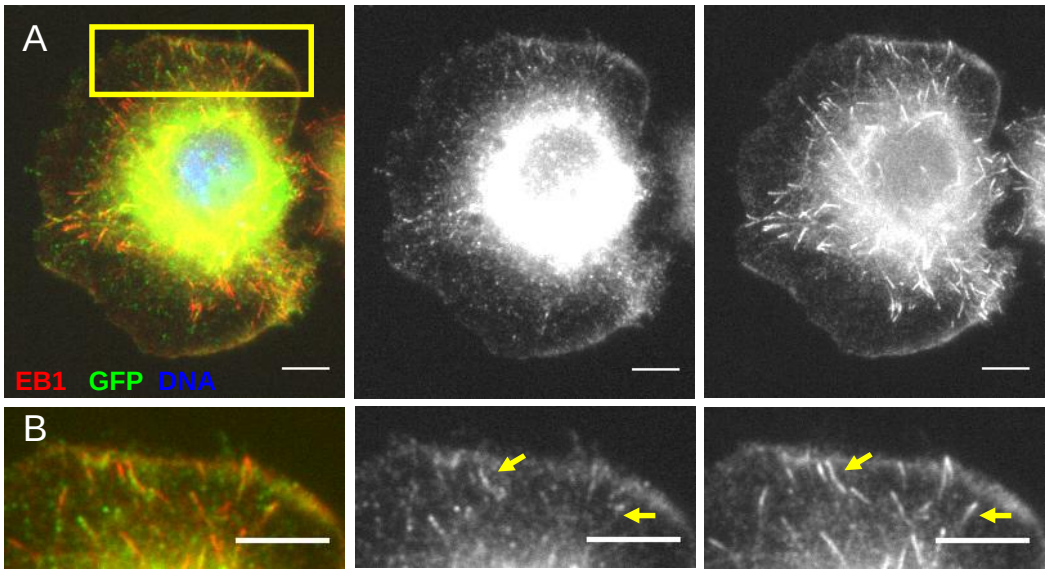

Figure 4.3 GFP-KANK colocalises with EB1 at microtubule growing ends. (A) S2 cells expressing GFP-KANK were coimmunostained for GFP and EB1. (B) The GFP signal was observed to localise to EB1 comets indicated by the yellow arrows. The GFP signal does not form comets and is more punctate than the EB1 signal. Scale bar is 5μm.

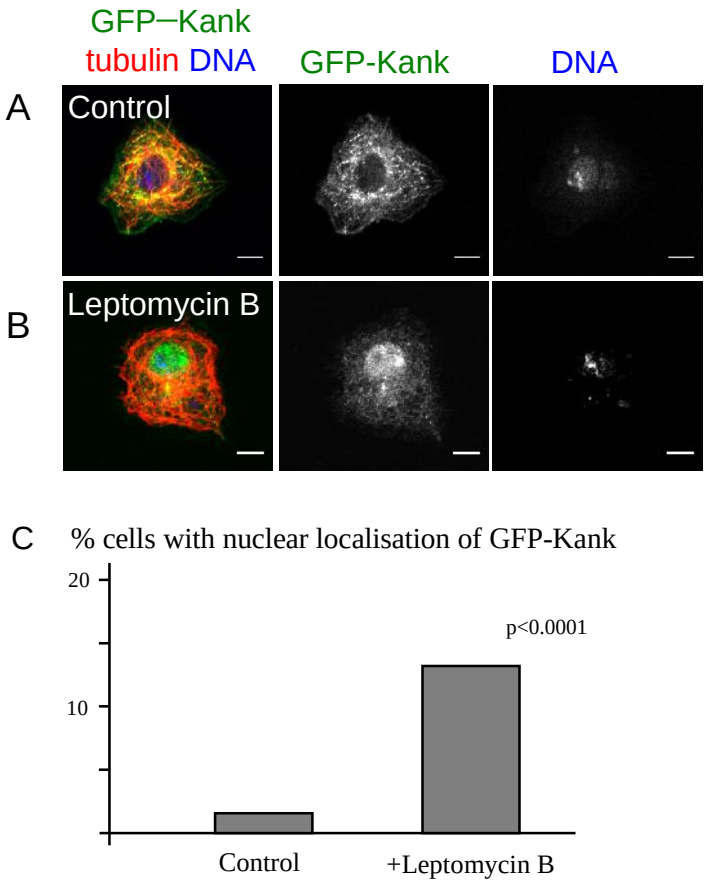

Figure 4.4 GFP-KANK can localise to the nucleus. S2 cells transfected with GFP-KANK were treated with Leptomycin-B or with methanol (control) for 3 hours and coimmunostained for GFP and tubulin. Nuclear localisation of the GFP signal is observed in ~13% of Leptomycin-B treated cells (A) while nuclear localisation is observed in <2% of methanol treated control cells (B). GFP-KANK can localise transiently to the nucleus and its export is CRM1-mediated. Scale bar is 5μm. (C) The increase in nuclear localisation was significant, as determined by student t-test.

4.1.6 Truncations of KANK Lacking the N or C terminus Have a Similar Localisation to GFP-KANK

To determine if the identified structural motifs contributed to the localisation of KANK; KANK(1-900) and KANK(489-1224) were labelled with GFP (Figure 4.7 A) and expressed in S2 cells under an actin promoter. Cells were then coimmunostained for GFP and tubulin.

Both truncations had a similar localisation to GFP-KANK and were localised to the cytoplasm, largely and microtubule ends (Figure 4.5A-B). This localisation was not as distinct as that seen in GFP-KANK transfected S2 cells. No nuclear localisation was observed. When transfected cells were co-immunostained for GFP and EB1, localisation of the GFP signal to EB1 comets was observed. 67% of GFP-KANK(1-900) transfected cells and 48% of GFP-KANK(489-1224) transfected cells have GFP signal localised to over half of the observable EB1 comets (Figure 4.6 A-B) although for KANK(489-1224) this reduction is significant (Figure 4.6 C) the colocalisation is still observable. Truncations of KANK lacking the N or C Terminal regions can localise to microtubule ends and are observed to colocalise with EB1.

4.1.7 Separated KANK Regions Do Not Have a Similar Localisation to GFP-KANK

To gain insight into the regions of KANK which contribute to microtubule localisation and its colocalisation with EB1, KANK was separated into three regions, each labelled with GFP and expressed in S2 cells under an actin promoter (Figure 4.7 A). KANK was separated into three regions, which resulted in separation and individual expression of the two structural domains found in the protein: the N-terminal, including the coiled coil domain of the protein, KANK(1-500) and the C-terminal of the protein, containing the ankyrin repeat domain, KANK(889-1224), and the middle region of the protein, KANK(489-900), which contains no known structure.

Transfected cells were stained for GFP and tubulin or EB1. Each region of KANK was largely diffuse within the cytoplasm although nuclear localisation was observed for KANK(1-500) and KANK(889-1224) (Figure 4.8). As no specific localisation was observed, transfected cell were immunoblotted and probed for GFP to confirm that the GFP-labelled proteins were expressed (Figure 4.7 B). None of

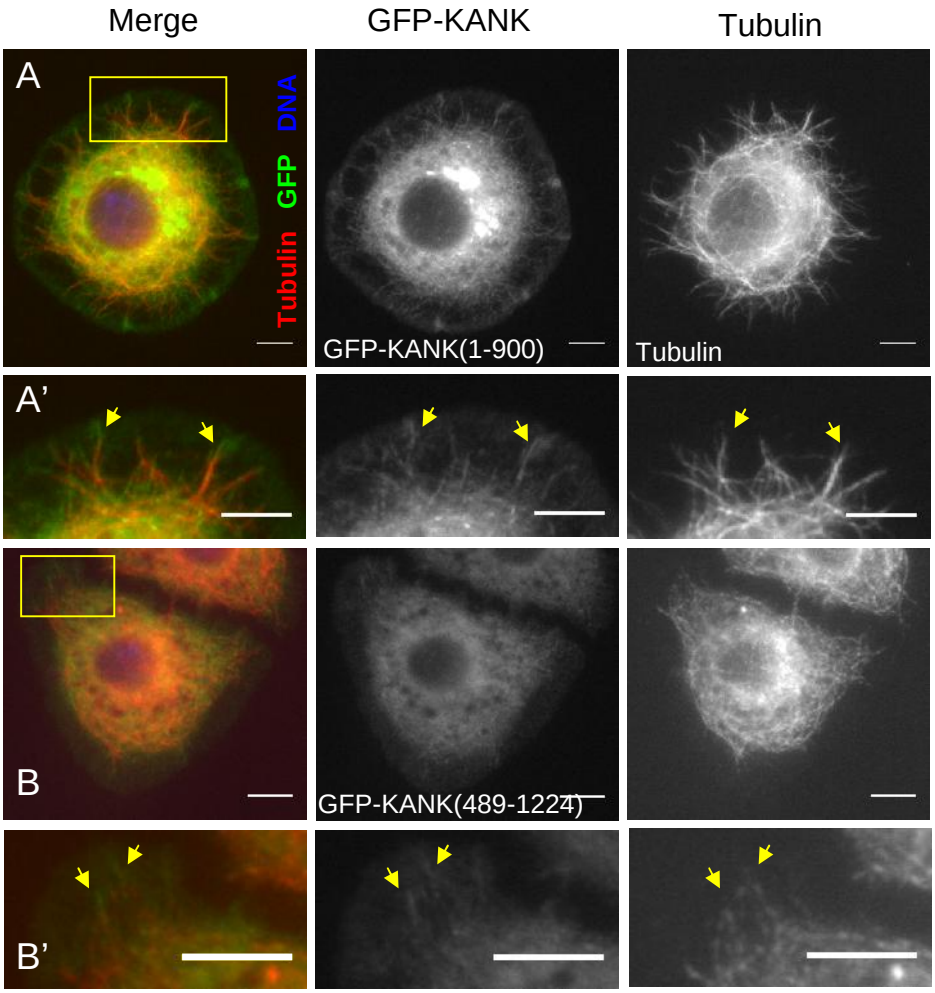

Figure 4.5 KANK can localise to microtubules in S2 cells when it lacks the C-terminal or the N-terminal but not both. Constructs with either C-terminal or N-terminal truncations of KANK were labelled with GFP (A) and transfected to S2 cells which were then coimmunostained for GFP and tubulin. The GFP signal localised to the cytoplasm for both constructs and was observed largely at microtubule ends (A-B). Nuclear localisation was not observed. Scale bar is 5μm.

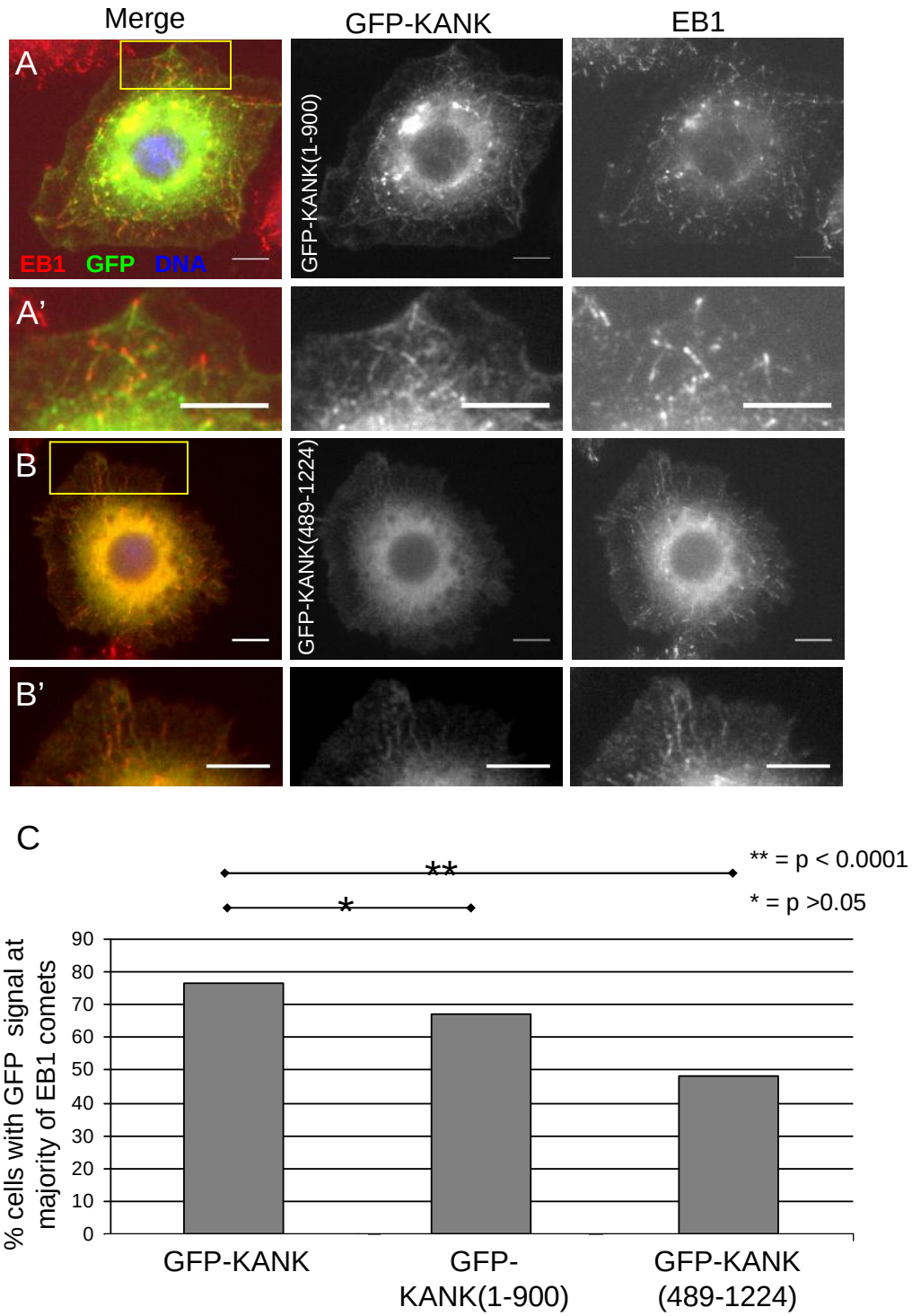

Figure 4.6 Deletion of the N-terminus or the C-terminus affects GFP-KANK localisation, though co-localisation with EB1 is still observed. S2 cells expressing GFP-KANK(1-924) or GFP-KANK(525-1224) were immunostained for GFP and EB1. Co-localisation of the GFP signal with EB1 was observed for both (A,B and inset A',B'). Scale bar is 5μm. (C) The percentage of cells with a strong GFP signal at EB1 comets was reduced for both constructs compared to GFP-KANK control. Significance determined by χ^2 test.

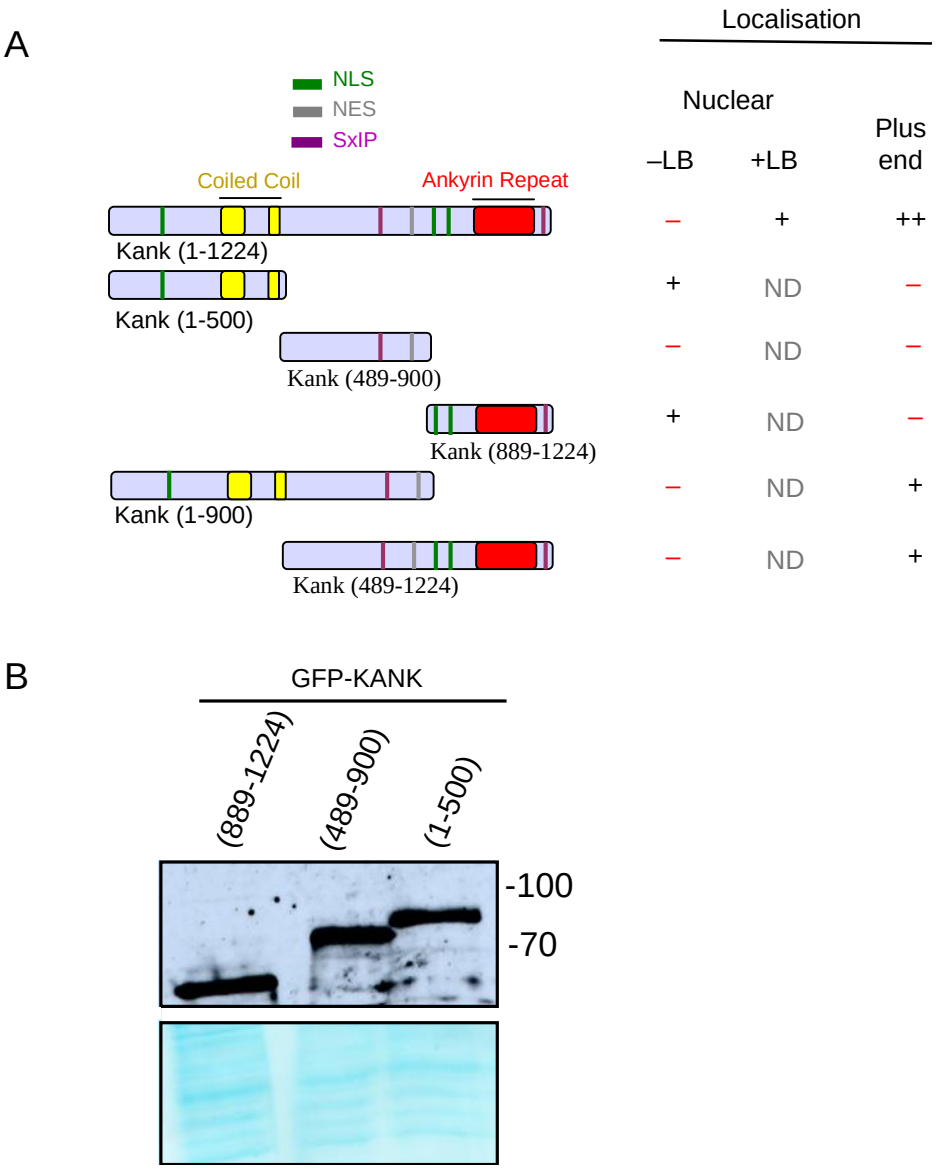

Figure 4.7 S2 cells were transfected with GFP labelled regions of KANK. KANK regions which reflected the structural domains of the protein were labelled with GFP (A) and transfected to S2 cells. A summary of the observed localisations is given. Three of the five GFP labelled regions displayed diffuse localisation in S2 cells, thus immunoblotting with an antibody specific for GFP was used to confirm expression of the entire region with the GFP label (B) No specific localisation was observed for three KANK regions. To ensure the regions were expressed, transfected cells were immunoblotted and probed for GFP. GFP-KANK(1-500) ~82kDa. GFP-KANK(489-900) ~72kDa. GFP-KANK(889-1224) ~64kDa.

these three regions have a similar localisation to GFP-KANK. It was not possible, therefore, to determine the region responsible for KANK localisation in S2 cells using this method.

4.1.8 Truncations of KANK Can Exhibit Nuclear Localisation.

GFP-KANK was observed to localise to the nucleus in fixed S2 cells, but this localisation was only apparent upon treatment of the cells with leptomycin-B. GFP-KANK(1-500) and GFP-KANK(889-1224) both exhibit strong nuclear localisation without leptomycin B treatment, in 75% and 98.5% of cells respectively (Figure 4.8). GFP-KANK(489-900) shows weak nuclear localisation in only a minority of cells. Nuclear localisation was not observed for KANK(1-900) or KANK(489-1224) (Figure 4.5 and 4.6).

These data suggest that both the N-terminal and the C-terminal regions of KANK contain nuclear localisation signals. The NLS found in the KN motif of other Kank family proteins is found in KANK, although it lacks the KN motif (Section 3.1). This NLS, found in GFP-KANK(1-500) may be responsible for nuclear localisation of this region. GFP-KANK(889-1224) contains 2 putative nuclear localisation signals. The N-terminal region and the C-terminal region can localise to the nucleus in S2 cells and it is likely that sequences in these regions are responsible for the observed nuclear localisation of GFP-KANK but their action can be inhibited by elements within the middle region of the protein (KANK(489-900)).

4.2 KANK Binds EB1 via an SxIP Motif and Requires This Interaction to Localise to Microtubule Ends

4.2.1 Background

EB1 is a highly conserved protein that binds the growing ends of microtubules autonomously and is critical for regulation of microtubule dynamics and growth. EB1 functions in microtubule dynamics by recruiting cargo proteins, such as CLIP-190 which has been shown to have a role in microtubule growth (Rogers and Rogers, 2008) and requires EB1 to localise at microtubule plus ends (Dzhindzhev et al., 2005).

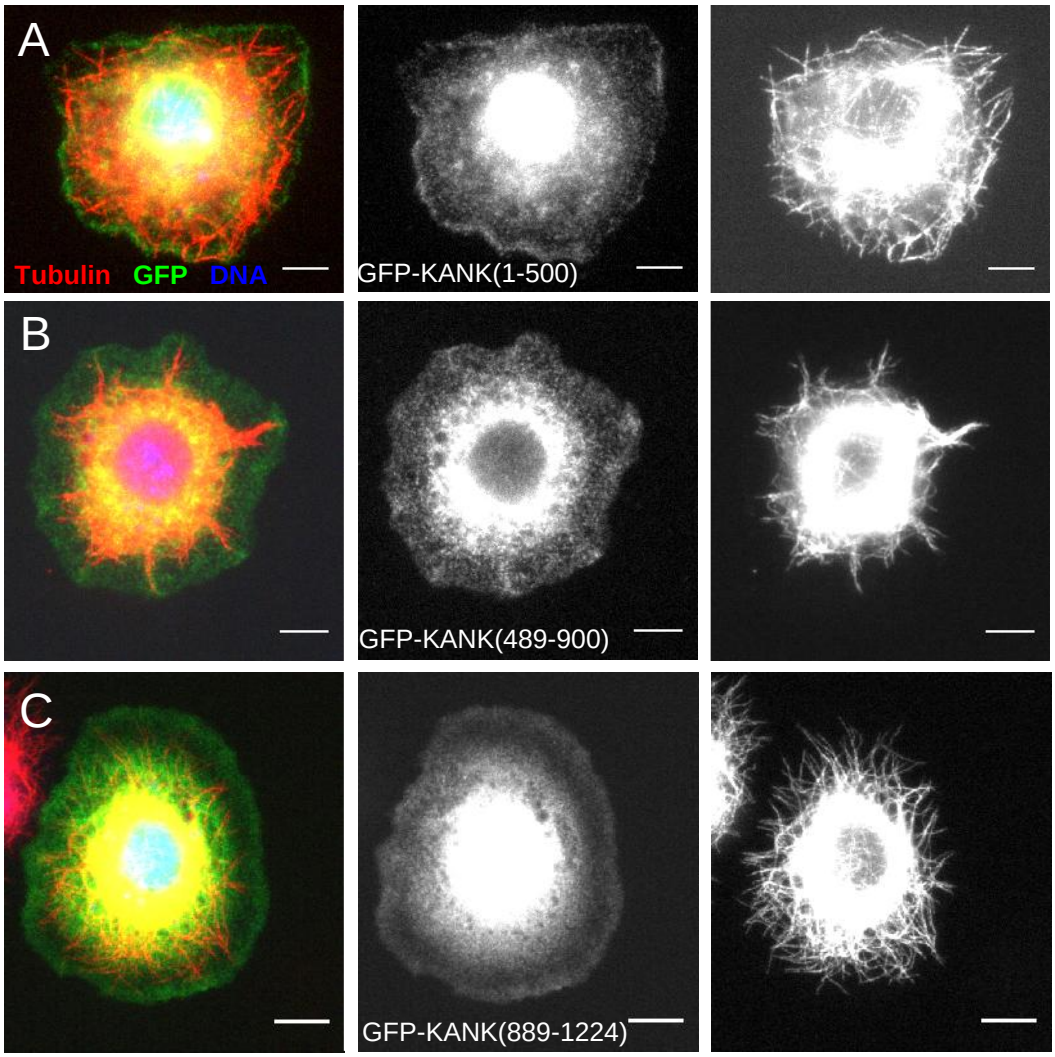

Figure 4.8 Truncations of KANK do not localise to microtubule ends in S2 cells. S2 cells were transfected with GFP labelled regions of KANK and immunostained for GFP and tubulin (A-C). Each GFP labelled region was observed to localise to the cytoplasm but specific localisation to microtubule ends was not seen. Nuclear localisation is evident for GFP-KANK(1-500) (A) and GFP-KANK(889-1224) (C) but is not observed for GFP-KANK(489-900) (B). Scale bar is 5μm.

KANK was identified in our lab as a protein which can directly bind EB1 *in vitro* and when KANK is expressed in S2 cells it can colocalise with EB1. In this section I determined if the interaction between KANK and EB1 was important for KANK localisation and identified the region of KANK required for EB1 dependent localisation in S2 cells.

4.2.2 EB1 RNAi Prevents KANK localisation to Microtubule Ends

EB1 is well known for recruiting proteins to microtubule plus ends. As KANK colocalises with EB1, I investigated if the localisation of KANK to microtubule ends was EB1 dependent. EB1 was depleted from S2 cells by RNAi. In parallel, RNAi of β-lactamase was performed on another population of S2 cells. As β-lactamase is not found in the genome of *Drosophila*, this acted as a control for any effects the cells may experience from undergoing the RNAi protocol. These two populations of cells were then transfected with GFP-KANK and costained for GFP and EB1. To confirm a reduction in the amount of EB1 in the cells an immunoblot probing for EB1 was performed. The immunoblot shows that compared to both β-lactamase RNAi and wild type cells, the amount of EB1 present in the EB1 RNAi cells is greatly reduced (Figure 4.9 A).

Localisation of GFP-KANK in β-lactamase RNAi cells was as previously described for GFP-KANK transfected S2 cells. In EB1 RNAi cells EB1 comets were fewer and their signal was perceived to be weaker. The number of EB1 and β-lactamase RNAi cells with GFP localised to more than half of the visible EB1 comets was counted (Figure 4.9 B). Localisation of GFP-KANK to EB1 comets is dramatically reduced in EB1 RNAi cells (2.1%) compared to control β-lactamase RNAi cells (65%) (Figure 4.9 C). The GFP-KANK signal was observed as a diffuse signal throughout the cytoplasm. Some colocalisation between GFP-KANK and EB1 was observed. This was expected as EB1 depletion was not 100% efficient. Depletion of EB1 results in alteration of KANK localisation, therefore KANK localisation to microtubule plus ends is dependent on EB1.

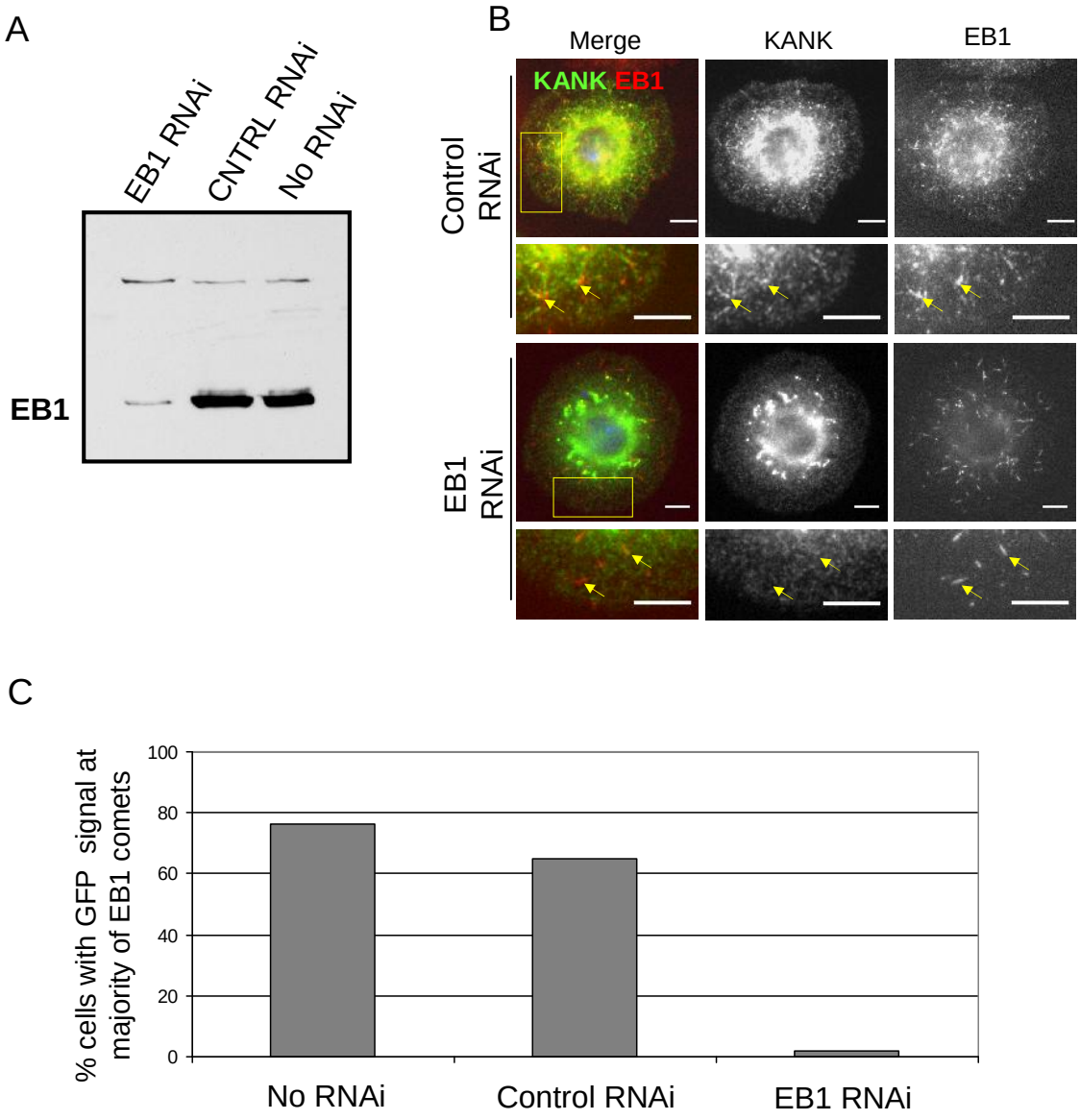

Figure 4.9: RNAi of EB1 in S2 cells abolishes KANK localisation at microtubule ends. RNAi of EB1 was carried out in S2 cells and confirmed by western blot (A), a non-specific band on the same immunoblot confirms roughly equal amounts of cell protein in each lane. These cells were transfected with GFP-KANK, fixed and stained. Comets were slightly affected in β-lactamase control cells. GFP-KANK did not localise to remaining EB1 in EB1 RNAi cells but did localise to EB1 in control RNAi cells (B) Scale bar is 5μm. (C) The percentage of cells with GFP localised to the majority of the visible EB1 comets was determined and it was found that EB1 RNAi abolishes KANK localisation to EB1 comets and to microtubule plus ends.

4.2.3 The Middle Region is Mainly Responsible For KANK/EB1 Interaction

KANK has been shown to directly bind EB1 *in vitro* (Dzhindzhev & Ohkura, personal communication) and EB1 is required for KANK localisation to microtubules in S2 cells. To determine the region of KANK which binds to EB1, KANK and its truncations were expressed *in vitro* using rabbit reticulocyte lysates and radioactively labelled with ^{35}S-methionine. The labelled proteins were incubated, separately, with bacterially produced MBP-EB1 and MBP coupled to amylose beads. The beads were washed and prepared as protein samples and run on an SDS gel, alongside samples of the labelled proteins taken before incubation. The gel was dried and exposed to a film. It was previously known that KANK can bind MBP-EB1 *in vitro* but does not bind MBP alone (Dzhindzhev & Ohkura, Personal Communication) therefore MBP was used as a positive control.

Binding between a labelled protein and EB1 was confirmed when the signal for the labelled protein bound to MBP-EB1 beads was higher than that of the signal for labelled protein bound to MBP beads. The unbound sample of labelled protein was used to confirm expression and molecular weight on the gel. EB1 binding was seen in long truncations which contained the middle region of the protein: KANK(502-1224), KANK(1-900). Inconsistent EB1 binding was seen for KANK(1-500) and KANK(502-900). The C-terminus of KANK when expressed alone did not bind EB1 (Figure 4.10). These results indicate that binding of KANK to EB1 is through the middle region of KANK, although the middle region expressed alone does not bind consistently. Some inconsistent binding can also occur via the N-terminal region of the protein.

4.2.4 KANK Binds EB1 via an SxIP motif

Truncations which contain the middle region of KANK can bind EB1 *in vitro*, while in S2 cells these truncations, apart from the GFP-KANK(489-900), show colocalisation with EB1 at microtubule ends. These data indicate that the middle region of KANK is responsible for KANK binding to EB1.

EB1 binding motifs are well-characterised, 4 amino acid motifs which have the defined sequence SxIP where x is variable (Honnappa et al., 2009; Jiang et al., 2012). KANK contains two putative SxIP sequences, in the middle region and in the ankyrin repeat domain. The ankyrin repeat domain alone does not exhibit EB1

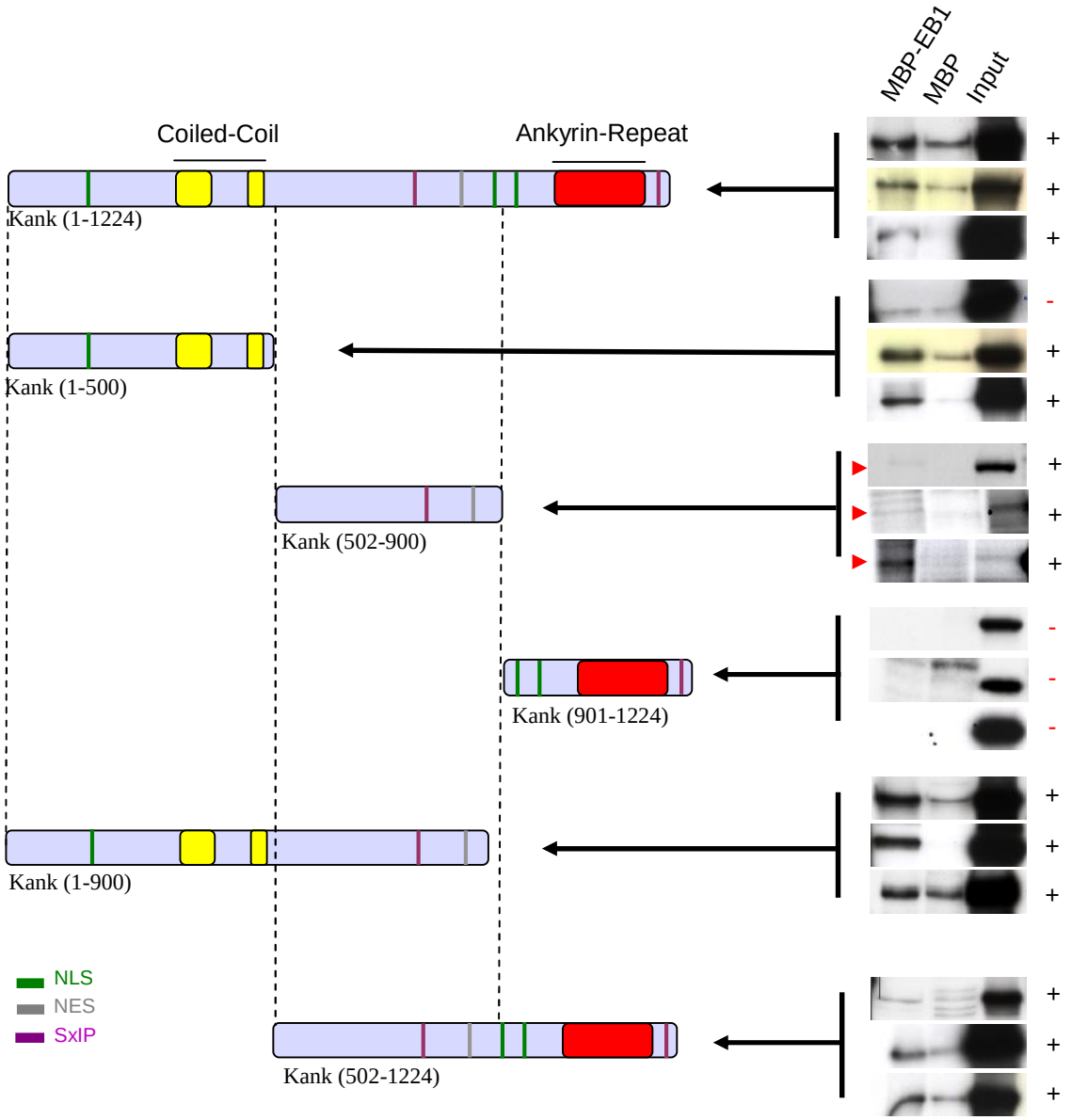

Figure 4.10 Truncations of KANK that contain the middle region and the coiled coil region can bind EB1 *in vitro*. The region of KANK with EB1 binding activity was identified by expressing radioactively labelled truncations of KANK *in vitro* and using MBP-EB1 to pull them down. MBP alone acted as a control. Some background binding was observed with MBP. Truncations which contained the middle region of KANK can bind MBP-EB1 stronger than MBP alone. The middle region of KANK binds EB1 weakly in this pull down. The middle region of KANK likely contains the EB1 binding region, while the coiled coil region is dispensable for binding but may contribute to the KANK/EB1 interaction.

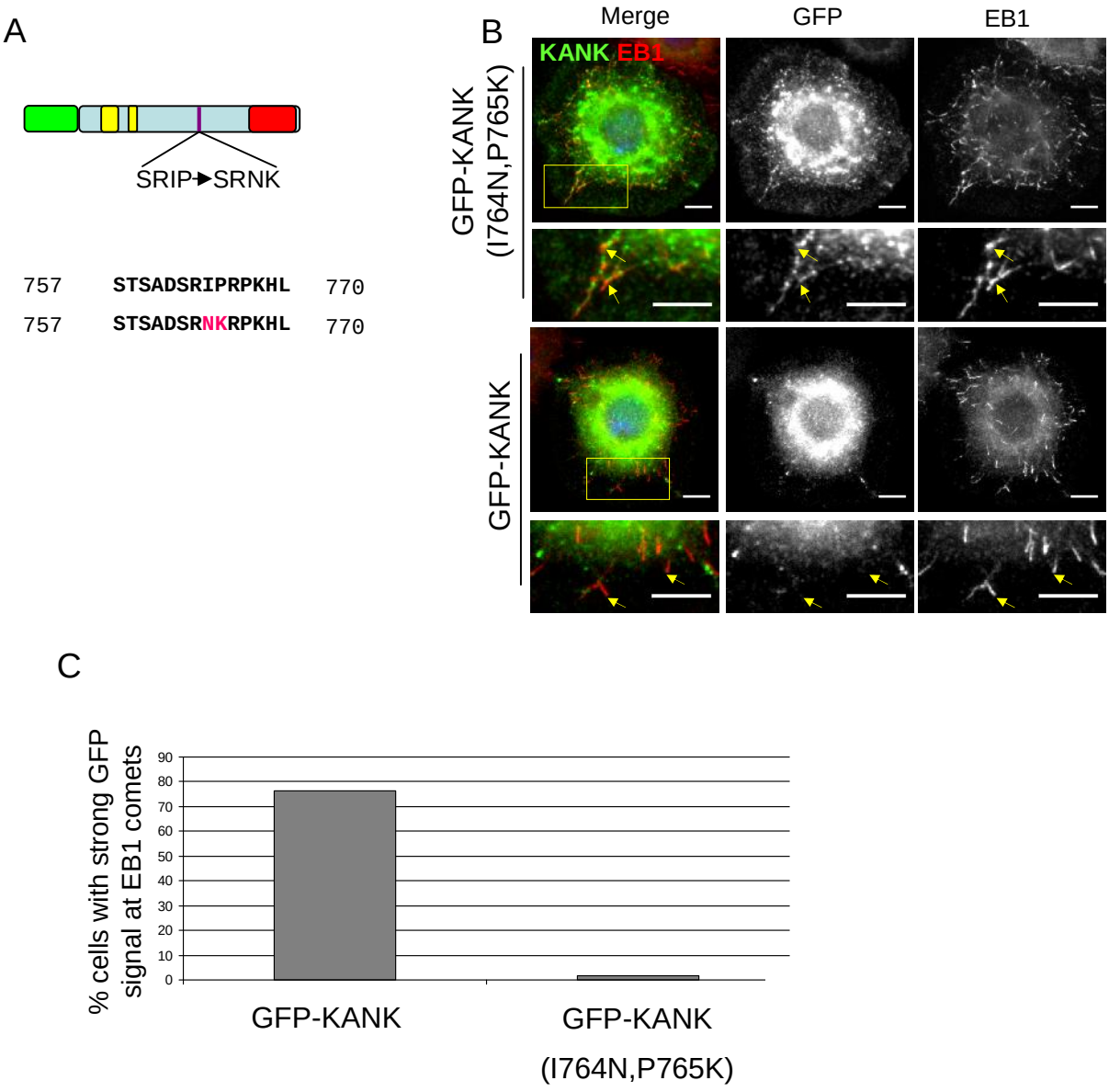

Figure 4.11 Mutation of an SxIP motif in KANK abolishes its co-localisation with EB1. (A). A two amino acid substitution was made in an SxIP motif of GFP-KANK to create GFP-KANK(I764,P765K) (B) S2 cells were transfected with GFP-KANK(I764,P765K) and coimmunostained for GFP and EB1. The GFP signal did not localise to EB1 comets in cells transfected with GFP-KANK(I764,P765K). Scale bar is 5μm. (C) The number of cells with a strong GFP signal at EB1 comets at microtubule ends was significantly lower than seen in cells transfected with GFP-KANK.

binding in S2 cells and is not pulled down by MBP-EB1 *in vitro*, therefore it is unlikely the motif in this region functions in EB1 binding. The motif in the middle region of the protein, however, is a good candidate for EB1 binding.

To determine if this SxIP motif was responsible for EB1 binding, the SxIP sequence was mutated to SxNK creating KANK (I764N,P765K) (Figure 4.11 A) which was then labelled with GFP and transfected to S2 cells (Figure 4.11 B). The transfected cells were coimmunostained for GFP and EB1. The GFP signal was observed to be diffuse within the cytoplasm with very little signal co-localised with EB1 to microtubule ends. The number of cells with GFP signal at more than half of the visible EB1 comets was counted and found to be greatly reduced in GFP- KANK (I764N,P765K) (1.5%) compared to cells expressing GFP-KANK(76.5%) (Figure 4.11 C).

Although KANK/EB1 interaction was not abolished, mutation of the SxIP motif in the middle region of KANK reduces its binding to EB1 and significantly delocalises the protein from microtubule ends. Therefore the SxIP motif in the middle region of KANK is required for the KANK/EB1 interaction.

4.3 Localisation of KANK in *Drosophila* embryos

4.3.1 Background

KANK was detectable in *Drosophila* embryos using immunoblotting. KANK is observed to increase in expression over the course of embryogenesis with protein expression detectable from 3-6 hours and reaching its peak at 15-18 hours of embryonic development (Section 3.4.3). An increase is embryonic lethality was observed in *kank* mutant embryos. These data indicate a role for KANK in embryogenesis. In this section I describe the observed localisation of KANK in *Drosophila* embryos. A summary of *kank* mutants is given in Figure 3.15.

4.3.2 Late Stage Embryos Display a Stereotypic Pattern of KANK Staining

To determine if KANK was detectable and could be visualised in fixed embryos, flies were left to lay eggs on grape juice plates and the embryos aged appropriately. After aging, embryos were collected and fixed in methanol. The

embryos were then coimmunostained for KANK and with 22c10. 22c10 stains the Map1b-like protein futsch, which localises along microtubules in the neurons of the peripheral nervous system (Hummel et al., 2000). Staining with 22c10 allows visualisation of neurons which is convenient to orient embryos and provides a map of the embryo body. Embryos from stages 10-15 were examined. However, localisation during these stages was not consistent between experiments.

In the later stages of *Drosophila* development, stages 16/17, KANK localisation becomes very distinct and consistent. Each hemi segment (half segment) distinctly displays eight spots of KANK signal, arranged as four spots in a line along the ventral-lateral axis and four parallel spots in a line along the dorsal-lateral axis, the posterior most spots are shifted ventrally (Figure 4.12). These lines of spots lie either side of the chordotonal organ, visible due to the staining with 22c10. No KANK staining was observed in *Δkank* embryos (Figure 4.13) which confirmed absence of KANK expression in *Δkank* embryos. Occasionally, staining of the pharynx was observed in both w^{1118} and *Δkank* embryos, indicating that this particular staining is non-specific.

As the chordotonal organ is situated at the lateral transverse muscles of the somatic musculature, whose structure may be reflected in KANK staining, it is possible KANK is expressed in muscle cells. Further KANK staining can be seen at intersegmental boundaries, which may reflect the topography of some somatic muscles which lie at these intersegmental areas.

4.3.3 KANK Localisation Reflects the Localisation of Myotendinous Junctions

Embryos were coimmunostained using antibodies specific for KANK and actin. The actin antibody apparently stained every individual cell in the embryos, allowing visualisation of certain cells, particularly those of the somatic musculature due to their distinct topography.

When the somatic musculature can be distinguished, KANK staining is observed at the sites of attachment between the somatic muscle and nearby tendon cells (Figure 4.14 A). Specifically, KANK staining is most apparent at the lateral transverse muscles as parallel lines of dots. KANK staining is also visible at the ends of muscle cells which have attachment sites to tendon cells at intersegmental borders,

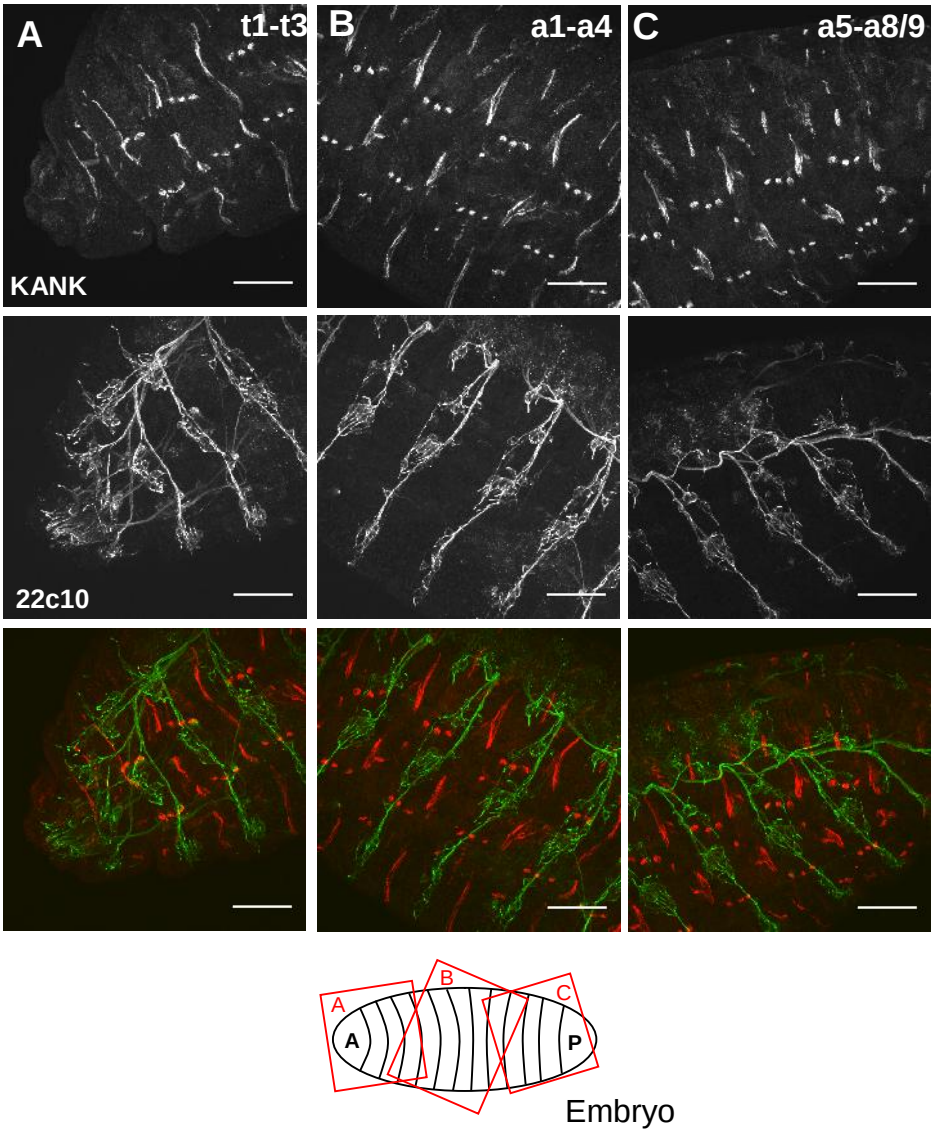

Figure 4.12 KANK antibody stains in a specific pattern. Embryos were co-immunostained for KANK and 22c10. The KANK antibody stains embryonic segments in a repeated, stereotypic pattern and stains intersegmental areas. t1-t3: Thoracic segments. a1-a9 Abdominal segments. Scale bar is 40µm.

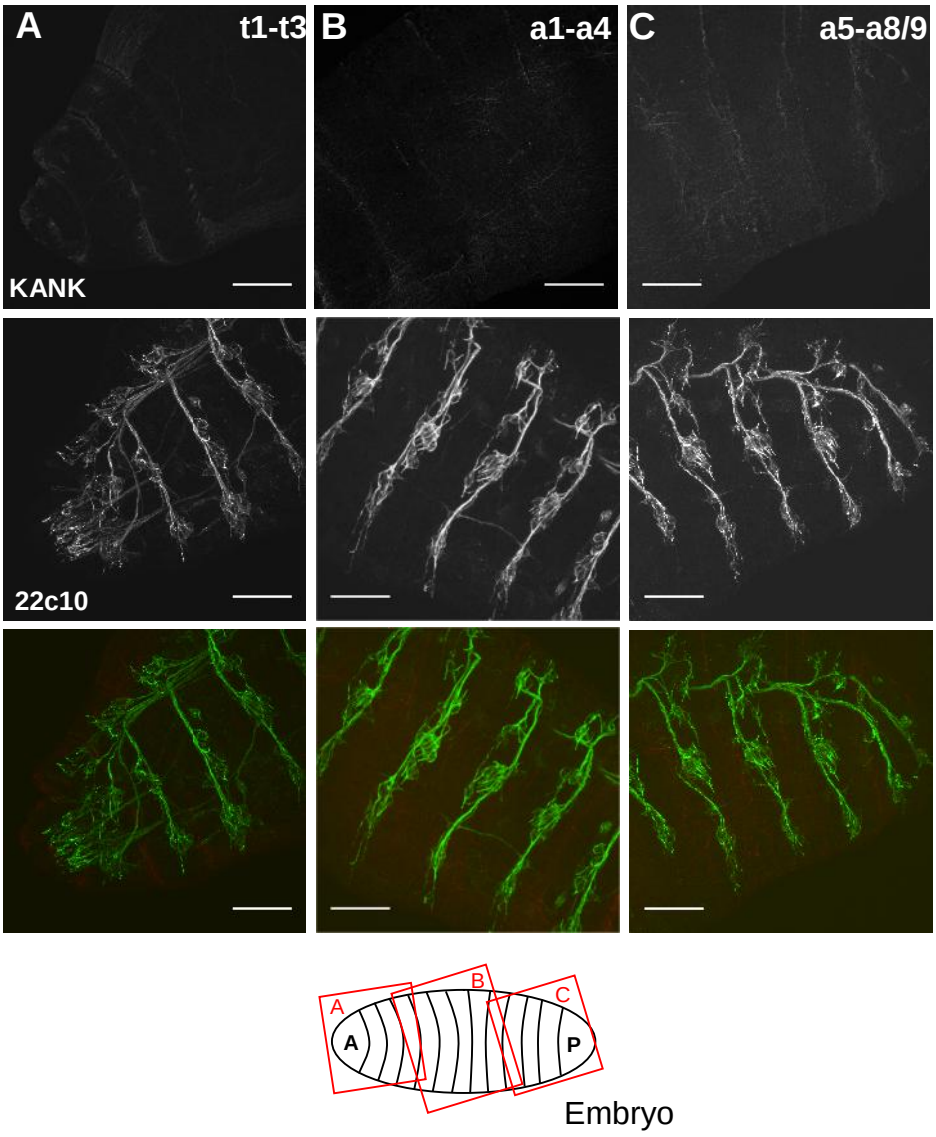

Figure 4.13 The KANK antibody does not show specific staining in *Δkank* embryos. Embryos were co-immunostained for KANK and 22c10. No KANK staining was seen in *Δkank* embryos. This both indicates the specificity of the antibody for endogenous KANK and confirms that the protein is not expressed in these mutants. t1-t3: Thoracic segments. a1-a9 Abdominal segments. Scale bar is 40μm.

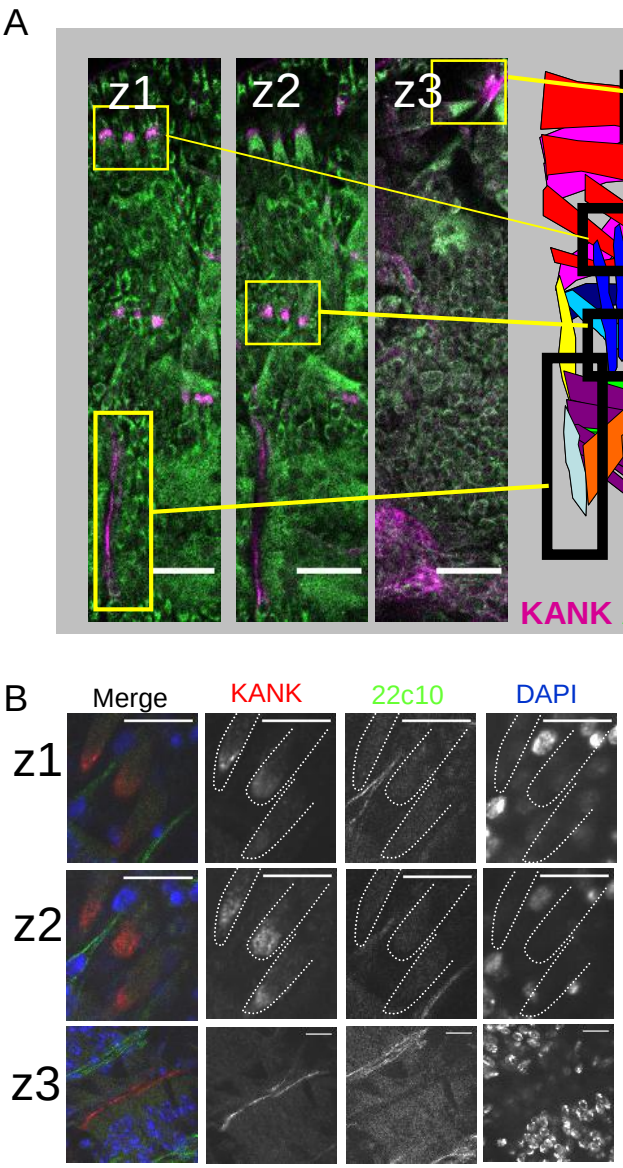

Figure 4.14 KANK localises at the attachment sites of somatic muscle cells. (A) Stage 16/17 *w*^{1118} embryos stained for KANK (magenta) and actin (green) show that KANK is localised to the ends of those cells which resemble the pattern of somatic musculature. Z1-3 show z-sections of the same embryo. The cells of the somatic musculature are visible. KANK staining corresponds with the borders of somatic muscle cells. Scale bar is 40μm. (B) Stage 16/17 embryos were stained for KANK (red) and with 22c10 (green). Background staining makes the structure of somatic muscles partially visible in late stage embryos. KANK staining is visible at the ends of muscle cells where attachment sites to tendon cells form. Z1-2 show two z sections of lateral transverse muscles in which KANK is observed localising towards the tips. Scale bar is 50 μm. (C) KANK localises to the periphery of dorsal muscles at intersegmental borders. Scale bar is 10μm.

that is, the borders of the larval body segments. Closer examination of the lateral transverse muscles, whose structure is visible as background staining in 22c10 stained embryos, indicates that KANK is likely present within the multinucleate muscle cell and seems localised towards the end of the muscle (Figure 4.14 B).

These muscle cells form attachment sites with epidermal cells, that is, the myotendinous junction (MTJ). Localisation of KANK staining is identical to that seen for other proteins which localise to the MTJ, such as the spectraplakin *shot* which localises to all MTJs in the developing embryo (Strumpf and Volk, 1998). However, while proteins which localise to the tendon side of the MTJ have a punctate appearance, KANK staining is not punctate and resembles the pattern seen for proteins which localise to the muscle side of the MTJ (Ellis et al., 2011). These data indicate that KANK localises at sites of muscle attachment to epidermally derived tendon cells in late stage embryos, specifically those attachment sites where a MTJ is forming or has formed.

4.3.4 Disruption of KANK Expression Does Not Affect KANK Localisation

Remobilisation of a P-element within the *kank* gene region resulted in imprecise excision of DNA from a nearby exon. These embryos ($kank^{\Delta 17}$) express KANK at a lower level than that seen in w^{1118}, though they have an increase in embryonic lethality similar to that seen in *Δkank*.

An attempt to rescue the embryo lethality by insertion of the *kank* gene elsewhere in the genome of *Δkank* flies resulted in embryos (*kank;res* strain) that have increased embryonic lethality compared to w^{1118} and *Δkank*. This increase in lethality may be due to lack of regulation of KANK expression.

To determine if KANK localisation was similar to that seen in w^{1118}, $kank^{\Delta 17}$and *kank;res* embryos were collected at stage 16/17 and fixed in methanol. Embryos were then co-immunostained for KANK and with 22c10. Although immunoblotting of embryos from $\Delta kank^{17}$ indicates that expression of KANK is lower than that seen for w^{1118}, KANK localises in a stereotypic pattern reflecting apparent MTJs, as seen in w^{1118} in 7 out of 10 embryos observed (Figure 4.15). In the remaining 3 embryos, no KANK expression was observed.

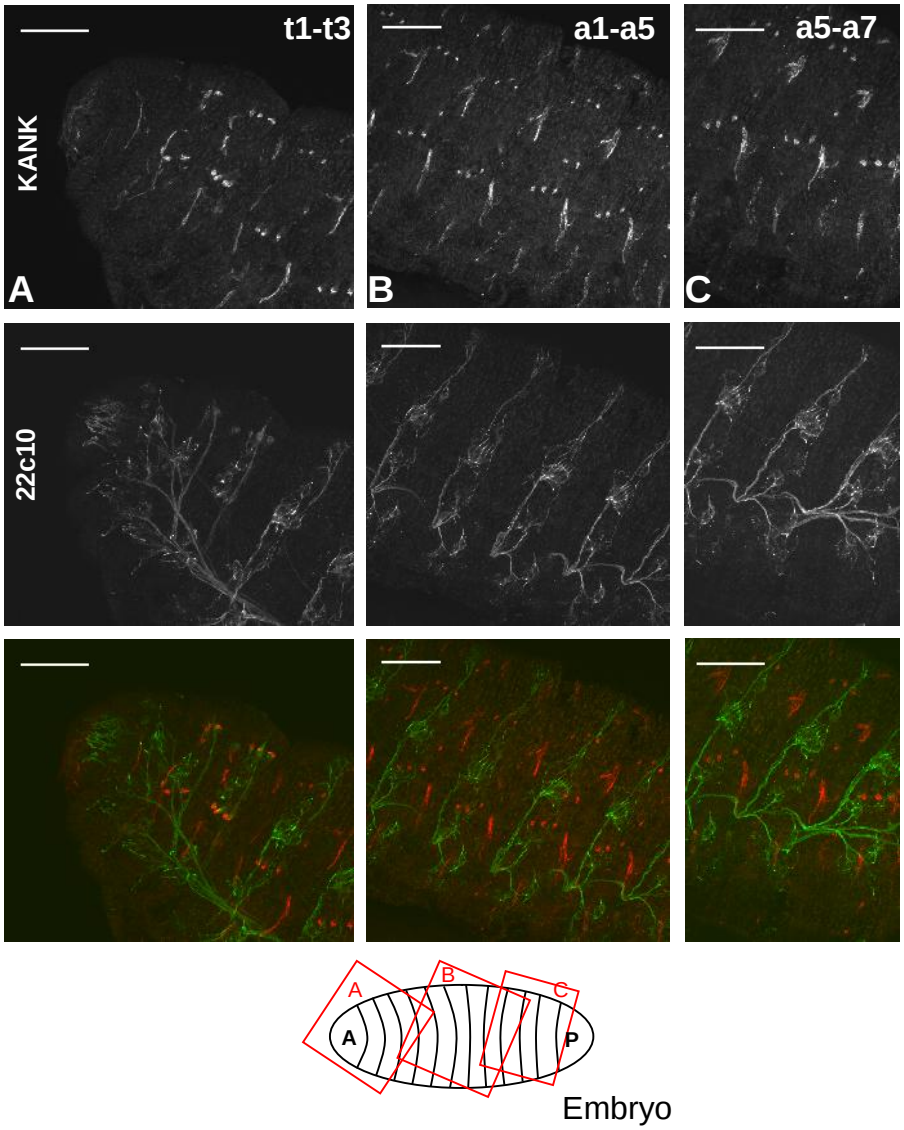

Figure 4.15 KANK staining in *kank*$^{\Delta 17}$ is similar to that seen in *w*^{1118}. Embryos were co-immunostained for KANK and with 22c10. The KANK antibody stains embryonic segments in a repeated, stereotypic pattern and stains intersegmental borders. This staining was observed in 7 out of 10 *kank*$^{\Delta 17}$ embryos. t1-t3: Thoracic segments. a1-a7 Abdominal segments. a8/a9 are not shown. Scale bar is 40µm.

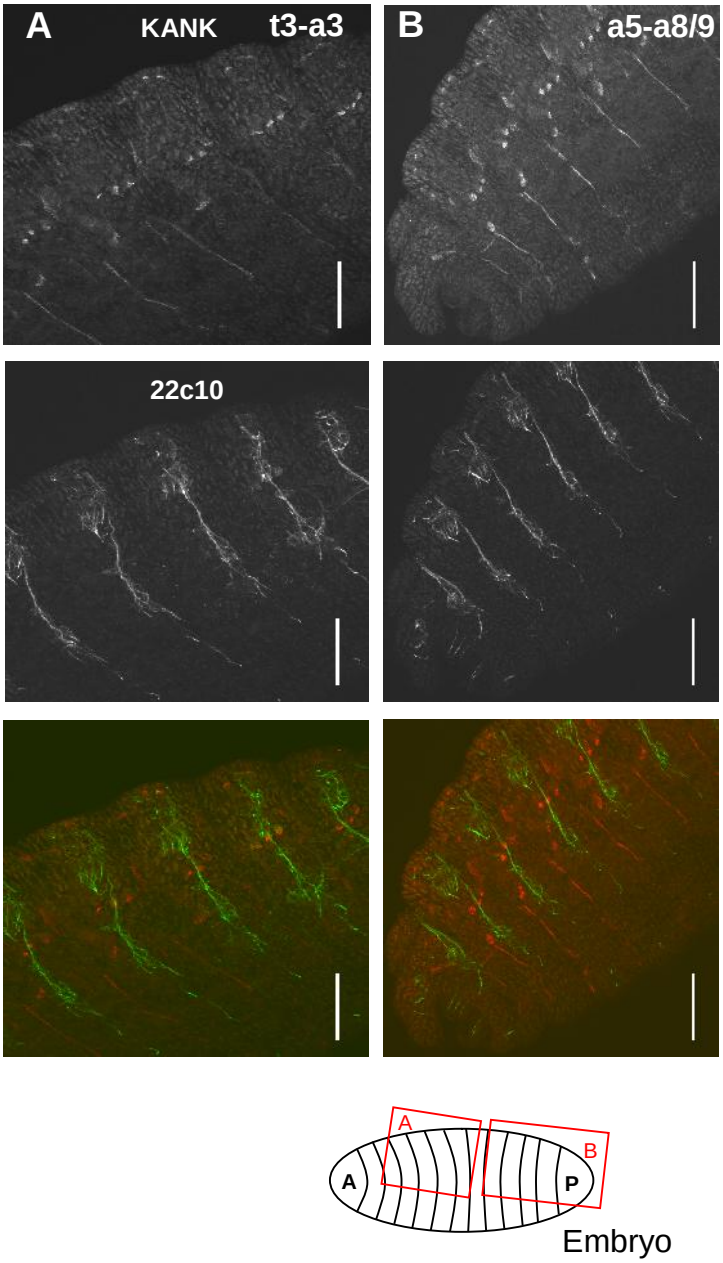

Figure 4.16 KANK staining in *kank;res* is similar to that seen in *w*^{1118}. *Kank;res* Embryos were co-immunostained for KANK and with 22c10. The KANK antibody stains embryonic segments in a repeated, stereotypic pattern and stains intersegmental borders. *kank;res* were only briefly examined. t1-t3: Thoracic segments. a1-a8/9 Abdominal segments. Scale bar is 40µm.

Embryos from *kank;res* were briefly examined (Figure 4.16). In *kank;res* embryos, KANK is localised in the stereotypic pattern observed for w^{1118} in 7 out of 7 embryos examined.

4.4 Discussion

4.4.1 KANK Localisation to Microtubule Ends Requires EB1

Endogenous KANK shows cytoplasmic localisation, and some localisation to microtubule ends in interphase S2 cells. This microtubule localisation becomes more apparent when GFP-KANK is expressed in these cells under an actin promoter. GFP-KANK localises to plus ends of microtubules, colocalising with EB1, though not directly overlapping with the EB1 comet. This distinct localisation was not reported for mammalian cell lines. It is unclear if this localisation is specific to *Drosophila* KANK or is common to all Kank family proteins and is so far unobserved.

Drosophila KANK was originally identified as an EB1 interacting protein (Dzhindzhev & Ohkura, Personal Communication) and human Kank proteins (Kank2 and Kank4) have been identified as putative EB1 interactors. This study has indicated that KANK interacts with EB1 in S2 cells directly predominantly through its SxIP motif. Firstly, Truncations of KANK which contained this region (amino acids 500-900) can be consistently pulled down by MBP-EB1 when expressed *in vitro*, although the poorly translated middle region KANK(502-900) does not bind consistently. Secondly, this region contains a motif that fits to the SxIP consensus sequence which has been found to facilitate EB1 binding (Honnappa et al., 2009; Buey et al., 2012). Mutation of this putative EB1 binding motif in KANK prevented KANK localisation to microtubule ends, as did RNAi of EB1. KANK requires EB1 to localise to microtubule ends and interacts with EB1 through an SxIP motif present in the middle region of KANK.

In vitro experiments indicated that some EB1 binding may occur through the N-terminal region of the protein. This is further supported by evidence from transfected S2 cells, in which KANK(489-1224) which lacks the N terminal region has a significant reduction in GFP/EB1 colocalisation while KANK(1-900) does not display a significant reduction. As the effect of the mutation in the SxIP motif was so

strong (Figure 4.11 C) if this region of KANK does contribute to EB1 binding in cells, the effect is minor. EB1 is an important microtubule binding protein and EB1 binding is the primary method of microtubule plus end localisation for a number of proteins (Section 1.3). Therefore the function of this KANK-EB1 interaction is likely to be localisation of KANK to the growing ends of microtubules. This localisation has not been demonstrated for other Kank proteins.

4.4.2 KANK Exhibits Nuclear Localisation

GFP- KANK can localise to the nucleus of S2 cells and accumulates there if cells are treated with leptomycin-B, an inhibitor of active nuclear export. However, this occurs in relatively few cells (~14%). Both GFP-KANK(1-500) and GFP-KANK(889-1224) localise to the nucleus in most S2 cells, therefore it is likely they contain nuclear localisation signals (NLS) and possibly lack a nuclear export signal (NES). KANK(1-500) contains an NLS which has the same sequence as the NLS found in the KN motif of other human Kank family proteins and was found to contribute to localisation of human Kank1 in some cultured cell lines (Wang et al., 2006). GFP-KANK(889-1224) contains two putative NLS (Section 3.1). GFP-KANK(1-900) and GFP-KANK(489-1224) do not localise to the nucleus, despite containing these putative NLS. There are three possible reasons for this.

Firstly, there is a putative NES in the overlapping region present in both of these truncations, which may prevent their accumulation in the nucleus. A second possibility is that this overlapping region contains a signal that inhibits nuclear import of the protein. Finally, a less likely possibility is that localisation of these truncations to the ends of microtubules prevents them from being available to enter the nucleus. Treatment of S2 cells with leptomycin-B would indicate if transient localisation of these truncations to the nucleus occurs.

KANK can localise to the nucleus and it is the middle region of the protein which prevents its accumulation there. KANK may have a nuclear function. Human Kank1 has been shown to accompany the transport of β-catenin from the cytoplasm to the nucleus (Wang et al., 2006) and it is possible this function is conserved in *Drosophila.*

4.4.3 KANK is Localised in Stereotypic Pattern Which is Reflective of Sites of Muscle Attachment to Epidermis

An antibody specific to KANK(489-900) stains in a stereotypic pattern in wild type embryos at stages 16/17. This staining is not seen in *Δkank* embryos, confirming loss of KANK expression in these flies and the specificity of the antibody. Unfortunately, distinct staining was seen with only one of the four antibodies created during this study. Some nonspecific staining of the embryonic pharyngeal cells was observed in both w^{1118} and *Δkank*, though this was not consistent. No staining was seen in neurons, despite some evidence for neuronal localisation of VAB-19 in *C.elegans* (Ding et al., 2003) and possible neuronal expression of KANK indicated by a mild RNAi phenotype in cultured primary neurons (Sepp et al., 2008).

The observed pattern for KANK staining is reflective of myotendinous junctions (MTJ) in developing embryos as seen in embryos stained for *shot* (Strumpf and Volk, 1998). This localisation is not affected in $kank^{\Delta 17}$despite disruption of KANK expression confirmed by immunoblotting or in *kank;res.* Though it was not observed, misregulation of *kank* expression in *kank;res* during embryogenesis may lead to expression of KANK in non-muscle cells which may in turn lead to the increased embryonic lethality in *kank;res* seen in Section 3.7, though that is purely speculative.

Kank proteins have not been conclusively localised in mammals. It is known that the long isoform of Kank1 (Kank-L) has higher expression in liver, heart kidney and skeletal muscle tissues than in other tissues. In *C. elegans*, GFP-VAB-19 localises to muscle-epidermal attachment structures, consistent with the localisation observed for KANK. However, GFP-VAB-19 was observed to localise in the epidermal cells which made contact with muscle. The function of KANK in muscle cells at MTJs has yet to be determined. Data from *C. elegans* indicates that VAB-19 is essential to maintain myotactin, VAB-10A and intermediate filaments at attachment sites. *Drosophila* does not contain any cytoplasmic intermediate filaments. The *Drosophila* homologue of myotactin, *sidekick,* functions in cell adhesion at synapses in the retina (Yamagata et al., 2002) but has no known function in *Drosophila* muscles. *Shot*, the *Drosophila* homologue of VAB10A has been

demonstrated to be required in tendon cells for MTJ formation and functions in an EB1 dependent manner. *Shot* also displays a similar localisation to KANK in the late stages of embryogenesis (Strumpf and Volk, 1998). It would be interesting to determine if *Shot* localisation is affected in *Δkank* embryos, or vice versa.

Chapter 5

Effects of KANK Disruption on *Drosophila melanogaster*

5.1 Haemocytes from *Δkank* flies do not have observable altered microtubule dynamics

KANK family proteins have been shown to play a role in cell migration, specifically in fibroblast migration during wound healing assays (Li *et al.*, 2011). In this study KANK was found to form a complex with the human proteins BIG1 and KIF21A, and this complex was necessary to alter cell polarity in response to external cues. Little is known about the *Drosophila* homologues of these proteins, Sec71 and KLP31E respectively.

When the *Δkank* strain, prior to the publication of suitable ModEncode data, was generated little expression data was available. However, Kank1 has been shown to affect the growth rates of naturally motile cells in humans – red and white blood cells (Kralovics et al., 2005) – as mentioned in Section 1.5. Haemocytes are migratory, motile cells which play a role in immune response in *Drosophila*. To determine if there is any affect of the KANK deletion in these natural motile cells in *Drosophila*, I compared the microtubule network in haemocytes which were obtained from 3rd instar larvae between three *Drosophila* strains: $\Delta kank^{B}$ and two controls w^{1118}, *yw;Df(2R)ED2423/SM6A*. W^{1118} cells were used as a wild type control. Homozygous *Δkank* larvae were obtained from *Δkank/Df(2R)ED2423.* For this reason, *yw;Df(2R)ED2423/SM6A* were used as a second control to ensure that if an affect was seen it was not due to mutations introduced to the *Δkank* strain from the deficiency strain. Haemocytes were prepared by puncturing an individual larva in Schneider media supplemented with a protease inhibitor. This media was then placed on a Concanavalin A coated coverslip and cells were allowed to adhere before being fixed with methanol. Haemocytes were immunostained for tubulin.

Four categories of microtubule network organisation were observed (Figure 5.1 A) classified as bundled, half bundled, spread and normal. However, no significant difference between the microtubule networks of the three strains was found (Figure 5.1 B). Retrospectively, it is unlikely that KANK is expressed in these cells, making this result far from surprising.

A

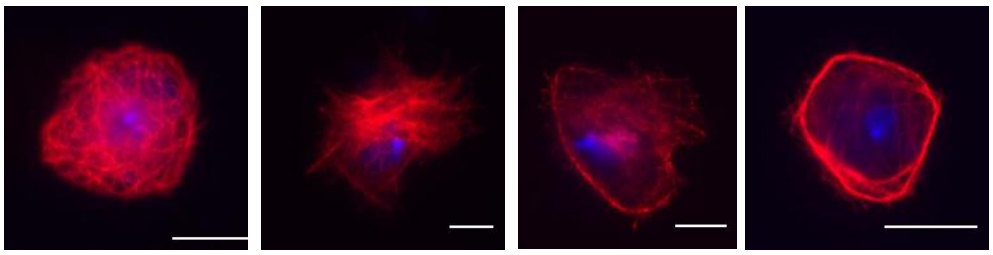

Normal Spread Half-Bundled Bundled

B

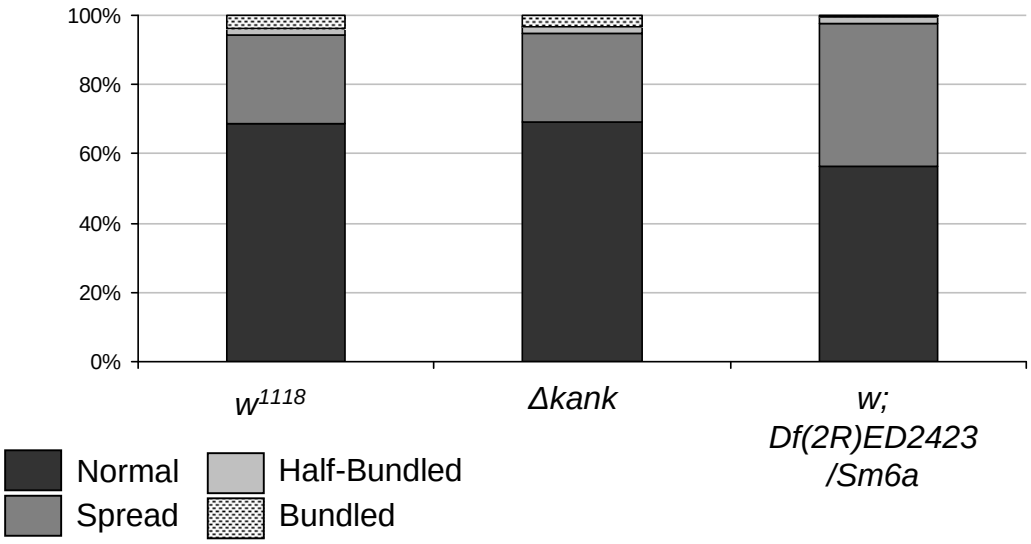

Figure 5.1 Deletion of *kank* does not effect the microtubule network of haemocytes. (A) Haemocytes from *Δkank* and two controls were prepared from 3rd instar larvae and immunostained for tubulin. 4 different morphologies were observed for the microtubule network of haemocytes on ConA coverslips Scale bar is 5μm. (B) The prevalence of each morphology was counted and results were compared between strains. Each strain showed a similar number percentage of each microtubule network morphology.

5.2 Neuronal Structures Are Mildly Affected By Loss of KANK Expression

5.2.1 Background

RNAi of KANK in cultured neurons leads to mild phenotypes (Sepp *et al.,* 2008) such as slight blebbing and increased axon complexity. KANK staining was not observed in the neurons of late stage embryos; however, the possibility that a loss of KANK expression might affect neuron development in *Drosophila* embryos was explored. A summary of *kank* mutants is given in Figure 3.15.

5.2.2 Deletion of KANK Results in a Mild neuronal Phenotype.

To determine if loss of KANK affected neuron growth, I fixed *Δkank* mutant embryos at stage 16/17 when neuron development is almost complete and stained with 22c10. This antibody stains the protein Futsch which binds microtubules in neuronal cells of the peripheral nervous system (PNS) and parts of the central nervous system. The overall pattern of the PNS is unaffected in embryos which lack KANK expression. However, subtle morphological abnormalities can be observed: Neurons in *Δkank* embryos display slight unbundling. The unbundling is particularly evident in the thoracic segments when axons projecting from the CNS begin to separate (Figure 5.2 A). Such unbundling was occasionally observed in w^{1118} but the extent of unbundling was noticeably lower and incidences were observed less frequently than in mutants. As whole mount embryos were viewed in this experiment, any method of quantification was unreliable as the angle of observation could not be accounted for.

This mild neuronal phenotype was also seen in flat preparations of *Drosophila* embryos (Figure 5.3).

5.2.3 Chordotonal Organs in kank Deletion Embryos Are Abnormally Positioned Compared to Wild type

To determine if morphological defects could be observed in more complex structures of the PNS, fixed embryos at stage 16/17 were stained with 22c10 and the abdominal chordotonal organs were observed.

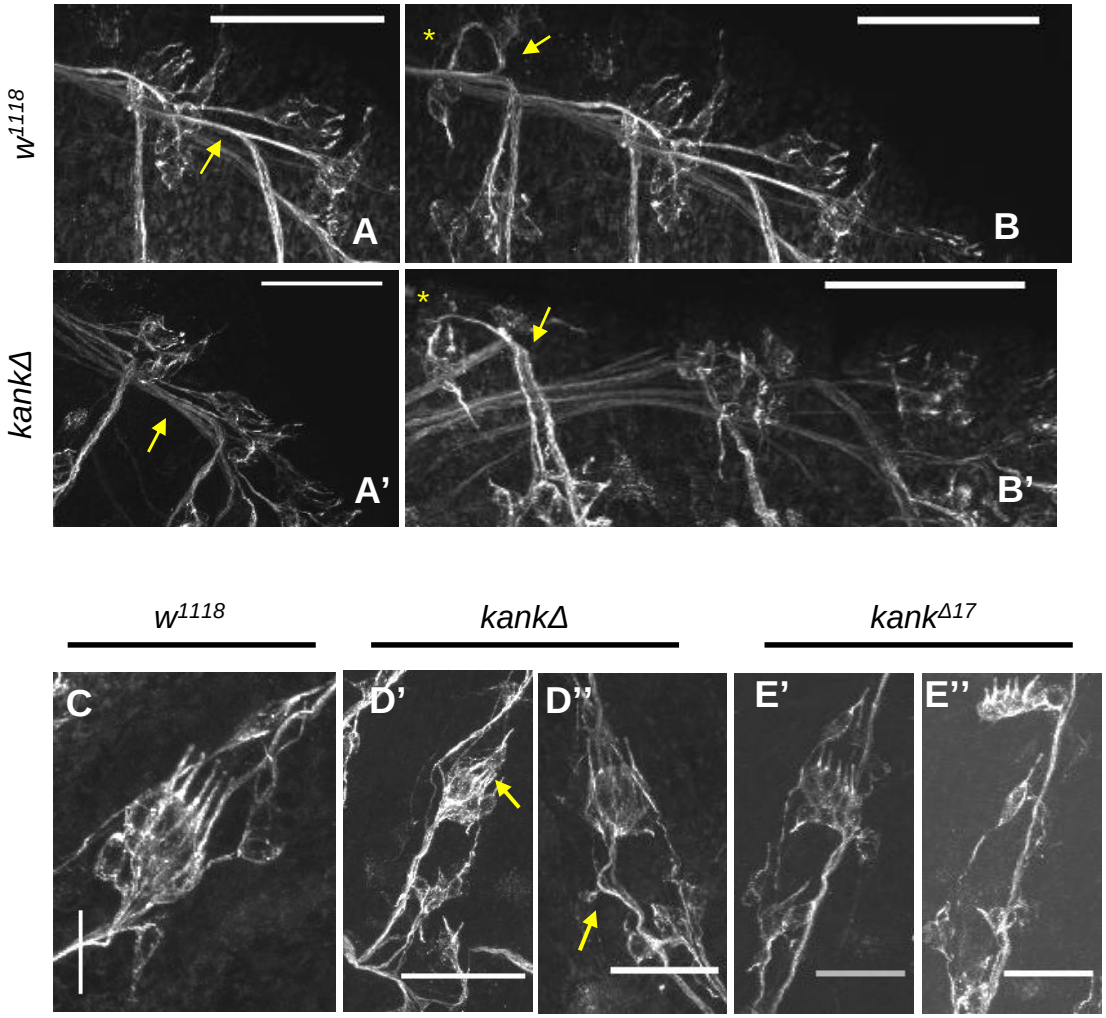

Figure 5.2 Mild abnormalities were observed in neurons of *Δkank* embryos. Neurons in *Δkank* mutant embryos displayed subtle abnormalities ranging from unbundled axons (A' and B', yellow arrows) and some abnormal positioning of neurons (asterisk). These abnormalities were occasionally seen in w^{1118} but never to same degree. Scale bar is 50 µm. (C) A wild type (w^{1118}) abdominal chordotonal organ (CO). (D'-D'') The COs of *Δkank* mutants are slightly mispositioned compared to w^{1118}. This looks to be a result from mispatterning of the surrounding neurons which is evident in the mildly twisted neuron (yellow arrow in D''). Occasionally the disorder is within the CO (yellow arrow in D'). (E'-E'') This phenotype was also observed in $kank^{\Delta 17}$ mutants. (E'). Occasionally an extreme phenotype was observed (E'') which has not been observed in w^{1118}. These incidences were rare. Scale bar 20µm.

In w^{1118} mildly abnormal chordotonal organs are seen in 5/50 abdominal segments, representing sections of 15 embryos (normal wild type is shown in Figure 5.2). Abnormality was generally characterised by chordotonal organs positioned mildly incorrectly relative to the surrounding neurons. The incidence of abnormality in the positioning of the chordotonal organ was greatly increased in *Δkank* embryos where mild abnormalities were observed in the chordotonal organs of 21/45 abdominal segments representing 13 embryos (Figure 5.2 D). Unbundling of the neurons leading from the CNS to the chordotonal organs was also seen in these embryos. This abnormal morphology was also detected in 18/38 chordotonal organs of $kank^{\Delta 17}$ embryos, in which *kank* genomic DNA is disrupted, representing 8 embryos (Figure 5.2 E).

5.3 Larvae lacking KANK expression do not show coordination or motility defects

5.3.1 Background

Kank proteins have been associated with cerebral palsy and congenital fibrosis of the extraocular muscles (CFEEOM) in humans (Lerer *et al.,* 2005; Kakinuma & Kiyama 2009). This implicates a role for Kank proteins in neuromuscular development. As KANK localises to myotendinous junction sites and *kank* mutants display a mild defect in neuron patterning, it was possible that coordination of muscles might be affected in mutant larvae. To determine if this was the case, motility and overall body coordination in $\Delta kank^{B}$ (*Δkank)* larvae were compared to w^{1118}. A second control (*yw;* y^{+}*Sco/CyO*) was also used. This strain is genetically dissimilar from the deletion mutant and the wild type control and was used to determine if the assays were fit for purpose. Four different motility assays were carried out. The burrowing assay outlined below was carried out with only one control (w^{1118}).

5.3.2 Larvae lacking KANK expression do not show motility defects

This assay determines if there are any effects of a mutation on overall larval movement and coordination (adapted from Batlevi *et al.,* 2010). The number of gridlines passed by an individual larva in a defined amount of time is measured.

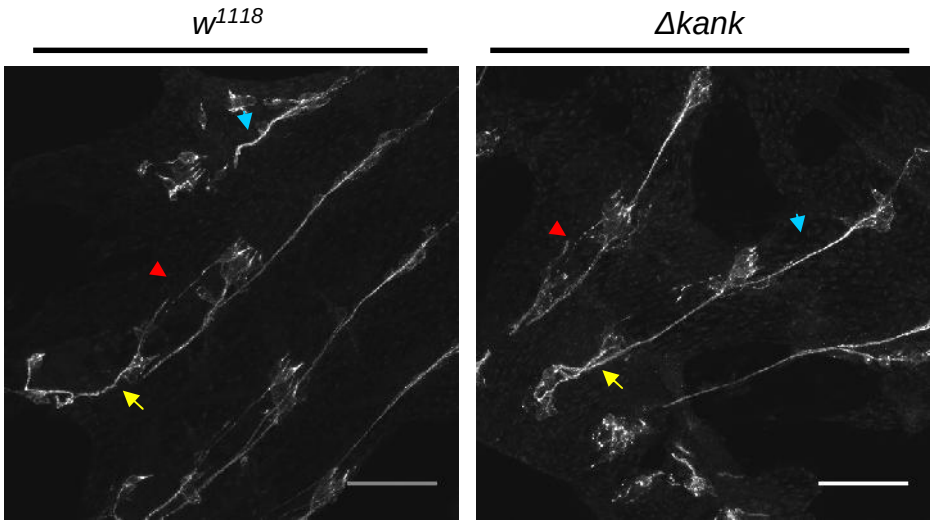

Figure 5.3 Flat preparations of *Drosophila* embryos show some abnormalities in neurons. Flat preparations of *Drosophila* neurons were made and the tissue stained with 22c10 antibody. Some abnormalities were observed in neurons, such as early branching (yellow arrow in *Δkank* – correctly branched neuron indicated by yellow arrow in w^{1118}) and some slight misrouting of neurons (yellow arrow – corresponding correctly formed neurons indicated by red arrowhead in w^{1118}). The technique, however, is difficult to perfect and some effect on the surrounding tissues was observed (blue arrowheads) indicating that this data may not be sound. Scale bars are 40 μm.

The number of gridlines crossed by the *Δkank* larvae was similar to that crossed by the w^{1118} control ($p>0.05$), while the *yw;* y^{+}*Sco/CyO* control showed a significant decrease in motility compared to w^{1118} ($p<0.05$) (Figure 5.4 A).

5.3.3 Larvae lacking KANK expression do no show muscle movement defects

This assay determines if the waves of muscle contraction and relaxation that larvae use to propel themselves (known as peristaltic waves) are coordinated and also tests if they occur at normal rates, relative to controls (adapted from Feiguin *et al.*, 2009). The peristaltic waves were closely examined to check they travel the entire length of the larva in a coordinated fashion. This was found to be the case for all three strains examined. The number of peristaltic waves a larva demonstrates within one minute was counted. The difference between the *Δkank* and w^{1118} was not significant ($p>0.05$). However, the *yw;* y^{+}*Sco/CyO* control showed a significant reduction ($p<0.05$) (Figure 5.4 B).

5.3.4 Larvae lacking KANK expression do not show righting defects

This assay addresses if larvae maintain coordination between their dorsal and ventral muscles (adapted from Ubhi *et al.*, 2007) and also muscle power as it a strenuous movement for a larva to right itself. Larvae were rolled from their dorsal to their ventral sides and righting was timed. The time taken by *Δkank* and w^{1118} was almost equivalent (~30 seconds) while the *yw;* y^{+}*Sco/CyO* control took less time to right (~15 seconds) (Figure 5.5 A).

5.3.5 Larvae Lacking KANK Display Wild type Burrowing Behaviours

In order to determine if any minor locomotor difficulties exist (adapted from Wu *et al.*, 2003). 30 larvae from each genotype were placed on top of food and put in the dark for two hours, after which the number of larvae remaining on top of the food was counted. It is thought that larvae with locomotor difficulties will not have the muscle strength or coordination to burrow efficiently. Three repeats showed that there was no significant difference between the *Δkank* and the w^{1118} larvae (Figure 5.5 B).

5.4 Larvae Lacking KANK React to Noxious Stimuli

Embryos lacking KANK have a mild neuronal phenotype which may be maintained during larval development. It is possible that, though larvae can move and coordinate themselves, they may have trouble communicating sensory signals. This assay is used to determine if larvae will react to noxious stimuli, in this case an uncomfortable stimulation with a blunt instrument which mimics the ovipositor of a parasitic wasp. 3rd instar larvae have been shown to attempt to evade this signal as a survival mechanism (Hwang *et al.*, 2007). Three strains were tested, w^{1118} $\Delta kank^{B}$ and *Δkank;P[kank]*. Larvae were placed on a Petri dish with some PBS. The larvae were then stimulated with a home-made Von-Frey fibre, which mimics the ovipositor of a parasitic wasp, across the abdominal and thoracic segments (Hwang et al., 2007). A maximum of 10 stimulations were applied per larva. A lack of response within 10 stimulations was marked as non-responsive.

A slight difference in larval responses was observed. While 8/44 w^{1118} and 9/43 $\Delta kank^{B}$ larvae were marked as non-responsive (roughly 20%), this number grew to 16/49 larvae for *Δkank;P[kank]* (33%). This difference was found not to be significant between strains ($p>0.05$). The number of stimulations required to illicit a response was averaged for each strain and were found to be the same (Figure 5.6) with a positive response recorded for each strain after an average of 3 stimulations. Loss of KANK and its effect on neuron development does not effect reactions of larvae to a noxious stimulus.

5.5 Discussion

5.5.1 Kank Deletion Mutants Display a Mild Neuronal Phenotype

KANK expression is maintained throughout the *Drosophila* lifecycle, its expression increases during embryonic development, and peaks at stage 16/17. Embryos at these stages are close to hatching and have fully formed muscles and neurons. No neuronal staining is observed with an antibody specific for KANK. Despite this, RNAi of KANK in primary neurons grown in culture results in a mild abnormal phenotype (Sepp et al., 2008) and an indication of VAB-19 localisation to neuronal processes in *C. elegans* (Ding et al., 2003b).

Subtle unbundling of neurons was observed in *Δkank* mutants, which was seen far less often in w^{1118}. This phenotype posed some difficulties for quantification as it did not represent a binary situation, neurons were not simply perfectly bundled or unbundled. This was further augmented by variations in embryo positioning, which made viewing thoracic neurons (where unbundling was most apparent) difficult. Chordotonal organs in *Δkank* embryos display a mild abnormal morphology. The effect was subtle; the position of chordotonal organs is somewhat skewed relative to the surrounding neurons. This was also observed in $kank^{\Delta 17}$ embryos. This effect may be a consequence of the 'unbundling' phenotype. It is possible that axonal growth along aberrant pathways may lead to incorrect positioning of chordotonal organs relative to the surrounding neurons.

KANK may affect neuron growth and mechanosensory organ positioning by directly affecting cytoskeletal organisation. The growth cone of developing axons relies on the tightly regulated cooperation between actin, microtubules and their associated regulators. KANK demonstrates EB1 binding (this study) and its homologues demonstrate a possibly conserved role in actin regulation (Ding et al., 2003b; Kakinuma et al., 2008a; Roy et al., 2008). Therefore, KANK may have a role in linking microtubules and actin in growth cones. For example, KANK may bind EB1 to hitchhike on growing microtubules to the actin rich P domain of the growth cone and, responding to regulatory cues, repress actin nucleation through by inhibiting Arp2/3. Inhibition of Arp2/3 in mammalian hippocampal neurons can negatively regulate growth cone translocation by increasing the ratio of tyrosinated to acetylated microtubules, which enhances axon elongation (Strasser et al., 2004).

The neuronal defect observed may account for the effect of lack of Kank1 expression in humans, namely a condition resembling cerebral palsy characterised by mental retardation and spastic quadriplegia. It is possible that the abnormal phenotype observed in humans is due to cerebral dysgenesis, abnormal brain formation. Although it is possible the subtle neuronal phenotype observed in *Δkank* contributes to the rise in embryonic lethality, it is unlikely that this is due to the effect on chordotonal organs. Mutants for *atonal* lack chordotonal organs and hypomorphic alleles for EB1 lead to aberrant chordotonal organ morphology, neither of these is lethal (Elliott et al., 2005; Jarman et al., 1993).

5.5.2 Lack of KANK Does Not Affect Larval Motility or Reaction to Noxious Stimuli

KANK displays localisation to muscle cells and does not localise to neurons but displays a mild neuronal phenotype. I intended to determine if larvae demonstrated motility, coordination or sensory defects. Two controls, w^{1118} representing wild type flies and *yw;Sco/CyO,y*$^{+}$, a balancer stock, were chosen. The use of two controls served to demonstrate if the assays were valid by determining if the results from two genetically dissimilar strains with no apparent neuronal or muscular defects were in agreement.

No significant difference is seen in locomotion, muscle coordination or muscle movement between *Δkank* and w^{1118} larvae. This indicates that KANK disruption does not affect motility. Results from the second control differed from w^{1118} in each assay, these differences were significant. In the righting assay where *yw;Sco/CyO,y*$^{+}$ was significantly slower in the motility test ($p<0.05$) and took significantly less time to right then the other two strains ($p<0.05$). A disruption in neuron patterning has been shown for *scutoid* mutants (Tom et al., 2011) though this was only demonstrated in olfactory neurons, it may be present in other sensory neurons. This may contribute to the difference seen between w^{1118} and *yw;Sco/CyO,y*$^{+}$.

The ability of larvae with disrupted KANK expression to respond to noxious stimuli, in this case prodding, is unaffected. Neither misexpression, in *Δkank;P[kank]* nor KANK deletion led to a disrupted nociceptive response. Both of the strains observed have increased embryonic lethality and it is possible that those embryos which survive to larval stages have overcome any deleterious effect of *kank* disruption.

It is possible, it must be said, that these assays were unsuitable for their intended purpose. However, it is more likely – since five assays were used and all are in agreement – that disruption of *kank* expression does not lead to any change in larval motility or defect in sensory signalling.

A

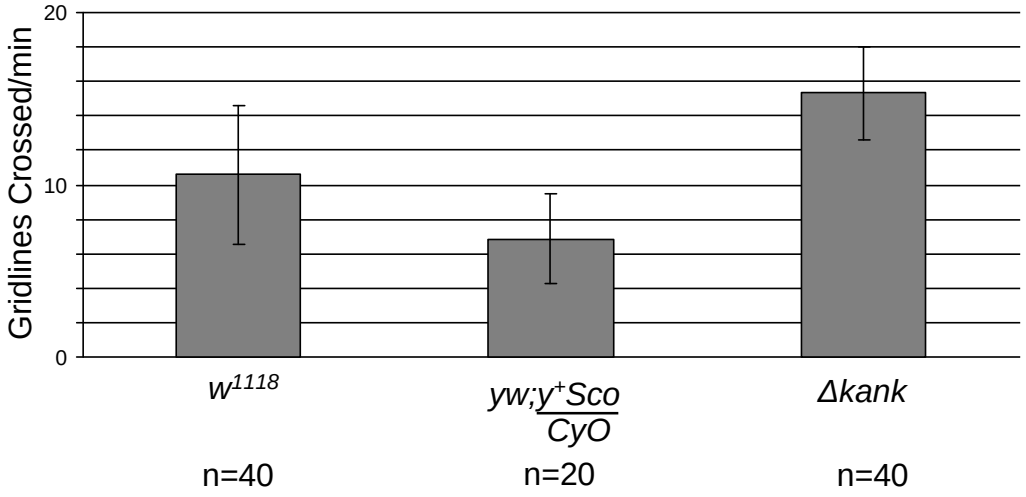

B

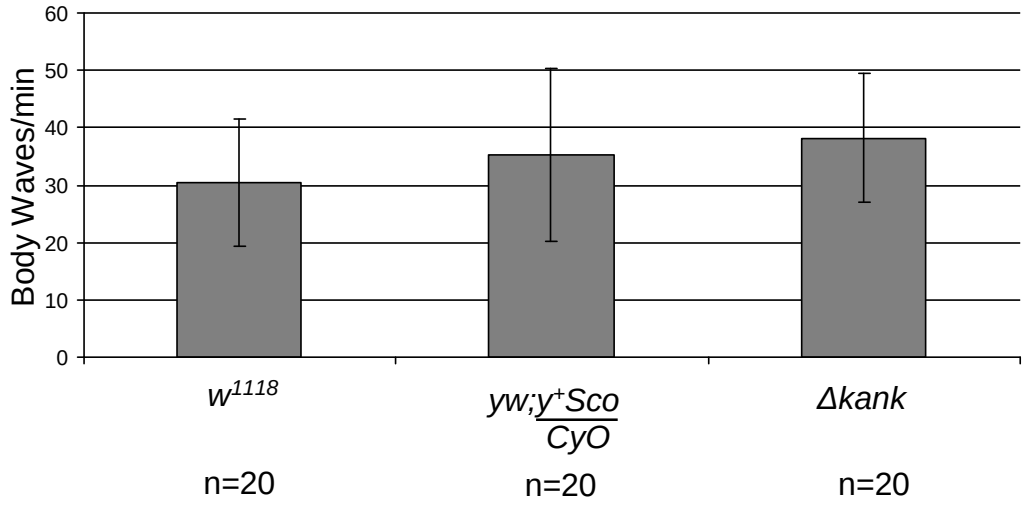

Figure 5.4 *Δkank* larvae do not show defects in motility. (A) The motility of late third instar larvae from two controls and *Δkank* was examined by allowing the larvae to crawl over gridlines on an agarose plate. The number of gridlines passed in 1 minute was counted. *Δkank* mutants did not differ from w^{1118} significantly ($p>0.05$). (B) The overall coordination and motility of larvae was then examined by counting the number of full body motile waves carried out by larvae in one minute. No significant difference was seen between *Δkank* and w^{1118} ($p>0.05$).

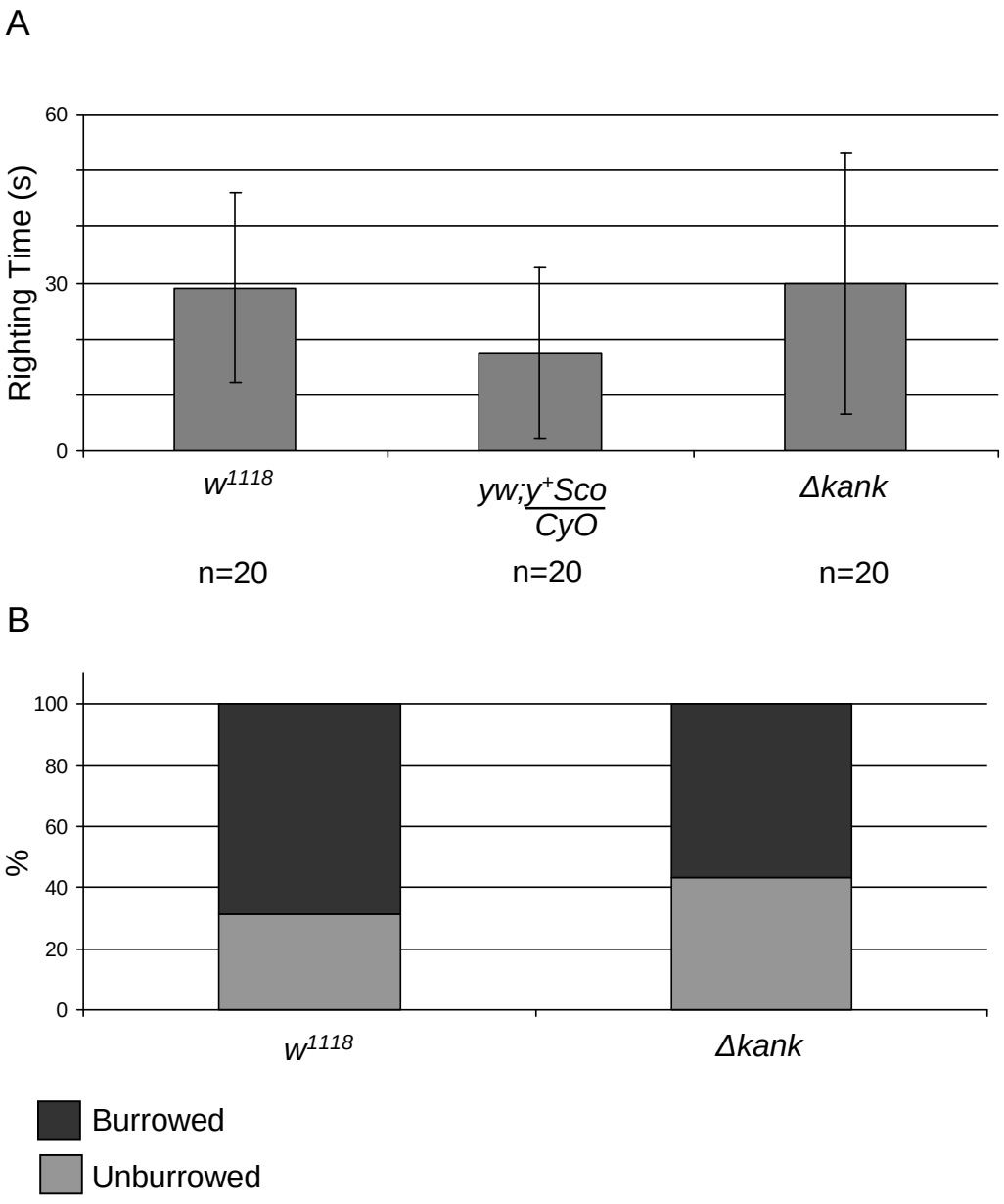

Figure 5.5 Motility assays with *Δkank* larvae do not show defects in motility. (A) Late third instar larvae were rolled from their ventral to their dorsal side while on an agarose plate. The time taken for them to right themselves was measured. *Δkank* larvae did not differ significantly from w^{1118} ($p>0.05$) (B) How well *Δkank* could burrow and move in food was determined. Third instar larva were placed on top of food in a bottle which was then placed in the dark for 2 hours. After this time, the number of larvae remaining on the food was counted. No significant difference was observed between strains ($p>0.05$).

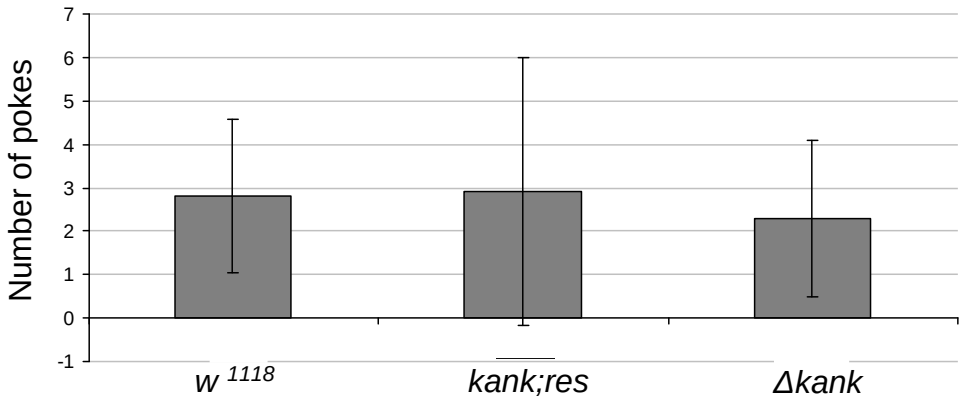

Figure 5.6 Reaction to noxious stimuli by 3rd instar larvae from three strains was similar. Larvae from each of the three strains: *w1118, kank;res, Δkank,* (n= 44, 49, 43 larvae respectively) were manually stimulated to elicit a response. The number of stimulations required to elicit a response was similar between strains. Disruption of KANK expression does not affect reaction to noxious stimuli.

Chapter 6
Discussion and Future directions

6.1 Summary and Conclusions

6.1.1 KANK Interacts Directly With EB1 in S2 Cells via an SxIP Motif

KANK interacts with EB1 directly to localise at microtubule growing ends. This interaction was confirmed by *in vitro* pull-down assays. An SxIP motif in the middle region of KANK was found to be predominantly responsible for this interaction as its mutation led to delocalisation of KANK. This interaction is likely to function in KANK localisation. SxIP motifs are found in human Kank1 and Kank4. However, a recent study which searched for mammalian EB1 binding proteins did not identify these proteins in EB protein binding assays, though did identify Kank2, which does not contain an SxIP motif. Localisation to microtubule ends was not observed for Kank1 in mammalian cells, therefore it is unclear if the interaction is conserved.

6.1.2 KANK Localises at Sites of Muscle-Epidermal Attachment

KANK localises in a stereotypic pattern in late stage embryos. This pattern reflects the pattern of myotendinous junctions (MTJ), sites of attachment between muscle and epidermally derived tendon cells which enable movement. This localisation is similar to that seen for GFP-VAB-19 in *C. elegans*, where GFP signal was seen at muscle attachment sites in developing nematodes. KANK localises at the ends of muscle cells at the sites of these junctions. Notably, GFP-VAB-19 localisation in *C. elegans*, as GFP signal was seen in epidermal cells.

VAB-19 is required for the maintenance of attachment structures in *C. elegans* during development and components of this structure become unlocalised in *vab-19* temperature sensitive mutants. It is possible that KANK has a role in maintenance of the MTJ in *Drosophila*. It would be interesting to determine of components of the MTJ remain localised in *Δkank* mutants.

6.1.3 Disruption of KANK Expression Increases Incidences of Embryonic Lethality

KANK is the only *Drosophila* member of the conserved Kank family of proteins. VAB-19, the single *C. elegans* Kank protein, is essential while disruption of Kank1 expression in humans leads to developmental disorders such as cerebral palsy.

Despite this, KANK expression was found to be expendable for the survival of in adult flies and no abnormal phenotypes were observed in adults.

Immunoblotting revealed that KANK expression begins in embryos between 3-6 hours after egg laying and peaks between 15-18 hours after egg laying, after which expression is reduced and maintained throughout the life cycle. Disruption of KANK expression leads to an increase in embryonic lethality, which was further increased when *kank* expression was restored from an insert which lacked regulatory elements from the *kank* genomic sequence. This indicates an important role for *kank* during embryonic development.

6.1.4 Disruption of KANK Expression Leads to Mild Disruption of Neuronal Patterning

Immunostaining late stage embryos with the 22c10 antibody revealed subtle abnormal patterning of the neurons. This was particularly evident in chordotonal organs of the abdomen. No localisation of KANK was observed in neurons, indicating that either expression in neurons is low, or KANK expression in muscle cells indirectly affects patterning of neurons during development. Interestingly, VAB-19 was seen to localise to neuronal processes in *C. elegans* where loss of VAB-19 also resulted in disruption of the localisation of myotactin and VAB10A (Ding et al., 2003a). The *Drosophila* homologues of these proteins, *sidekick* and *shot* respectively, have both been shown to affect neuron development. *Sidekick* can affect cell adhesion in retinal synapses(Yamagata et al., 2002) while *shot* is necessary to link actin and microtubules during axonal growth (Alves-Silva et al., 2012).

As KANK is an upstream inhibitor of actin nucleation (Kakinuma et al., 2008b; Roy et al., 2008; Strasser et al., 2004) it is also possible that a mild loss of actin regulation in growth cones results in axon paths which deviate slightly from the expected route.

Neuromuscular defects are seen in humans with Kank1 disruption. No affect on motility, muscle movement was observed. Importantly, these assays were performed on 3rd instar larvae. It is plausible that embryos which hatch have overcome any neuromuscular defects caused by the absence of KANK.

6.2 Future Directions

6.2.1 Confirming the KANK Phenotype

As previously mentioned (Section 3.7.3) the crosses carried out to create mutants with disrupted KANK expression (*Δkank* and $kank^{\Delta 17}$) use some of the same strains. In addition, insertion of part of the *kank* gene region elsewhere in the genome did not rescue the embryonic lethal phenotype. Therefore it has not been conclusively determined that *kank* disruption is responsible for the observed developmental defects. In order to confirm *kank* as the culprit, it will be necessary to attempt to replicate the phenotype through other means, for example, to determine if KANK RNAi flies also exhibit increased embryonic lethality and display mild neuronal defects. If *kank* is shown to be definitively responsible then this study has highlighted the importance of regulated KANK expression during embryogenesis. Embryos lacking KANK are nearly three times more likely than wild type to suffer arrest during embryogenesis. How this occurs, however, remains unanswered.

It is possible that no abnormal phenotype is observed in post-embryo *Drosophila* stages of *Δkank* as those embryos which are most affected do not hatch. It will be important to confirm this by determining if a mild neuronal phenotype is present in *Δkank* larvae. Determination of KANK localisation in older *Drosophila* life-cycle stages will also be necessary.

6.2.2 Investigation of the KANK-EB1 Interaction in Flies

Whether the KANK-EB1 interaction occurs in flies and its exact role remains to be uncovered. To determine if KANK and EB1 colocalise a fly strain with both GFP-EB1 and mCherry-KANK insertions might be created and somatic musculature and neurons observed during embryogenesis to determine if the proteins have a similar localisation. This can be done in fixed or live samples. I created a strain containing mCherry-KANK during this project though it has not been used thus far. It will be interesting to see if EB1 in necessary for KANK localisation in the multicellular organism. This particular question poses some difficulties as disruption of EB1 can affect many different proteins. As we have the *kank* BAC plasmid (*P[kank, w^+]*) it is possible to introduce base-pair mutations which result in a mutation of the SxIP

motif in KANK, as performed in S2 cells. Introduction of this mutated insert to *Δkank* flies and determination of the localisation of KANK in such flies might help determine if KANK localisation in *Drosophila* embryos is EB1 dependent.

6.2.3 Further Investigation of Myogenesis in KANK Mutants

To investigate the role of KANK during embryogenesis further, I feel it will be necessary to observe the pattern of somatic musculature in late stage embryos of *Δkank* mutants. Human Kank1 has established roles in polarity and actin regulation (Kakinuma et al., 2008a; Li et al., 2011; Roy et al., 2008) which may affect the growth of muscle cells towards the epidermis and thus muscle formation in late stage embryos. Disruption of this process may contribute to the increase in embryonic lethality observed. Somatic musculature can be visualised in strains of flies expressing GFP under a *myosin-heavy chain* (*Mhc*) promoter, which would allow differentiation between these cells and other cells in the embryo which was not possible with immunostaining against actin. Given the KANK-EB1 interaction observed, it will also be interesting to see if microtubules in muscle cells are affected which can be achieved using GFP-tau expressed under a *Mhc* promoter.

The localisation of KANK may reflect a role in formation or maintenance of the myotendinous junction on the muscle-side. Correct formation of the muscle-side hemi-adherens junction can be visualised by immunostaining for integrins associated with its formation, specifically *inflated* (αPS2).

6.2.4 Further Investigation of Neurogenesis in KANK Mutants

KANK localisation was not observed in neurons, though they show abnormal morphology in mutants with disrupted KANK expression. Targeted RNAi of KANK in muscle cells and subsequent examination of the neurons will be useful in determining if the expression of KANK in these cells indirectly affects neuron growth. Data from *C. elegans* implicates a role for KANK in synaptogenesis (interaction with myotactin/sidekick and EPS-8/Arouser-see below). Determination of synapse number in the brains of *Δkank* mutants may be worth investigating as such a phenotype may confirm the role of KANK in neurogenesis. Synapses in the

brain can be visualised upon introduction of the synapse marker synaptotagmin-GFP under a UAS promoter *kank* mutants and wild type.

6.2.5 Analysis of KANK Interactors May Contribute to Understanding KANK Function

EB1 is highly unlikely to be the only binding partner of KANK. Data from other organisms indicates that KANK may interact with a host of proteins. For example, EPS-8 was identified as a binding partner of VAB-19 in *C. elegans*. Disruption of the *Drosophila* homologue of EPS-8, Arouser, has recently been shown to increase the number of synaptic terminals in post-embryonic stages, a phenotype which was identified when adult flies showed increased sensitivity to ethanol (Eddison et al., 2011). An attempt to determine if KANK interacts with Arouser through an *in vitro* pulldown assay was hampered as consistent transcription and translation of the Arouser clone from the *Drosophila* Gold Collection was not achieved. It would be of great future interest to determine if KANK partakes in the same cytoskeletal signalling pathways as human Kank proteins.

Bibliography

ADAMS, M.D. (2000). The Genome Sequence of *Drosophila melanogaster*. *Science* (80-.). 287, 2185–2195.

AKHMANOVA, A, HOOGENRAAD, C.C., DRABEK, K., STEPANOVA, T., DORTLAND, B., VERKERK, T., VERMEULEN, W., BURGERING, B.M., DE ZEEUW, C.I., GROSVELD, F., ET AL. (2001). Clasps are CLIP-115 and -170 associating proteins involved in the regional regulation of microtubule dynamics in motile fibroblasts. *Cell* 104, 923–935.

AL-BASSAM, J., LARSEN, N. A, HYMAN, A. A, AND HARRISON, S.C. (2007). Crystal structure of a TOG domain: conserved features of XMAP215/Dis1-family TOG domains and implications for tubulin binding. *Cell* 15, 355–362.

AL-BASSAM, J., KIM, H., BROUHARD, G., VAN OIJEN, A., HARRISON, S.C., AND CHANG, F. (2010). CLASP promotes microtubule rescue by recruiting tubulin dimers to the microtubule. *Developmental Cell* 19, 245–258.

ALVES-SILVA, J., SÁNCHEZ-SORIANO, N., BEAVEN, R., KLEIN, M., PARKIN, J., MILLARD, T.H., BELLEN, H.J., VENKEN, K.J.T., BALLESTREM, C., KAMMERER, R. A, ET AL. (2012). Spectraplakins promote microtubule-mediated axonal growth by functioning as structural microtubule-associated proteins and EB1-dependent +TIPs (tip interacting proteins). *Journal of Neuroscience* 32, 9143–9158.

AMOS, L., AND KLUG, A (1974). Arrangement of subunits in flagellar microtubules. *Journal of Cell Science*. 14, 523–549.

AOYAGI, T., AND KIYAMA, R. (2005). Alternative splicing of the human Kank gene produces two types of Kank protein. *Biochemical and Biophysical Research Communications* 330, 1247–1253.

APPLEWHITE, D.A., GRODE, K.D., KELLER, D., ZADEH, A., SLEP, K.C., AND ROGERS, S.L. (2010). The spectraplakin Short stop is an actin-microtubule cross-linker that contributes to organization of the microtubule network. *Molecular Biology of The Cell* 21, 1714–1724.

ASHBURNER, M. (1989). *Drosophila*: A laboratory handbook (Cold Spring Harbor Laboratory Press).

BARTOLINI, F., MOSELEY, J.B., SCHMORANZER, J., CASSIMERIS, L., GOODE, B.L., AND GUNDERSEN, G.G. (2008). The formin mDia2 stabilizes microtubules independently of its actin nucleation activity. *Journal of Cell Biology* 181, 523–536.

BATE, M. (1990). The embryonic development of larval muscles in *Drosophila*. *Development* 110, 791–804.

BATEMAN, J.R., LEE, A.M., AND WU, C. (2006). Site-specific transformation of *Drosophila* via phiC31 integrase-mediated cassette exchange. *Genetics* 173, 769–777.

BATLEVI, Y., MARTIN, D.N., PANDEY, U.B., SIMON, C.R., POWERS, C.M., TAYLOR, J.P., AND BAEHRECKE, E.H. (2010). Dynein light chain 1 is required for autophagy, protein clearance, and cell death in *Drosophila*. *Procedures of the National Academy of Science U.S.A.* 107, 742–747.

BERRUETA, L., TIRNAUER, J.S., SCHUYLER, S.C., PELLMAN, D., AND BIERER, B.E. (1999). The APC-associated protein EB1 associates with components of the dynactin complex and cytoplasmic dynein intermediate chain. *Current Biology* 9, 425–428.

BHAT, K.M. (2005). Slit-roundabout signaling neutralizes netrin-Frazzled-mediated attractant cue to specify the lateral positioning of longitudinal axon pathways. *Genetics* 170, 149–159.

BIEDERER, T., AND STAGI, M. (2008). Signaling by synaptogenic molecules. *Current Opinion in Neurobiology*

BILBE, G., DELABIE, J., BRUGGEN, J., RICHENER, H., ASSELBERGS, F.A.M., CERLETTI, N., SORG, C., ODINK, K., TARCSAY, L., WIESENDANGER, W., ET AL. (1992). Restin : a novel intermediate filament-associated protein highly expressed in the Reed -Sternberg cells of Hodgkin ' s disease. *EMBO* 11, 2103–2113.

BODENMILLER, B., MALMSTROM, J., GERRITS, B., CAMPBELL, D., LAM, H., SCHMIDT, A., RINNER, O., MUELLER, L.N., SHANNON, P.T., PEDRIOLI, P.G., ET AL. (2007). PhosphoPep--a phosphoproteome resource for systems biology research in *Drosophila* Kc167 cells. *Molecular Systems Biology* 3, 139.

BODMER, R., CARRETTO, R., AND JAN, Y.N. (1989). Neurogenesis of the peripheral nervous system in *Drosophila* embryos: DNA replication patterns and cell lineages. *Neuron* 3, 21–32.

BOGAERT, T., BROWN, N., AND WILCOX, M. (1987). The *Drosophila* PS2 antigen is an invertebrate integrin that, like the fibronectin receptor, becomes localized to muscle attachments. *Cell* 51, 929–940.

BOGGETTI, B., JASIK, J., TAKAMIYA, M., STRÄHLE, U., REUGELS, A.M., AND CAMPOS-ORTEGA, J. A (2012). NBP, a zebrafish homolog of human Kank3, is a novel Numb interactor essential for epidermal integrity and neurulation. *Developmental Biology* 365, 164–174.

BORKOWSKI, O.M., BROWN, N.H., AND BATE, M. (1995). Anterior-posterior subdivision and the diversification of the mesoderm in *Drosophila*. *Development* 121, 4183–4193.

BOSHER, J.M., HAHN, B.-S., LEGOUIS, R., SOOKHAREEA, S., WEIMER, R.M., GANSMULLER, A., CHISHOLM, A.D., ROSE, A.M., BESSEREAU, J.-L., AND LABOUESSE, M. (2003). The Caenorhabditis elegans vab-10 spectraplakin isoforms protect the epidermis against internal and external forces. *Journal of Cell Biology* 161, 757–768.

BOUNOUTAS, A., O'HAGAN, R., AND CHALFIE, M. (2009). The multipurpose 15-protofilament microtubules in *C. elegans* have specific roles in mechanosensation. *Current Biology* 19, 1362–1367.

BOUQUET, C., AND NOTHIAS, F. (2007). Molecular mechanisms of axonal growth. *Advances in Expermental Medical Biology* 621, 1–16.

BOWNES, M. (1975). A photographic study of *Development* in the living embryo of *Drosophila melanogaste*r. *Journal of Embryology and Experimental Morphology* 33, 789–801.

BRIDGES, C. (1913). Non-disjunction of the sex chromosomes of Drosophila. *Journal of Experimental Zoology* 15, 587–606.

BRIDGMAN, P.C., AND DAILEY, M.E. (1989). The organization of myosin and actin in rapid frozen nerve growth cones. *Journal of Cell Biology* 108, 95–109.

BRITTLE, A.L., AND OHKURA, H. (2005). Mini spindles, the XMAP215 homologue, suppresses pausing of interphase microtubules in Drosophila. *EMBO* J. 24, 1387–1396.

BROUHARD, G.J., STEAR, J.H., NOETZEL, T.L., AL-BASSAM, J., KINOSHITA, K., HARRISON, S.C., HOWARD, J., AND HYMAN, A. A (2008). XMAP215 is a processive microtubule polymerase. *Cell* 132, 79–88.

BU, W., AND SU, L.-K. (2003). Characterization of functional domains of human EB1 family proteins. *Journal of Biological Chemistry* 278, 49721–49731.

BUEY, R.M., SEN, I., KORTT, O., MOHAN, R., GFELLER, D., VEPRINTSEV, D., KRETZSCHMAR, I., SCHEUERMANN, J., NERI, D., ZOETE, V., ET AL. (2012). Sequence determinants of a microtubule tip localization signal (MtLS). *Journal of Biological Chemistry* 287, 28227–28242.

BUNCH, T. A, GRANER, M.W., FESSLER, L.I., FESSLER, J.H., SCHNEIDER, K.D., KERSCHEN, A, CHOY, L.P., BURGESS, B.W., AND BROWER, D.L. (1998). The PS2 integrin ligand tiggrin is required for proper muscle function in Drosophila. *Development* 125, 1679–1689.

C. B. BRIDGES (1935). SALIVARY CHROMOSOME MAPS: With a Key to the Banding of the Chromosomes of Drosophila Melanogaster. *Journal of Heredity* 26, 60–64.

CAJAL, S.R. (1890). À quelle époque apparaissent les expansions des cellules nerveuses de la moëlle épinière du poulet? *Anatomomischer Anzeiger* 21-22, 609–639.

CAMPELLONE, K.G., AND WELCH, M.D. (2010). A nucleator arms race: cellular control of actin assembly. *Nature Reviews Molecular Cell Biology*. 11, 237–251.

CASTRESANA, J., AND SARASTE, M. (1995). Does Vav bind to F-actin through a CH domain? *FEBS Letters* 374, 149–151.

CHANANA, B., GRAF, R., KOLEDACHKINA, T., PFLANZ, R., AND VORBRÜGGEN, G. (2007). AlphaPS2 integrin-mediated muscle attachment in Drosophila requires the ECM protein Thrombospondin. *Mechanisms of Development*124, 463–475.

CHANDRA, B., AOYAGI, T., SARKAR, S., NOMURA, K., KANDA, H., IWAYA, K., TACHIBANA, M., AND KIYAMA, R. (2005). Pathological characterization of Kank in renal cell carcinoma. *Experimental Molecular Pathology* 78, 41 – 48.

CHARRASSE, S., SCHROEDER, M., GAUTHIER-ROUVIERE, C., ANGO, F., CASSIMERIS, L., GARD, D.L., AND LARROQUE, C. (1998). The TOGp protein is a new human microtubule-associated protein homologous to the Xenopus XMAP215. *Journal of Cell Science*. 111 (Pt 1, 1371–1383.

CIFERRI, C., PASQUALATO, S., SCREPANTI, E., VARETTI, G., SANTAGUIDA, S., DOS REIS, G., MAIOLICA, A., POLKA, J., DE LUCA, J.G., DE WULF, P., ET AL. (2008). Implications for kinetochore-microtubule attachment from the structure of an engineered Ndc80 complex. *Cell* 133, 427–439.

COQUELLE, F., AND CASPI, M. (2002). LIS1, CLIP-170's key to the dynein/dynactin pathway. *Cell Biology*. 22, 3089–3102.

CRISP, S., EVERS, J.F., FIALA, A., AND BATE, M. (2008). The development of motor coordination in Drosophila embryos. *Development* 135, 3707–3717.

CULLEN, C.F., DEÁK, P., GLOVER, D.M., AND OHKURA, H. (1999). mini spindles: A gene encoding a conserved microtubule-associated protein required for the integrity of the mitotic spindle in Drosophila. *Journal of Cell Biology* 146, 1005–1018.

DAVID-PFEUTY, T., ERICKSON, H.P., AND PANTALONI, D. (1977). Guanosinetriphosphatase activity of tubulin associated with microtubule assembly. *Procedures of the National Academy of Science U.S.A.* 74, 5372–5376.

DENT, E.W., GUPTON, S.L., AND GERTLER, F.B. (2011). The growth cone cytoskeleton in axon outgrowth and guidance. Cold Spring Harb. Perspect. Biol. 3.

DESAI, A, VERMA, S., MITCHISON, T.J., AND WALCZAK, C.E. (1999). Kin I kinesins are microtubule-destabilizing enzymes. *Cell* 96, 69–78.

DIETZL, G., CHEN, D., SCHNORRER, F., SU, K., BARINOVA, Y., FELLNER, M., GASSER, B., KINSEY, K., OPPEL, S., SCHEIBLAUER, S., ET AL. (2007). A genome-wide transgenic RNAi library for conditional gene inactivation in Drosophila. *Nature* 448.

DING, M., GONCHAROV, A., JIN, Y., AND CHISHOLM, A.D. (2003a). *C. elegans* ankyrin repeat protein VAB-19 is a component of epidermal attachment structures and is essential for epidermal morphogenesis. *Development* 130, 5791–5801.

DIXIT, R., BARNETT, B., LAZARUS, J.E., TOKITO, M., GOLDMAN, Y.E., AND HOLZBAUR, E.L.F. (2009). Microtubule plus-end tracking by CLIP-170 requires EB1. *Procedures of the National Academy of Science U.S.A.* 106, 492–497.

DJIANE, A., KREJCI, A., BERNARD, F., FEXOVA, S., MILLEN, K., AND BRAY, S.J. (2013). Dissecting the mechanisms of Notch induced hyperplasia. *EMBO J*. 32, 60–71.

DOUGHERTY, G.W., ADLER, H.J., RZADZINSKA, A., GIMONA, M., TOMITA, Y., LATTIG, M.C., MERRITT JR, R.C., AND KACHA, B. (2005). CLAMP, a novel microtubule-associated protein with EB-type calponin homology. *Cell Motility and Cytoskeleton* 62, 141–156.

DUJARDIN, D., WACKER, U.I., MOREAU, A, SCHROER, T. A, RICKARD, J.E., AND DE MEY, J.R. (1998). Evidence for a role of CLIP-170 in the establishment of metaphase chromosome alignment. *Journal of Cell Biology* 141, 849–862.

DZHINDZHEV, N.S., ROGERS, S.L., VALE, R.D., AND OHKURA, H. (2005). Distinct mechanisms govern the localisation of Drosophila CLIP-190 to unattached kinetochores and microtubule plus-ends. *Journal of Cell Science*. 118, 3781–3790.

EDDISON, M., GUARNIERI, D.J., CHENG, L., LIU, C.-H., MOFFAT, K.G., DAVIS, G., AND HEBERLEIN, U. (2011). Arouser Reveals a Role for Synapse Number in the Regulation of Ethanol Sensitivity. *Neuron* 70, 979–990.

EGELMAN, E. (1985). The structure of F-actin. *The Journal of Muscle Research and Cell Motility* 6, 129–151.

Elliott, S.L., Cullen, C.F., Wrobel, N., Kernan, M.J., and Ohkura, H. (2005). EB1 is essential during Drosophila development and plays a crucial role in the integrity of chordotonal mechanosensory organs. *Molecular Biology of The Cell* 16, 891–901.

ELLIS, S.J., PINES, M., FAIRCHILD, M.J., AND TANENTZAPF, G. (2011). In vivo functional analysis reveals specific roles for the integrin-binding sites of talin. *Journal of Cell Science*. 124, 1844–1856.

ENGLUND, C., STENEBERG, P., FALILEEVA, L., XYLOURGIDIS, N., AND SAMAKOVLIS, C. (2002). Attractive and repulsive functions of Slit are mediated by different receptors in the Drosophila trachea. *Development* 129, 4941–4951.

FEIGUIN, F., GODENA, V.K., ROMANO, G., D'AMBROGIO, A., KLIMA, R., AND BARALLE, F.E. (2009). Depletion of TDP-43 affects Drosophila motoneurons terminal synapsis and locomotive behavior. *FEBS Letters* 583, 1586–1592.

FORSCHER, P., AND SMITH, S.J. (1988). Actions of cytochalasins on the organization of actin filaments and microtubules in a neuronal growth cone. *Journal of Cell Biology* 107, 1505–1516.

FRIEDEN, C. (1982). The Mg2+-induced conformational change in rabbit skeletal muscle G-actin. *Journal of Biological Chemistry* 257, 2882–2886.

FRIEDEN, C., AND PATANE, K. (1985). Differences in G-actin containing bound ATP or ADP: the Mg2+-induced conformational change requires ATP. *Biochemistry* 24, 4192–4196.

FROMMER, G., VORBRÜGGEN, G., PASCA, G., JÄCKLE, H., AND VOLK, T. (1996). Epidermal egr-like zinc finger protein of Drosophila participates in myotube guidance. *EMBO J.* 15, 1642–1649.

GARD, D.L., AND KIRSCHNER, M.W. (1987). A microtubule-associated protein from Xenopus eggs that specifically promotes assembly at the plus-end. *Journal of Cell Biology* 105, 2203–2215.

GILSOHN, E., AND VOLK, T. (2010). Slowdown promotes muscle integrity by modulating integrin-mediated adhesion at the myotendinous junction. *Development* 137, 785–794.

GNAD, F., REN, S., COX, J., OLSEN, J. V, MACEK, B., OROSHI, M., AND MANN, M. (2007). PHOSIDA (phosphorylation site database): management, structural and evolutionary investigation, and prediction of phosphosites. *Genome Biology* 8, R250.

GOSHIMA, G., AND VALE, R.D. (2003). The roles of microtubule-based motor proteins in mitosis: comprehensive RNAi analysis in the Drosophila S2 cell line. *Journal of Cell Biology* 162, 1003–1016.

GOTWALS, P., AND FESSLER, L. (1994). Drosophila PS1 integrin is a laminin receptor and differs in ligand specificity from PS2. *Procedures of the National Academy of Sciences U.S.A.* 91, 11447–11451.

GRAVELEY, B.R., BROOKS, A.N., CARLSON, J.W., DUFF, M.O., LANDOLIN, J.M., YANG, L., ARTIERI, C.G., VAN BAREN, M.J., BOLEY, N., BOOTH, B.W., ET AL. (2011). The developmental transcriptome of Drosophila melanogaster. *Nature* 471, 473–479.

GREGORY, S.L., AND BROWN, N.H. (1998). Kakapo, a Gene Required for Adhesion Between and Within Cell Layers in Drosophila Encodes a Large Cytoskeletal Linker Protein Related to Plectin and Dystrophin. *Journal of Cell Biology* 143, 1271–1282.

GRODEN, J., THLIVERIS, A, SAMOWITZ, W., CARLSON, M., GELBERT, L., ALBERTSEN, H., JOSLYN, G., STEVENS, J., SPIRIO, L., AND ROBERTSON, M. (1991). Identification and characterization of the familial adenomatous polyposis coli gene. *Cell* 66, 589–600.

GU, C., ZHOU, W., PUTHENVEEDU, M. A, XU, M., JAN, Y.N., AND JAN, L.Y. (2006). The microtubule plus-end tracking protein EB1 is required for Kv1 voltage-gated K+ channel axonal targeting. *Neuron* 52, 803–816.

HALL, A. (1994). Small GTP-binding proteins and the regulation of the actin cytoskeleton. *Annual Review in Cell Biology* 10, 31–54.

HALPERN, E., JOHANSEN, M., AND KESHISHIAN, H. (1989). Stereotypic Morphology of Glutamatergic Muscle Cells of Drosophila Larvae Synapses on Identified. *Journal of Neuroscience* 9, 710–725.

HARADA, J.N., BOWER, K.E., ORTH, A.P., CALLAWAY, S., NELSON, C.G., LARIS, C., HOGENESCH, J.B., VOGT, P.K., AND CHANDA, S.K. (2005). Identification of novel mammalian growth regulatory factors by genome-scale quantitative image analysis. *Genome Research* 15, 1136–1144.

HATINI, V., AND DINARDO, S. (2001). Divide and conquer: pattern formation in Drosophila embryonic epidermis. *Trends in Genetics*. 17, 574–579.

HAYASHI, I., AND IKURA, M. (2003). Crystal structure of the amino-terminal microtubule-binding domain of end-binding protein 1 (EB1). *Journal of Biological Chemistry* 278, 36430–36434.

HIGHTOWER, ROBIN C. MEAGHER, R.B. (1986). The molecular evolution of actin. *Genetics* 114, 315–332.

HILL, T.L., AND CHEN, Y. (1984). Phase changes at the end of a microtubule with a GTP cap Biology : *Procedures of the National Academy of Science U.S.A.* 81, 5772–5776.

HO, R., BALL, E., AND GOODMAN, C. (1983). Muscle pioneers: large mesodermal cells that erect a scaffold for developing muscles and motoneurones in grasshopper embryos. *Nature* 301, 66–69.

HOLMES, K., POPP, D., GEBHARD, W., AND KABSCH, W. (1990). Atomic model of the actin filament. *Nature* 347, 44 – 49.

HONG, J.-W., PARK, K.W., AND LEVINE, M.S. (2013). Temporal regulation of single-minded target genes in the ventral midline of the Drosophila central nervous system. *Developmental Biology* 380, 335–343.

HONNAPPA, S., JOHN, C.M., KOSTREWA, D., WINKLER, F.K., AND STEINMETZ, M.O. (2005). Structural insights into the EB1-APC interaction. *EMBO J.* 24, 261–269.

HONNAPPA, S., GOUVEIA, S.M., WEISBRICH, A., DAMBERGER, F.F., BHAVESH, N.S., JAWHARI, H., GRIGORIEV, I., VAN RIJSSEL, F.J. A, BUEY, R.M., LAWERA, A., ET AL. (2009). An EB1-binding motif acts as a microtubule tip localization signal. *Cell* 138, 366–376.

HOPWOOD, N.D., PLUCK, A, AND GURDON, J.B. (1989). A Xenopus mRNA related to Drosophila twist is expressed in response to induction in the mesoderm and the neural crest. *Cell* 59, 893–903.

HUMMEL, T., KRUKKERT, K., ROOS, J., DAVIS, G., AND KLÄMBT, C. (2000). Drosophila Futsch/22C10 is a MAP1B-like protein required for dendritic and axonal development. *Neuron* 26, 357–370.

HWANG, R., ZHONG, L., XU, Y., AND JOHNSON, T. (2007). Nociceptive Neurons Protect Drosophila Larvae from Parasitoid Wasps. *Current Biology* 17, 2105–2116.

IHARA, S., HAGEDORN, E.J., MORRISSEY, M.A., CHI, Q., MOTEGI, F., KRAMER, J.M., AND SHERWOOD, D.R. (2011). Basement Membrane Sliding and Targeted Adhesion Remodels Tissue Boundaries During Unterine-vulval Attachment in *C. elegans*. *Nature Cell Biology* 13, 641–651.

ISSHIKI, T., PEARSON, B., HOLBROOK, S., AND DOE, C.Q. (2001). Transcription Factors which Specify the Temporal Identity of Their Neuronal Progeny 1254 University of Oregon. *Cell* 106, 511–521.

JAKUS, M., AND HALL, C. (1947). Studies of Actin and Myosin. *Journal of Biological Chemistry* 163, 705–.

Jarman, a P., Grau, Y., Jan, L.Y., and Jan, Y.N. (1993). atonal is a proneural gene that directs chordotonal organ formation in the Drosophila peripheral nervous system. *Cell* 73, 1307–1321.

JIANG, K., TOEDT, G., MONTENEGRO GOUVEIA, S., DAVEY, N.E., HUA, S., VAN DER VAART, B., GRIGORIEV, I., LARSEN, J., PEDERSEN, L.B., BEZSTAROSTI, K., ET AL. (2012). A Proteome-wide screen for mammalian SxIP motif-containing microtubule plus-end tracking proteins. *Current Biology* 22, 1800–1807.

JOSHI, H.C., PALACIOS, M.J., MCNAMARA, L., AND CLEVELAND, D. (1992). Gamma-Tubulin is a centrosomal protein required for cell cycle-dependent microtubule nucleation. *Nature* 356.

KABSCH, W., MANNHERZ, H., SUCK, D., PAI, E., AND HOLMES, K. (1990). Atomic structure of the actin: DNase I complex. *Nature* 347, 37 – 44.

KAKINUMA, N., AND KIYAMA, R. (2009). A major mutation of KIF21A associated with congenital fibrosis of the extraocular muscles type 1 (CFEOM1) enhances translocation of Kank1 to the membrane. *Biochemical and Biophysical Research Communications* 386, 639–644.

KAKINUMA, N., ROY, B.C., ZHU, Y., WANG, Y., AND KIYAMA, R. (2008a). Kank regulates RhoA-dependent formation of actin stress fi bers and cell migration via 14-3-3 in PI3K – Akt signaling. *Cell* 181, 537–549.

KAKINUMA, N., ROY, B.C., ZHU, Y., WANG, Y., AND KIYAMA, R. (2008b). Kank regulates RhoA-dependent formation of actin stress fibers and cell migration via 14-3-3 in PI3K-Akt signaling. *Journal of Cell Biology* 181, 537–549.

KAKINUMA, NAOTO, ZHU, Y., WANG, Y., ROY, B.C., AND KIYAMA, R. (2009). Kank proteins: structure, functions and diseases. *Cell and Molecular Life Sciences* 66, 2651–2659.

KANAI, M.I., OKABE, M., AND HIROMI, Y. (2005). seven-up Controls switching of transcription factors that specify temporal identities of Drosophila neuroblasts. *Developmental Cell* 8, 203–213.

KENNEDY, S. A, FRAZIER, M.L., STEINIGER, M., MAST, A.M., MARZLUFF, W.F., AND REDINBO, M.R. (2009). Crystal structure of the HEAT domain from the Pre-mRNA processing factor Symplekin. *Journal of Molecular Biology* 392, 115–128.

KESKIN, O., DURELL, S.R., BAHAR, I., JERNIGAN, R.L., AND COVELL, D.G. (2002). Relating molecular flexibility to function: a case study of tubulin. *Biophysical Journal* 83, 663–680.

KIDD, T., BLAND, K.S., AND GOODMAN, C.S. (1999). Slit is the midline repellent for the robo receptor in Drosophila. *Cell* 96, 785–794.

KOHNO, T., OTSUKA, A., GIRARD, L., SATO, M., IWAKAWA, R., OGIWARA, H., SANCHEZ-CESPEDES, M., MINNA, J.D., AND YOKOTA, J. (2010). A Catalog of Genes Homozygously Deleted in Human Lung Cancer and the Candidacy of PTPRD as a Tumor Suppressor Gene. *Cancer*

KOMAROVA, Y. A, AKHMANOVA, A.S., KOJIMA, S.-I., GALJART, N., AND BORISY, G.G. (2002). Cytoplasmic linker proteins promote microtubule rescue in vivo. *Journal of Cell Biology* 159, 589–599.

KRALOVICS, R., TEO, S., BUSER, A.S., BRUTSCHE, M., TIEDT, R., TICHELLI, A., PASSAMONTI, F., PIETRA, D., CAZZOLA, M., AND SKODA, R.C. (2005). Altered gene expression in myeloproliferative disorders correlates with activation of signaling by the V617F mutation of Jak2. *Blood* 106, 3374–3376.

KRAMER, S.G., KIDD, T., SIMPSON, J.H., AND GOODMAN, C.S. (2001). Switching repulsion to attraction: changing responses to slit during transition in mesoderm migration. *Science* 292, 737–740.

KREBS, A, ROTHKEGEL, M., KLAR, M., AND JOCKUSCH, B.M. (2001). Characterization of functional domains of mDia1, a link between the small GTPase Rho and the actin cytoskeleton. *Journal of Cell Science*. 114, 3663–3672.

DE LA TORRE, J.R., HÖPKER, V.H., MING, G.L., POO, M.M., TESSIER-LAVIGNE, M., HEMMATI-BRIVANLOU, A, AND HOLT, C.E. (1997). Turning of retinal growth cones in a netrin-1 gradient mediated by the netrin receptor DCC. *Neuron* 19, 1211–1224.

LEE, L. A, LEE, E., ANDERSON, M. A, VARDY, L., TAHINCI, E., ALI, S.M., KASHEVSKY, H., BENASUTTI, M., KIRSCHNER, M.W., AND ORR-WEAVER, T.L. (2005). Drosophila genome-scale screen for PAN GU kinase substrates identifies Mat89Bb as a cell cycle regulator. *Developmental Cell* 8, 435–442.

LEE, T., LANGFORD, K.J., ASKHAM, J.M., BRÜNING-RICHARDSON, A, AND MORRISON, E.E. (2008). MCAK associates with EB1. *Oncogene* 27, 2494–2500.

LEPTIN, M. (1991). twist and snail as positive and negative regulators during Drosophila mesoderm development. *Genes and Develeopment.* 5, 1568–1576.

LEPTIN, M., AEBERSOLD, R., AND WILCOX, M. (1987). Drosophila position-specific antigens resemble the vertebrate fibronectin-receptor family. *EMBO* J. 6, 1037–1043.

LEPTIN, M., BOGAERT, T., LEHMANN, R., AND WILCOX, M. (1989). The function of PS integrins during Drosophila embryogenesis. *Cell* 56, 401–408.

LERER, I., SAGI, M., MEINER, V., COHEN, T., ZLOTOGORA, J., AND ABELIOVICH, D. (2005). Deletion of the ANKRD15 gene at 9p24.3 causes parent-of-origin-dependent inheritance of familial cerebral palsy. *Human Molecular Genetetics* 14, 3911–3920.

LI, C.-C., KUO, J.-C., WATERMAN, C.M., KIYAMA, R., MOSS, J., AND VAUGHAN, M. (2011). Effects of brefeldin A-inhibited guanine nucleotide-exchange (BIG) 1 and KANK1 proteins on cell polarity and directed migration during wound healing. *Procedures of the National Academy of Science U.S.A.* 108, 19228–19233.

LIOU, J., KIM, M.L., HEO, W. DO, JONES, J.T., MYERS, J.W., FERRELL, J.E., AND MEYER, T. (2005). STIM is a Ca2+ sensor essential for Ca2+-store-depletion-triggered Ca2+ influx. *Current Biology* 15, 1235–1241.

LIU, Z.C., AND GEISBRECHT, E.R. (2011). Moleskin is essential for the formation of the myotendinous junction in Drosophila. *Developmental Biology* 359, 176–189.

LÜER, K., AND TECHNAU, G.M. (2009). Single cell cultures of Drosophila neuroectodermal and mesectodermal central nervous system progenitors reveal different degrees of developmental autonomy. Neural Dev. 4, 30.

MACKRELL, A.J., BLUMBERG, B., HAYNES, S.R., AND FESSLER, J.H. (1988). The lethal myospheroid gene of Drosophila encodes a membrane protein homologous to vertebrate integrin beta subunits. *Procedures of the National Academy of Science U.S.A.* 85, 2633–2637.

MAEKAWA, M. (1999). Signaling from Rho to the Actin Cytoskeleton Through Protein Kinases ROCK and LIM-kinase. *Science* (80-.). 285, 895–898.

MAIATO, H., FAIRLEY, E. A L., RIEDER, C.L., SWEDLOW, J.R., SUNKEL, C.E., AND EARNSHAW, W.C. (2003). Human CLASP1 is an outer kinetochore component that regulates spindle microtubule dynamics. *Cell* 113, 891–904.

MANDELKOW, E., AND SCHULTHEISS, R. (1986). On the surface lattice of microtubules: helix starts, protofilament number, seam, and handedness. *Journal of Cell Biology* 102, 1067–1073.

MANEY, T., HUNTER, A W., WAGENBACH, M., AND WORDEMAN, L. (1998). Mitotic centromere-associated kinesin is important for anaphase chromosome segregation. *Journal of Cell Biology* 142, 787–801.

MAURER, S.P., FOURNIOL, F.J., BOHNER, G., MOORES, C.A., AND SURREY, T. (2012). EBs Recognize a NucleotideDependent Structural Cap at Growing Microtubule Ends. *Cell* 149, 371–382.

MCGINNIS, W., GARBER, R.L., WIRZ, J., KUROIWA, A, AND GEHRING, W.J. (1984). A homologous protein-coding sequence in Drosophila homeotic genes and its conservation in other metazoans. *Cell* 37, 403–408.

MCKEOWN, C., PRAITIS, V., AND AUSTIN, J. (1998). sma-1 encodes a betaH-spectrin homolog required for Caenorhabditis elegans morphogenesis. *Development* 125, 2087–2098.

MCMAHON, A., REEVES, G.T., SUPATTO, W., AND STATHOPOULOS, A. (2010). Mesoderm migration in Drosophila is a multi-step process requiring FGF signaling and integrin activity. *Development* 137, 2167–2175.

MEDVES, S., DUHOUX, F.P., FERRANT, A, TOFFALINI, F., AMEYE, G., LIBOUTON, J.-M., POIREL, H. A, AND DEMOULIN, J.-B. (2010). KANK1, a candidate tumor suppressor gene, is fused to PDGFRB in an imatinib-responsive myeloid neoplasm with severe thrombocythemia. Leukemia 24, 1052–1055.

MEIRELES, A.M., DZHINDZHEV, N.S., AND OHKURA, H. (2011). Kebab: kinetochore and EB1 associated basic protein that dynamically changes its localisation during Drosophila mitosis. PLoS One 6, e24174.

MIKI, H., YAMAGUCHI, H., SUETSUGU, S., AND TAKENAWA, T. (2000). IRSp53 is an essential intermediate between Rac and WAVE in the regulation of membrane ruffling. *Nature* 408, 732–735.

MILLER (1950). The internal anatomy and histology of the imago of Drosophila melanogaster. In The Biology of Drosophila, (New York, Hafner Press), pp. 468–480.

MILLER, R.K., CHENG, S.C., AND ROSE, M.D. (2000). Bim1p/Yeb1p mediates the Kar9p-dependent cortical attachment of cytoplasmic microtubules. *Molecular Biology of The Cell* 11, 2949–2959.

MIMORI-KIYOSUE, Y., SHIINA, N., AND TSUKITA, S. (2000). The dynamic behavior of the APC-binding protein EB1 on the distal ends of microtubules. *Current Biology* 10, 865–868.

MISRA, S., CROSBY, M. A, MUNGALL, C.J., MATTHEWS, B.B., CAMPBELL, K.S., HRADECKY, P., HUANG, Y., KAMINKER, J.S., MILLBURN, G.H., PROCHNIK, S.E., ET AL. (2002). Annotation of the Drosophila melanogaster euchromatic genome: a systematic review. Genome Biol. 3, RESEARCH0083.

MITCHISON, T., AND KIRSCHNER, M. (1984a). Microtubule assembly nucleated by isolated centrosomes. *Nature* 312, 232–237.

MITCHISON, T., AND KIRSCHNER, M. (1984b). Dynamic instability of microtubule growth. *Nature* 312, 237–242.

MOORE, A.T., RANKIN, K.E., VON DASSOW, G., PERIS, L., WAGENBACH, M., OVECHKINA, Y., ANDRIEUX, A., JOB, D., AND WORDEMAN, L. (2005). MCAK associates with the tips of polymerizing microtubules. *Journal of Cell Biology* 169, 391–397.

MORGAN, T. (1911). An attempt to analyze the constitution of the chromosomes on the basis of sex-limited inheritance in Drosophila. *Journal of Experimental Zoology* 11, 365–413.

MORGAN, T. (1914). No crossing over in the male of Drosophila of genes in the second and third pairs of chromosomes. Biol. Bull. 26, 195–204.

MORGAN, T., AND LYNCH, C. (1912). The linkage of two factors in Drosophila that are not sex linked. Biol. Bull. 174–182.

MORRISON, E.E., WARDLEWORTH, B.N., ASKHAM, J.M., MARKHAM, A F., AND MEREDITH, D.M. (1998). EB1, a protein which interacts with the APC tumour suppressor, is associated with the microtubule cytoskeleton throughout the cell cycle. Oncogene 17, 3471–3477.

MOSAVI, L.K., CAMMETT, T.J., DESROSIERS, D.C., AND PENG, Z. (2004). The ankyrin repeat as molecular architecture for protein recognition. *Cell* Cycle 1435–1448.

MULLER, H. (1914). A FACTOR FOR THE FOURTH CHROMOSOME OF DROSOPHILA. *Science* (80-.). 39, 906.

MULLER, H. (1918). Genetic variability, twin hybrids and constant hybrids, in a case of balanced lethal factors. *Genetics* 3, 422–499.

MÜLLER-REICHERT, T., CHRÉTIEN, D., SEVERIN, F., AND HYMAN, A A (1998). Structural changes at microtubule ends accompanying GTP hydrolysis: information from a slowly hydrolyzable analogue of GTP, guanylyl (alpha,beta)methylenediphosphonate. *Procedures of the National Academy of Science U.S.A.* 95, 3661–3666.

NI, J.-Q., ZHOU, R., CZECH, B., LIU, L.-P., HOLDERBAUM, L., YANG-ZHOU, D., SHIM, H.-S., TAO, R., HANDLER, D., KARPOWICZ, P., ET AL. (2011). A genome-scale shRNA resource for transgenic RNAi in Drosophila. *Nature Methods* 8, 405–407.

NÜSSLEIN-VOLHARD, C., AND LOHS-SCHARDIN, M. (1980). A dorso-ventral shift of embryonic primordia in a new maternal-effect mutant of Drosophila. *Nature* 283, 474–476.

NÜSSLEIN-VOLHARD, C., AND WIESCHAUS, E. (1980). Mutations affecting segment number and polarity in Drosophila. *Nature*.

OAKLEY, C.E., AND OAKLEY, B.. (1989). Identification of gamma tubulin, a new member of the tubulin superfamily encoded by mipA gene of Apergillus nidulans. *Nature* 338.

OHNISHI, T. (1962). Extraction of actin- and myosin-like proteins from liver mitochondria. *Journal of Biochemistry.* 52, 230–231.

OLIVER, B., AND LEBLANC, B. (2003). How many genes in a genome? *Genome Biology.* 5, 204.

PAINTER, T.S. (1934). The morphology of the X chromosome in salivary glands of Drosophila melanogaster and a new type of chromsome map for this element. *Journal of Heredity* 25, 448–469.

PANDEY, U., AND NICHOLS, C. (2011). Human disease models in Drosophila melanogaster and the role of the fly in therapeutic drug discovery. *Pharmacological Review*. 63, 411–436.

PARSONS, L., HARRIS, K.-L., TURNER, K., AND WHITINGTON, P.M. (2003). Roundabout gene family functions during sensory axon guidance in the drosophila embryo are mediated by both Slit-dependent and Slit-independent mechanisms. *Developmental Biology* 264, 363–375.

PERIS, L., THERY, M., FAURÉ, J., SAOUDI, Y., LAFANECHÈRE, L., CHILTON, J.K., GORDON-WEEKS, P., GALJART, N., BORNENS, M., WORDEMAN, L., ET AL. (2006). Tubulin tyrosination is a major factor affecting the recruitment of CAP-Gly proteins at microtubule plus ends. *Journal of Cell Biology* 174, 839–849.

PIELAGE, J., AND KLÄMBT, C. (2001). Glial cells aid axonal target selection. *Trends in Neuroscience*. 24, 432–433.

PIERRE, P., SCHEEL, J., RICKARD, J.E., AND KREIS, T.E. (1992). CLIP-170 Links Endocytic Vesicles to Microtubules. *Cell* 70, 887–900.

PIERRE, P., PEPPERKOK, R., AND KREIS, T.E. (1994). Molecular characterization of two functional domains of CLIP-170 in vivo. *Journal of Cell Science*. 107, 1909–1920.

POZO-GUISADO, E., CASAS-RUA, V., TOMAS-MARTIN, P., LOPEZ-GUERRERO, A.M., ALVAREZ-BARRIENTOS, A., AND MARTIN-ROMERO, F.J. (2013). Phosphorylation of STIM1 at ERK1/2 target sites regulates interaction with the microtubule plus-end binding protein EB1. *Journal of Cell Science*. 126, 3170–3180.

PROKOP, A (1999). Integrating bits and pieces: synapse structure and formation in Drosophila embryos. *Cell Tissue Research.* 297, 169–186.

PROKOP, A., BEAVEN, R., QU, Y., AND SÁNCHEZ-SORIANO, N. (2013). Using fly genetics to dissect the cytoskeletal machinery of neurons during axonal growth and maintenance. *Journal of Cell Science*. 126, 2331–2341.

REITER, L.T., POTOCKI, L., CHIEN, S., GRIBSKOV, M., AND BIER, E. (2001). A systematic analysis of human disease-associated gene sequences in Drosophila melanogaster. *Genome Research.* 11, 1114–1125.

ROGERS, S.L., AND ROGERS, G.C. (2008). Culture of Drosophila S2 *Cell*s and their use for RNAi-mediated loss-of-function studies and immunofluorescence microscopy.

ROY, B.C., KAKINUMA, N., AND KIYAMA, R. (2008). Kank attenuates actin remodeling by preventing interaction between IRSp53 and Rac 1. *Journal of Cell Biology* 184, 253–267.

ROY, B.C., KAKINUMA, N., AND KIYAMA, R. (2009). Kank attenuates actin remodeling by preventing interaction between IRSp53 and Rac1. *Journal of Cell Biology* 184, 253–267.

RUBINFELD, B., SOUZA, B., ALBERT, I., MULLER, O., CHAMBERLAIN, S., MASIARZ, F., MUNEMITSU, S., AND P, P. (1993). Association of the APC gene product with beta-catenin. *Science* (80-.). 262.

RUDOLF, A., BUTTGEREIT, D., REXER, K.-H., AND RENKAWITZ-POHL, R. (2012). The syncytial visceral and somatic musculature develops independently of β3-Tubulin during Drosophila embryogenesis, while maternally supplied β1-Tubulin is stable until the early steps of myoblast fusion. *European Journal of Cell Biology* 91, 192–203.

RUSHTON, E., DRYSDALE, R., ABMAYR, S.M., MICHELSON, A M., AND BATE, M. (1995). Mutations in a novel gene, myoblast city, provide evidence in support of the founder cell hypothesis for Drosophila *muscle* development. *Development* 121, 1979–1988.

SABBIONI, S., VERONESE, A, TRUBIA, M., TARAMELLI, R., BARBANTI-BRODANO, G., CROCE, C.M., AND NEGRINI, M. (1999). Exon structure and promoter identification of STIM1 (alias GOK), a human gene causing growth arrest of the human tumor cell lines G401 and RD. *Cytogenetic Cell Genetics.* 86, 214–218.

SAMBROOK, J., FRITSCH, E., AND MANIATIS, T. (1989). Molecular cloning: a laboratory manual (Cold Spring Harbour Press, New York).

SANGER, J. (1975). Changing Patterns of Actin Localization During *Cell* Division. *Procedures of the National Academy of Sciences U.S.A.* 72, 1913–1916.

SARGENT, M.G., AND BENNETT, M.F. (1990). Identification in Xenopus of a structural homologue of the Drosophila gene snail. *Development* 109, 967–973.

SARKAR, S., ROY, B., HATANO, N., AND AOYAGI, T. (2002a). A novel ankyrin repeat-containing gene (Kank) located at 9p24 is a growth suppressor of renal cell carcinoma. *Journal of Biological Chemistry* 277, 36585–36591.

SARKAR, S., ROY, B.C., HATANO, N., AOYAGI, T., GOHJI, K., AND KIYAMA, R. (2002b). A novel ankyrin repeat-containing gene (Kank) located at

9p24 is a growth suppressor of renal cell carcinoma. *Journal of Biological Chemistry* 277, 36585–36591.

SCHAEFER, A.W., KABIR, N., AND FORSCHER, P. (2002). Filopodia and actin arcs guide the assembly and transport of two populations of microtubules with unique dynamic parameters in Neuronal growth cones. *Journal of Cell Biology* 158, 139–152.

SCHROEDER, T.E. (1973). Actin in dividing *Cell*s: contractile ring filaments bind heavy meromyosin. *Procedures of the National Academy of Science U.S.A.* 70, 1688–1692.

SEHER, T.C., NARASIMHA, M., VOGELSANG, E., AND LEPTIN, M. (2007). Analysis and reconstitution of the genetic cascade controlling early mesoderm morphogenesis in the Drosophila embryo. *Mechanisms of Development*124, 167–179.

SEN, I., VEPRINTSEV, D., AKHMANOVA, A., AND STEINMETZ, M.O. (2013). End binding proteins are obligatory dimers. *PLoS One* 8, e74448.

SEPP, K.J., SCHULTE, J., AND AULD, V.J. (2000). Developmental dynamics of peripheral glia in Drosophila melanogaster. *Glia* 30, 122–133.

SEPP, K.J., HONG, P., LIZARRAGA, S.B., LIU, J.S., MEJIA, L. A, WALSH, C. A, AND PERRIMON, N. (2008). Identification of neural outgrowth genes using genome-wide RNAi. *PLoS Genetics* 4, e1000111.

SHERWOOD, N.T., SUN, Q., XUE, M., ZHANG, B., AND ZINN, K. (2004). Drosophila spastin regulates synaptic microtubule networks and is required for normal motor function. *PLoS Biology* 2, e429.

SLEP, K.C., ROGERS, S.L., ELLIOTT, S.L., OHKURA, H., KOLODZIEJ, P. A, AND VALE, R.D. (2005). Structural determinants for EB1-mediated recruitment of APC and spectraplakins to the microtubule plus end. *Journal of Cell Biology* 168, 587–598.

SLOBODA, R.D., RUDOLPH, S. A, ROSENBAUM, J.L., AND GREENGARD, P. (1975). Cyclic AMP-dependent endogenous phosphorylation of a microtubule-associated protein. *Procedures of the National Academy of Science U.S.A.* 72, 177–181.

SMITH, D.E., AND FISHER, P. A (1984). Identification, developmental regulation, and response to heat shock of two antigenically related forms of a major nuclear envelope protein in Drosophila embryos: application of an improved method for affinity purification of antibodies using polypeptides. *Journal of Cell Biology* 99, 20–28.

SMITH, D.E., FRANCO DEL AMO, F., AND GRIDLEY, T. (1992). Isolation of Sna, a mouse gene homologous to the Drosophila genes snail and escargot: its expression pattern suggests multiple roles during postimplantation development. *Development* 116, 1033–1039.

SOUSA, A., REIS, R., SAMPAIO, P., AND SUNKEL, C.E. (2007). The Drosophila CLASP homologue, Mast/Orbit regulates the dynamic behaviour of interphase microtubules by promoting the pause state. *Cell Motility and Cytoskeleton* 64, 605–620.

SPITTLE, C., CHARRASSE, S., LARROQUE, C., AND CASSIMERIS, L. (2000). The interaction of TOGp with microtubules and tubulin. *Journal of Biological Chemistry* 275, 20748–20753.

ST PIERRE, S.E., PONTING, L., STEFANCSIK, R., AND MCQUILTON, P. (2014). FlyBase 102--advanced approaches to interrogating FlyBase. *Nucleic Acids Research.* 42, D780–8.

STRASSER, G. A, RAHIM, N.A., VANDERWAAL, K.E., GERTLER, F.B., AND LANIER, L.M. (2004). Arp2/3 is a negative regulator of growth cone translocation. *Neuron* 43, 81–94.

STRAUB, F.B. (1942). Studies from the Institute of Medical Chemistry University Szeged Vol. 2. pp. 3–15.

STRUMPF, D., AND VOLK, T. (1998). Kakapo, a novel cytoskeletal-associated protein is essential for the restricted localization of the neuregulin-like factor, vein, at the muscle-tendon junction site. *Journal of Cell Biology* 143, 1259–1270.

STURTEVANT, A. (1913). imperialA third group of linked genes in Drosophila ampelophilia. *Science* (80-.). 37, 990–992.

SU, L., BURRELL, M., HILL, D., GYURIS, J., AND BRENT, R. (1995). APC binds to the novel protein EB1. *Cancer Research.* 2972–2977.

SUBRAMANIAN, A., PROKOP, A., YAMAMOTO, M., SUGIMURA, K., UEMURA, T., BETSCHINGER, J., KNOBLICH, J.A., AND VOLK, T. (2003). Shortstop Recruits EB1 / APC1 and Promotes Microtubule Assembly at the Muscle-Tendon Junction. *Current Biology* 13, 1086–1095.

TAI, C.-Y., DUJARDIN, D.L., FAULKNER, N.E., AND VALLEE, R.B. (2002). Role of dynein, dynactin, and CLIP-170 interactions in LIS1 kinetochore function. *Journal of Cell Biology* 156, 959–968.

TAKENAWA, T., AND MIKI, H. (2001). WASP and WAVE family proteins: key molecules for rapid rearrangement of cortical actin filaments and *Cell* movement. *Journal of Cell Science*. 114, 1801–1809.

THIBAULT, S.T., SINGER, M. A, MIYAZAKI, W.Y., MILASH, B., DOMPE, N. A, SINGH, C.M., BUCHHOLZ, R., DEMSKY, M., FAWCETT, R., FRANCIS-LANG, H.L., ET AL. (2004). A complementary transposon tool kit for Drosophila melanogaster using P and piggyBac. *Nature Genetics*. 36, 283–287.

THORPE, H.M., WILSON, S.E., AND SMITH, M.C. (2000). Control of directionality in the site-specific recombination system of the Streptomyces phage phiC31. *Molecular Microbiology.* 38, 232–241.

TILNEY, L.G., BRYAN, J., BUSH, D.J., FUJIWARA, K., MOOSEKER, M.S., MURPHY, D.B., AND SNYDER, D.H. (1973). Microtubules: evidence for 13 protofilaments. *Journal of Cell Biology* 59, 267–275.

TIRNAUER, J., O'TOOLE, E., BERRUETA, L., BIERER, B., AND PELLMAN, D. (1999). Yeast Bim1p promotes the G1-specific dynamics of microtubules. *Journal of Cell Biology* 145, 993–1007.

TOM, W., DE BRUYNE, M., HAEHNEL, M., CARLSON, J.R., AND RAY, A. (2011). Disruption of olfactory receptor neuron patterning in Scutoid mutant Drosophila. *Molecular and Cellular Neurosciences*. 46, 252–261.

TORTOSA, E., GALJART, N., AVILA, J., AND SAYAS, C.L. (2013). MAP1B regulates microtubule dynamics by sequestering EB1/3 in the cytosol of developing Neuronal *Cell*s. *EMBO J.* 32, 1293–1306.

UBHI, K.K., SHAIBAH, H., NEWMAN, T. A, SHEPHERD, D., AND MUDHER, A. (2007). A comparison of the neuronal dysfunction caused by Drosophila tau and human tau in a Drosophila model of tauopathies. *Invertabrate Neuroscience.* 7, 165–171.

VAUGHAN, K.T. (2005). TIP maker and TIP marker; EB1 as a master controller of microtubule plus ends. *Journal of Cell Biology* 171, 197–200.

VENKEN, K.J.T., CARLSON, J.W., SCHULZE, K.L., PAN, H., SPOKONY, R., WAN, K.H., KORIABINE, M., JONG, P.J. DE, KEVIN, P., BELLEN, H.J., ET AL. (2009). Versatile P(acman) BAC Libraries for Transgenesis Studies in Drosophila melanogaster. *Nature Methods* 6, 431–434.

VOLK, T., AND VIJAYRAGHAVAN, K. (1994). A central role for epidermal segment border cells in the induction of muscle patterning in the Drosophila embryo. *Development* 120, 59–70.

WANG, Y., KAKINUMA, N., AND KIYAMA, R. (2006a). Nucleo-cytoplasmic shuttling of human Kank protein accompanies intracellular translocation of beta-catenin. *Journal of Cell Science*. 119, 4002–4010.

WEISBRICH, A., HONNAPPA, S., JAUSSI, R., OKHRIMENKO, O., FREY, D., JELESAROV, I., AKHMANOVA, A., AND STEINMETZ, M.O. (2007). Structure-

function relationship of CAP-Gly domains. *Nature Structural and Molecular Biology*. 14, 959–967.

WEN, Y., ENG, C., SCHMORANZER, J., CABRERA-POCH, NOEMI MORRIS, E., CHEN, M., WALLAR, B., ALBERTS, A., AND GUNDERSEN1, G.G. (2004). EB1 and APC bind to mDia to stabilize microtubules downstream of Rho and promote cell migration. *Nature Cell Biology* 6, 820–830.

WILCOX, M., BROWER, D.L., AND SMITH, R.J. (1981). A position-specific cell surface antigen in the drosophila wing imaginal disc. *Cell* 25, 159–164.

WOLF, C., THISSE, C., STOETZEL, C., THISSE, B., GERLINGER, P., AND PERRIN-SCHMITT, F. (1991). The M-twist gene of Mus is expressed in subsets of mesodermal cells and is closely related to the Xenopus X-twi and the Drosophila twist genes. *Developmental Biology* 143.

WORDEMAN, L., AND MITCHISON, T.J. (1995). Identification and partial characterization of mitotic centromere-associated kinesin, a kinesin-related protein that associates with centromeres during mitosis. *Journal of Cell Biology* 128, 95–104.

WU, Q., WEN, T., LEE, G., PARK, J.H., CAI, H.N., AND SHEN, P. (2003). Developmental control of foraging and social behavior by the Drosophila neuropeptide Y-like system. *Neuron* 39, 147–161.

XIONG, W.C., OKANO, H., PATEL, N.H., BLENDY, J. A, AND MONTELL, C. (1994). repo encodes a glial-specific homeo domain protein required in the Drosophila nervous system. *Genes and Development.* 8, 981–994.

YAMAGATA, M., WEINER, J. A, AND SANES, J.R. (2002). Sidekicks: synaptic adhesion molecules that promote lamina-specific connectivity in the retina. *Cell* 110, 649–660.

YARNITZKY, T., MIN, L., AND VOLK, T. (1997). The Drosophila neuregulin homolog Vein mediates inductive interactions between myotubes and their epidermal attachment cells. *Genes and Development*. 11, 2691–2700.

ZHAI, B., VILLÉN, J., BEAUSOLEIL, S.A., MINTSERIS, J., AND GYGI, S.P. (2008). Phosphoproteome Analysis of Drosophila melanogaster Embryos. *Journal of Proteome Research* 7, 1675–1682.

ZHANG, T., ZAAL, K.J.M., SHERIDAN, J., MEHTA, A., GUNDERSEN, G.G., AND RALSTON, E. (2009). Microtubule plus-end binding protein EB1 is necessary for muscle cell differentiation, elongation and fusion. *Journal of Cell Science*. 122, 1401–1409.

ZHANG, Y., ZHANG, H., LIANG, J., YU, W., AND SHANG, Y. (2007). SIP, a novel ankyrin repeat containing protein, sequesters steroid receptor coactivators in the cytoplasm. *EMBO J.* 26, 2645–2657.

ZHU, Y., KAKINUMA, N., WANG, Y., AND KIYAMA, R. (2008). Kank proteins: a new family of ankyrin-repeat domain-containing proteins. *Biochemica et Biophysica Acta* 1780, 128–133.

ZIMNIAK, T., STENGL, K., MECHTLER, K., AND WESTERMANN, S. (2009). Phosphoregulation of the budding yeast EB1 homologue Bim1p by Aurora/Ipl1p. *Journal of Cell Biology* 186, 379–391.